Ferdowsi University of Mashhad

Iranian Food Science and Technology Research Journal

Iranian food science and technology Association

Vol.22 No.3

2026

ISSN:1735-4161

Contents

Iranian Food Science and Technology Research Journal

Vol. 22 No. 3 2026

Published by: Ferdowsi University of Mashhad, (College of Agriculture), Iran
Executive Manager: N. Shahnoushi, Department of Agricultural Economics, Ferdowsi University of Mashhad, Iran

Publisher Ferdowsi University of Mashhad
Address: College of Agriculture, Ferdowsi University of Mashhad, Iran
P.O.BOX: 91775- 1163
Fax: (98)051-38787430
E-Mail: ifstrj@um.ac.ir
Web Site: https://ifstrj.um.ac.ir

Contents

Iranian Food Science and Technology Research Journal
Homepage: https://ifstrj.um.ac.ir

Research Article
Vol. 22, No. 3, July- August. 2026, p. 225-240

Phytochemical Characterization and Evaluation of Contaminants in the Processed Products of Organically Produced *Moringa oleifera* from the Niger Sahel

M. Mahamane[1], I. Amadou[2*], X-R. Cheng[3]

1- School of Post Graduate (SISE), Dan Dicko Dankoulodo University of Maradi, Niger
2- Department of Crop Production, Faculty of Agronomy and Environmental Sciences. Dan Dicko Dankoulodo University of Maradi, Niger
(*- Corresponding Author Email: amadou.issoufou@uddm.edu.ne)
3- School of Food Science and Technology, Jiangnan University, Wuxi, China

Received: 26.10.2025
Revised: 19.04.2026
Accepted: 25.04.2026
Available Online: 24.05.2026

How to cite this article:
Mahamane, M., Amadou, I., & Cheng, X-R. (2026). Phytochemical characterization and evaluation of contaminants in the processed products of organically produced *Moringa oleifera* from the Niger Sahel. *Iranian Food Science and Technology Research Journal*, *22*(3), 225-240. https://doi.org/10.22067/ifstrj.202696126.1498

Abstract

In the Nigerien Sahel, *Moringa oleifera* processing presents a valuable economic opportunity for local communities; however, product quality and safety are closely linked to the processing methods employed. This study investigated the phytochemical composition and contamination markers of Moringa leaf extracts (MLE) and Moringa seed oil (MSO) using GC–MS analysis. The results demonstrated a significant influence of processing on chemical profiles. Fatty acids dominated the compositions (32.93%). Room-dried MLE was enriched in esters (39.9%) and terpenes (18.84%), while solar-dried samples showed elevated aldehyde content (25.3%), reflecting lipid oxidation. Sun-dried extracts uniquely contained N,N-dimethyltryptamine and phenylquinonine, indicating the presence of photochemically induced metabolites. In MSO, fatty acids were predominant (72.76%), and extraction conditions affected the stability of bioactive compounds. Cold extraction preserved thermolabile molecules such as squalene (0.29%), which were absent from heat-treated samples. Contamination markers were also identified, including di-n-octyl phthalate (1.68%) in room-dried MLE and 2-dimethylaminoethyl methacrylate (2%) in Solar dryer-dried extracts. Industrial contaminants, such as 10-undecenoyl chloride (3.68%) and 13-oxabicyclo[10.1.0]tridecane (5.85%), were detected in the control MSO. Overall, GC–MS profiling revealed that each processing method yields a distinct phytochemical fingerprint with specific nutritional, pharmacological, and safety implications. These findings highlight the need for optimized processing and packaging strategies to enhance the quality and market value of Moringa-based products in the Sahel.

Keywords: Chromatography, Infestation, Processing, Sahel

https://doi.org/10.22067/ifstrj.202696126.1498

Introduction

Moringa oleifera is a multipurpose plant native to subtropical regions, now widely cultivated across tropical and arid zones, particularly in Africa, Asia, and South America (El Bilali *et al.*, 2024). In the Nigerien Sahel, where food insecurity and chronic malnutrition remain significant challenges, its cultivation offers a promising alternative within agroforestry systems. The species is valued primarily for its leaves, which are rich in essential nutrients and widely used in human diets, and for its seeds, which yield a high-quality edible oil (Uzair, 2021; Latla, 2020). Moringa leaves, often regarded as the most nutritious part of the plant, provide key vitamins (B, C, K, and beta-carotene/provitamin A), minerals, and proteins, making them an essential dietary resource (Ndong, Wade, Dossou, Guiro, & Gning, 2007; Luoh, Sheu, Wu, & Yang, 2015; Tamilselvi & Arumugam, 2019). Beyond its nutritional value, Moringa cultivation and marketing generate substantial income and play an increasingly important role in local economies (Hassoumi, 2017; Outani, Adamou, Mahamadou, & Delmas, 2023; Mahamane, Amadou, & Moussa, 2025).

However, conventional farming systems often rely heavily on agrochemicals, raising concerns regarding the safety and quality of Moringa-derived products. Valorizing locally cultivated *M. oleifera*—whether for nutritional or pharmacological applications could therefore enhance community resilience and reduce dependence on humanitarian aid (Djeneba, Dembélé, Touré, & Iknane, 2023). Yet, the composition and quality of bioactive compounds in Moringa products are influenced by multiple factors, including cultivation practices, post-harvest processing, and storage conditions. Such variability has important implications for their nutritional efficacy and pharmacological safety (Djeneba *et al.*, 2023). Notably, a recent study reported that 68% of Moringa samples exceeded the maximum permissible limits for pesticide residues (Adeyeye *et al*., 2020).

In this context, profiling the chemical composition of processed Moringa leaves and seed oils is essential. Particular attention must be paid to assessing the effects of agricultural practices, particularly organic production systems, to ensure both product quality and consumer safety. Accordingly, this study aims to characterize the chemical profile of extracts from organically produced dried leaves and seed oil of *M. oleifera* in the Nigerien Sahel. Using gas chromatography coupled with mass spectrometry (GC-MS), the study evaluates both nutritional constituents and contaminant marker compounds to ensure the safety and quality of Moringa products.

Materials and methods

Materials

Dried Moringa Leaves

Fresh leaves of *M. oleifera* were collected from mature Moringa plants at the Kanambakache Maradi organic Moringa production site and subjected to a washing and cleaning protocol (Mahamane *et al*., 2025; Mahamane, Laminou, Amadou, & Hamadou, 2024). The methods for processing fresh Moringa leaves included room drying (away from sunlight) for 48 hours, sun-drying for 8 hours, and drying in a solar dryer at 55±5°C for at least 46 hours. The control sample of dried Moringa leaves was purchased from the local market in Maradi.

Moringa Leaf Extract (MLE)

Moringa oleifera leaf powder was extracted using distilled water and methanol. A 5% (w/v) solution was prepared at a solid-to-solvent ratio of 1:10 (1 g of powder per 10 mL of solvent). The suspension was maintained under continuous stirring at 45 °C for 8 h. The resulting mixture was filtered through Whatman No. 1 filter paper, and the filtrate was collected as the crude extract containing phytochemicals.

Moringa Seed Oil Extraction

The transformation of Moringa seeds into oil was undertaken using two distinct physical

extraction methods, in line with the principles outlined by Moneim (2024): cold-press and hot-press techniques. Following the methodology described by Al-Maqtari, Bahadi, Al-Maydama, & Barfed, (2024), cold-press extraction was performed by pressing thoroughly cleaned Moringa seeds at controlled temperatures not exceeding 50 °C for 90 minutes, thereby preserving the integrity of thermolabile compounds. In contrast, hot-press extraction was performed by subjecting the seeds to temperatures above 80 °C for a continuous 2 hours, a process intended to enhance oil yield but with potential implications for the stability of bioactive components.

Methods

GC-MS Analysis of Dried Moringa Leaf Extracts and Moringa Seed Oil Extracts

Phytochemical analyses of dried moringa leaf extracts (MLE) and moringa seed oil (MSO) were performed using a gas chromatograph equipped with a SHIMADZU GCMS-QP2010 Plus mass selective detector. A comparative analysis of the phytochemical profiles of MLE and MSO was conducted according to the protocol established by Bhalla, Ingle, Patri, & Haranath, (2021). The chromatographic parameters were characterized by an initial column oven temperature of 80.0 °C at 0 min, which was increased to 280.0 °C and maintained for 5 min. The injection was conducted at 250 °C with a 20:1 split ratio and a linear-velocity flow-control mode of 46.3 cm/s. The DB-5MS GC column (30 m × 0.25 mm, 0.25 µm) was used, with helium (99.99% purity) as the carrier gas. Extracts were injected using a multi-mode autosampler in solvent vent injection mode.

The injector operating conditions were as follows: injection volume, 13 µL. The injector temperature was maintained at 80 °C (held for 1 minute) during the solvent evaporation step, to 280 °C at a rate of 10 °C/min for 5 minutes. The total analysis time was 24 minutes. The triple quadrupole mass spectrometer was operated in electron impact (EI) ionization at 70 eV.

The relative amounts of each component were calculated and compared with the average peak area relative to the total area. The peaks of the phytochemical compounds in the chromatogram were identified by comparison with the elemental mass spectra in the National Institute of Standards and Technology (NIST) database (Halket *et al.*, 2004).

Detection and Identification of Phytochemicals

The spectrometer offers several detection modes. This detection mode allows for compound identification using mass spectral libraries. Phytochemical identification is based on retention times (RT), characteristic fragment ions (m/z), and relative peak intensities. The relative concentration of the Total Ion Chromatogram (% TIC area) of the peaks is determined by dividing the peak area of the identified compound by the total area of all the peaks in the extract. However, accurate peak detection has often been challenging due to interference from the complex matrix of compounds (fatty acids, esters, alcohols, phenols, aldehydes and ketones, terpenes, sterols, heterocyclic and aromatic compounds, glycosides, hydrocarbons, etc.) present in plant extracts (Kind & Fiehn, 2007; Halket *et al.*, 2004).

Statistical Analysis

A statistical analysis was conducted to evaluate the impact of extract types (MLE and MSO) on the phytochemical composition. The relative concentrations of compounds, expressed as a percentage of the chromatographic peak TIC, were summarized using descriptive statistics (mean and standard deviation). Principal component analysis (PCA) was performed to identify interrelationships among phytochemical compounds and to assess their similarity or

dissimilarity in discriminating compounds, based on chromatographic variables. An ascending hierarchical classification (HAC) of the contamination marker compounds was performed, enabling analysis of interclass (Between-class) and intraclass (Within-class) variances to assess dissimilarity or similarity between clusters of chemical compounds. This statistical analysis attests to the robustness of the classification of chemical compound groups. These statistical analyses were conducted using XLSTAT 5.3.

Results and Discussion

Results

GC-MS Analysis of Moringa Leaf Extracts (MLE)

The MLE extracts (Fig. 1), analyzed by GC-MS, exhibit distinct chromatographic peaks, each corresponding to a compound identified by its retention time. The number of peaks indicates the presence and diversity of phytochemical constituents (PICs) in each extract. Among the samples, the room-dried leaves (Fig. 1C) showed the highest number of peaks (35), followed by the solar-dried leaves (Fig. 1B) with 26 peaks. The sun-dried leaves (Fig. 1A) and the control sample (Fig. 1D) recorded the lowest counts, each with 19 peaks. The retention times (R.T.) of the detected compounds ranged as follows: 5.735–29.372 min for sun-dried leaves (Fig. 1A), 4.391–27.465 min for solar-dried leaves (Fig. 1B), 4.811–27.171 min for room-dried leaves (Fig. 1C), and 6.117–27.856 min for the control sample (Fig. 1D).

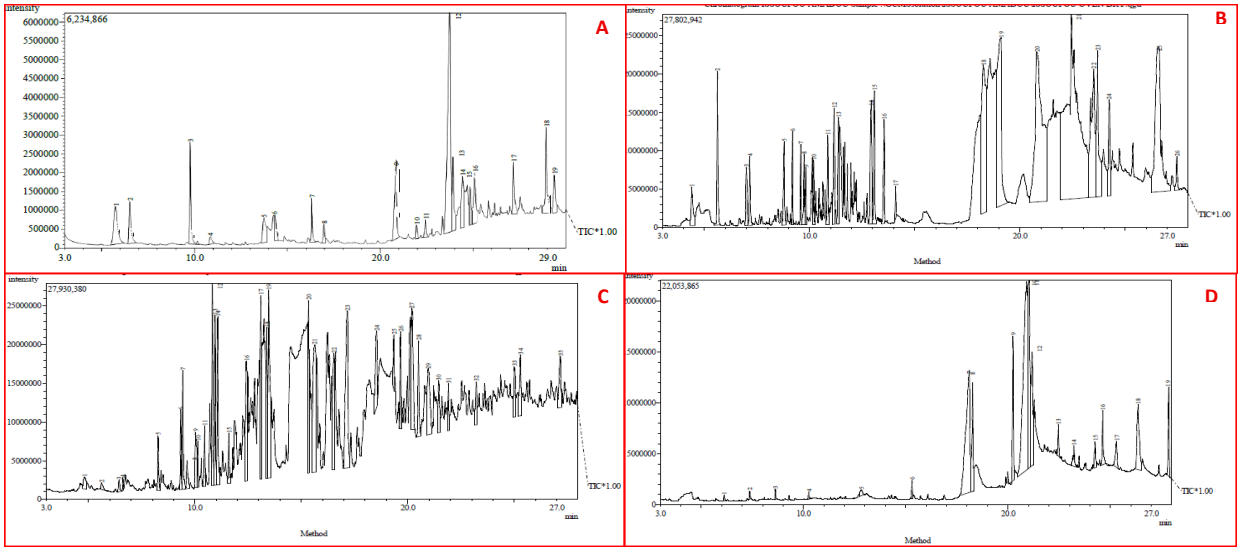

Fig. 1. Chromatogram profile of analysis of dried leaves of *M. oleifera*; (A): Sun-dried leaves; (B): Solar dryer-dried leaves; (C): room-dried leaves; (D): Control sample

Phytochemical Profiles of Dried Moringa Leaf Extracts

A comparative assessment of the chemical profiles (Table 1) from four Moringa leaf drying methods revealed a pronounced impact of processing on the composition of the resulting extracts. The chemical constituents varied significantly across techniques, with high standard deviations observed in most compound groups.

Fatty acids (Essential oils): Fatty acids emerged as the most abundant chemical family, with the highest proportion (55.85% to 9.92%) and a value across treatments of 32.93%. However, their distribution was uneven across treatments. The control extract exhibited the highest concentration of fatty acids (55.85%), with the most proportional fatty acids being linoleic acid (30.1%) and palmitic acid (18.7%). Sun-dried MLE

followed with 46.7% fatty acids, dominated by oleic acid (37.6%) and stearic acid (7.2%). In contrast, the room-dried extract contained only 9.92% fatty acids and showed a modest level of erucic acid (4.28%).

Table 1- Profiling of phytochemical compounds of Dried Moringa Leaf Extracts (MLE)

N°	Identified compounds/(Chemical)	Area percentage of Dried Moringa Leaf Extracts			
		Control	Solar drayer drying	Sun drying	Room drying
Fatty acids and derivatives		55.85	19.24	46.7	9.92
1	Palmitic acid	18.7	9	0	0
2	Stearic acid	7.05	0	7.2	0
3	Oleic acid	0	10.24	37.6	0
4	Linoleic acid	30.1	0	0	0
5	Decanoic acid	0	0	1.9	0
6	Erucic acid	0	0	0	4.28
7	Heptadecanoic acid	0	0	0	5.64
Esters		7.6	32.74	5.1	39.9
8	Ethyl Palmitate	5.2	7.9	0	0
9	Ethyl Linoleate	0	14.12	0	0
10	Ethyl E-11-Hexadecenoate	0	6.4	0	0
11	Ethyl Stearate	1.5	0	0	0
12	Methyl 11-Octadecenoate	0	0	1.2	5.05
13	Methyl Stearate	0	0	0	2.29
14	Methyl Erucate	0.9	0	0	0
15	Ethyl Icosanoate	0	3.78	0	0
16	Ethyl Docosanoate	0	0.54	0	0
17	Methoxyacetic Acid. 3-Tridecyl Ester	0	0	0	7.41
18	Benzyl Benzoate	0	0	0	2.49
19	Tridecanoic Acid. Methyl Ester	0	0	0	9.07
20	Trans-. Beta. -Terpinyl Benzoate	0	0	0	2.86
21	Bornyl Cinnamate	0	0	0	1.54
22	Benzyl Stearate	0	0	0	2.5
23	9-Hexadecenoic Acid. Phenylmethyl Ester. (Z)-	0	0	0	2.16
24	Methyl 4.6-Decadienyl Ether	0	0	0	4.62
25	Hexadecyl 3-Methyl-2-Butenoate	0	0	3.9	0
Phenols		5.03	6.62	17.01	14.27
26	Phytol	5.03	0	0	0
27	τ-Muurolol	0	2.28	0	0
28	1-Nonanol	0	0	6.81	0
29	Guaiol	0	0	0	5.42
30	Farnesol	0	0	0	1.88
31	2-Phenylethylbenzyl alcohol	0	0	0	0.66
32	2-Tetradecanol	0	0	0	3.94
33	11-Hexadecen-1-ol. (Z)-	0	0	0	2.02
34	1.3-Propanediol. 2-ethyl-2-(hydroxymethyl)	0	0	0.9	0
35	2-Dodecyl-1.3-propanediol	0	0	5.9	0
36	2-Methyl-3.13-octadecadienol	0	0	3.4	0
37	2.3-Pinanediol	0	1.15	0	0
38	α-Cadinol	0	1.96	0	0
39	δ-Cadinol	0	1.23	0	0
40	Phenol. 2.6-dimethyl-	0	0	0	0.35
Aldehydes and ketones		16.4	26.3	6.5	12.27
41	9-Hexadecenal	14.9	0	6.5	0
42	9-Octadecenal (E)	1.5	0	0	0

43	(Z)-9.17-Octadecadienal	0	26.3	0	0
44	2-Undecanone	0	0	0	3.25
45	2-Tetradecanone	0	0	0	3.44
46	3-Decen-2-one	0	0	0	1.02
47	8-Pentadaneton	0	0	0	4.56
Terpenes and sterols		3.2	11.2	0	18.84
48	α-Phellandrene	0	0.8	0	0
49	Limonene	0	0	0	0.68
50	β-Linalool. α-Terpineol	0	2.9	0	0
51	Sabinol	0	0.8	0	0
52	Squalene	3.2	0	0	0
53	Acetic acid. 1.7.7-trimethyl-bicyclo [2.2.1] hept-2-yl ester	0	0	0	1.1
54	Dihydrocarvyl acetate	0	0	0	1.44
55	p-Menth-1-en-8-yl acetate	0	0	0	2.39
56	Beta-Vatirenene	0	0	0	0.88
57	Vatirenene (isomer)	0	0	0	1.23
58	2.7.7-Trimethylbicyclo [2.2.1] hept-2-ene	0	0	0	9.66
59	α-Guaiene	0	0	0	1.46
60	α-Cubebene	0	0.8	0	0
61	Copaene	0	0.6	0	0
62	Germacrene D	0	0.7	0	0
63	Cedrene	0	0.6	0	0
64	β-Bisabolene	0	0.6	0	0
65	α-Curcumene	0	1.1	0	0
66	α-Muurolene	0	1.7	0	0
67	γ-Muurolene	0	0.6	0	0
Heterocyclic and aromatic		0.8	0	3.7	2.68
68	Benzyl nitrile	0.2	0	0	0
69	2.3-Benzofuran	0.3	0	0	0
70	2-Methoxy-4-vinylphenol	0.3	0	0	0
71	4-[5-Dimethylamino-2-hydroxy-2-pentyl]-2-phenylquinonine	0	0	3.7	0
72	Ethanone. 2-amino-1-phenyl-	0	0	0	0.29
73	1.4-dimethoxy-2.3.5.6-tetramethylbenzene	0	0	0	2.29
74	p-Benzophenetidide (N-(4-Ethoxyphenyl) benzamide)	0	0	0	0.1
Glycosides. Amides. Amines		10.12	3.9	16.9	0.29
75	Methyl 3.6-anhydrohexopyranoside	0	2	0	0
76	octyl-β-D-glucopyranoside	0	0	10.2	0
77	Oleamide	1.12	0	0	0
78	Monopalmitine. Monoolein	7.5	0	0	0
79	Propylhexedrine. Amines	0	2	2	0.29
80	N. N-dimethyl-1-heptadencanamin	0	0	2	0
81	2-Acetonyl-9-[3-deoxy-β-d-ribouranosyl] hypoxanthine	0	0	2.7	0
82	2-(Dimethylamino)ethyl methacrylate	0	1.9	0	0
83	L-glutamine	0.9	0	0	0
84	Ethyl-D-glucopyranoside	0.6	0	0	0
Hydrocarbons		0.6	0	0	0
85	1-Octadecyne	0.6	0	0	0
Phthalate		0	0	0	1.68
86	Di-n-octyl phthalate	0	0	0	1.68

TIC: Total Ion Chromatogram (% TIC area)

Esters: Ester compounds showed distinct patterns, with high concentrations in room-dried (39.9%) and solar dryer-dried (32.74%) MLE, and much lower levels in sun-dried (7.6%) and control (5.1%) samples. Notably, the room-dried extract contained a diverse array of methyl esters, accounting for 22.03% of its composition.

Alcohols and phenols: This group included phytol (5.03%), predominantly found in the control extract. Alcohols and phenols were more prevalent in sun-dried (17.4%) and room-dried (14.27%) MLE, while solar-dried samples contained the least (6.62%).

Aldehydes and ketones: These compounds displayed marked variability. Solar-dried MLE had the highest concentration (26.3%), mainly (Z)-9,17-octadecadienal. Room-dried MLE featured several ketones, including 2-undecanone (3.25%), 2-tetradecanone (3.44%), 8-pentadanetone (4.56%), and 3-decan-2-one (1.02%). The control extract contained 16.4% aldehydes, mainly 9-hexadecenal (14.98%) and 9-octadecenal (1.5%).

Heterocyclic and aromatic compounds: This group exhibited a mean concentration of 1.80, indicating high variability. The control extract was notable for the presence of benzyl nitrile (0.2%), 2,3-benzofuran (0.3%), and 2-methoxy-4-vinylphenol (0.3%). The sun-dried extract uniquely contained N,N-Dimethyltryptamine (DMT) and 4-[5-Dimethylamino-2-hydroxy-2-pentyl]-2-phenylquinoline, each at 3.7%.

Miscellaneous compounds (Glycosides, Amides, Amines): This group had a moderate concentration (12.45) and considerable heterogeneity. The control extract was distinguished by oleamide (1.12%), monopalmitin, and mono-olein (7.55%). Sun-dried MLE was rich in glucopyranoses, notably octyl-β-D-glucopyranoside (10.2%).

Terpenes and sterols: These compounds exhibited moderate variability (8.31). Room-dried MLE had the highest content (18.84%), followed by dryer-dried MLE (11.2%). The control extract contained only 3.2%.

Hydrocarbons and other compounds: The hydrocarbon group was represented solely by 1-Octadecyne, found exclusively in the control sample. Additionally, phthalate was detected in the room-dried MLE at a low concentration (1.68%).

GC-MS Analysis of Moringa Seed Oil Extracts (MSO)

Moringa seed oil extracts (Fig. 2) show that the cold extract has the highest number of peaks (18 peaks), followed by the control sample (Fig. 1D) with (14 peaks) and the hot extract (Fig. 2E) with (13 peaks). The chromatogram analysis of Moringa seed oil shows that the RTs of the identified compounds vary from 16.056 to 22.418 min for the hot MSO (Fig. 2E), 15.464 to 23.651 min for the cold extract (Fig. 2F), and 16.024 to 22.122 min for the control sample (Fig. 2G). The retention time was used to characterize the compounds identified in the chromatograms and to determine their polarity, volatility, and mass.

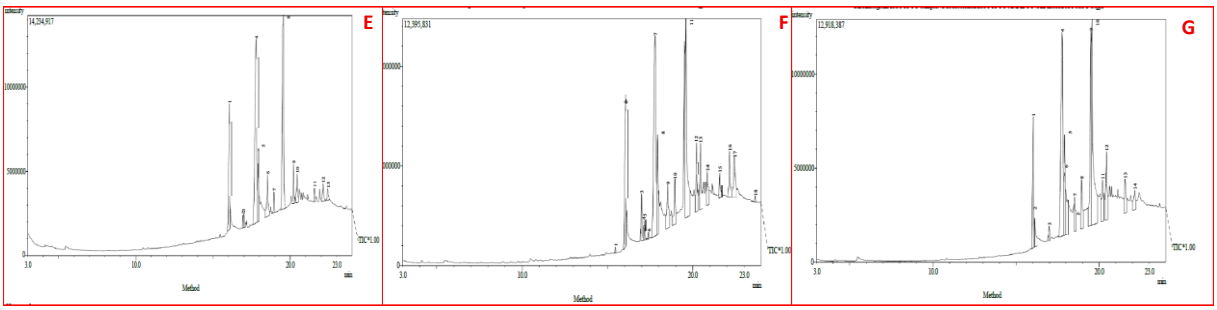

Fig. 2. Chromatogram profile of *M. oleifera* seed oil analysis; (E) Hot extract; (F): Cold extract; (G): Control sample

Phytochemical Compositions of Moringa Seed Oil Extracts

A comparative analysis of the three oil extraction methods (Table 2) reveals a significant influence of the extraction processes on the chemical profiles of the compounds. Table 2 shows the dominance of

the average relative concentration of the TIC area and also the stability of the fatty acids (72.76%) in the three MSO. Within this chemical family, oleic acid is the predominant compound (28.03%), while stearic acid is the most stable with the lowest variability (6.08). Finally, ricinoleic acid is detected exclusively in the control extract (20.66%) and is absent from the other extraction methods. In contrast, hot extraction is distinguished by its high undecenoic acid content (29.6%). However, the ester composition shows a strong presence of ethyl esters in the control extract, as well as other specific compounds, such as chloride and glyceryl. Conversely, the cold extract produces methyl esters, including linoleate, stearate, and 2-monopalmitin. On the other hand, the hot extract exhibits selectivity for compounds such as lactones and ethers. The aldehyde composition is the most variable in the cold extract, which clearly favors its formation (23.57%) and exhibits specificities, such as (Z)-7-tetradecenal. Thus, other specific compounds, present in low quantities, such as ketones, are found in all the extracts. On the other hand, hydrocarbons containing squalene at a trace level (0.29%) are present only in the cold extract.

Table 2- Profiling of phytochemical compounds of Moringa Seed Oil Extracts (MSO)

N°	Identified compounds / (Chemical families)	Area percentages in MSO		
		MSO Control	**MSO Hot extraction**	**MSO Cold extraction**
Fatty Acids		73.85	80.58	63.84
1	Palmitic acid	7.84	12.4	10.56
2	Oleic acid	24.44	32.59	27.07
3	Stearic acid	6.04	5.99	6.22
4	Indecenoic acid	14.87	29.6	19.99
5	Ricinoleic acid	20.66	0	0
Esters and Glycerides		14.21	5.24	8.58
6	Allyl decanoate	0	0.7	0
7	Methyl 14-methylpentadecanoate	0	0	0.24
8	Methyl linoleate	0	0	0.78
9	Methyl 11-octadecenoate	0	0	0.57
10	Methyl stearate	0	0	0.39
11	Methyl 2-methylhexadecanoate	2.3	0	0
12	Ethyl stearate	2.44	0	0
13	2.3-Dihydroxypropyl palmitate	0	1.4	0
14	2-Monopalmitin	0	0	6.6
15	Glyceryl 2-pentadecanoate	3.62	0	0
16	13-Oxabicyclo[10.1.0]tridecane	5.85	3.14	0
Aldehydes		4.87	12.22	23.57
17	9-Octadecenal	2.6	5.56	4.71
18	7.11-Hexadecadienal	2.27	2.95	4.82
19	10-Undecenal	0	0	5.34
20	9-Tetradecnal (Z)	0	2.28	0
21	(Z)-9-Tetradecnal	0	1.43	0
22	(Z)-7-Tetradecnal	0	0	4.96
23	13-Octadecenal. (Z)-	0	0	3.74
Ketones		2.75	1.08	1.53
24	1-(2.2-Dimethylcyclopentyl) ethanone	2.75	1.08	1.53
Hydrocarbon		0	0	0.29%
25	Squalène	0	0	0.29
Lactones		0.64	0.89	2.19
26	13-Hexyloxacyclotridec-10-en-2-one	0.64	0.89	2.19
Chlorides		3.68	0	0
27	10-Undecenoyl chloride	3.68	0	0

TIC: Total Ion Chromatogram (% TIC area)

Characterization of Contamination Marker Compounds

Analysis of chemical contamination marker compounds (Table 3) revealed their presence in two Moringa leaf processing methods. The chemical compounds identified in the room-grown MLE were composed of di-n-octyl phthalate (DNOP) products with a TIC abundance of 1.68%, benzyl benzoate (2.49%), and benzyl stearate (2.5%). DNOP, a di-n-octyl phthalate ester, is a synthetic plastic-derived compound that can enter the product from the environment (Li, Liu, Kang, Liu, & Wang, 2022; Waring, Harris, & Mitchell, 2018). Benzyl benzoate is a compound that can be natural or synthetic. Benzyl stearate is a derivative of plant-based and synthetic compounds. However, in the dryer MLE, 2-dimethylaminoethyl methacrylate was identified with a TIC abundance of 2%. In contrast, the control MLE sample, which contained two detected compounds, benzyl nitrile (0.2%) and 2,3-benzofuran (0.3%), had a very low TIC concentration. Benzyl nitrile is widely produced by chemical synthesis from benzyl chloride. Benzofuran can originate from natural or synthetic sources.

Table 3- Profile of contamination marker compounds

Extract Type Method		Identified Compound	% TIC	TR (min)
MLE	Room	Di-n-octyl phthalate	1.68	25
		Benzyl benzoate	2.49	15
		Benzyl stearate	2.5	25
	Sun dried	2-Dimethylaminoethyl methacrylate	2	24.251
	Control	Benzyl nitrile	0.2	6.12
		2.3-Benzofuran	0.3	7.36
MSO	Control	10-Undecenoyl chloride	3.68	20.194
		1-(2.2-dimethylcyclopentyl) ethanone	2.75	21.549
		13-Oxabicyclo[10.1.0]tridecane	5.85	20.431

TIC: Total Ion Chromatogram (% TIC area); MLE: Moringa leaf extract; MSP: Moringa seed oil

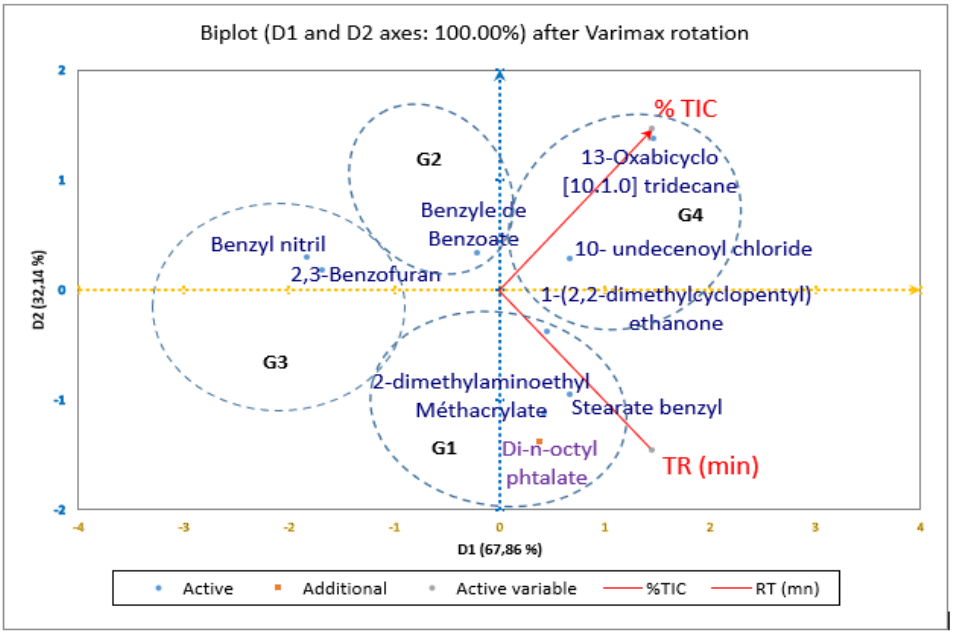

Fig. 3. Principal component analysis (PCA) of compounds

In the MSO, only the control sample contained compounds detected as a source of contamination: 10-undecenoyl chloride (3.68%), 1-(2,2-dimethylcyclopentyl) ethanone (2.75%), and 13-oxabicyclo[10.1.0]tridecane (5.85%).

Comparative Analysis of Contaminants

Principal component analysis (Fig. 3) facilitated the classification and differentiation of compounds based on key variables extracted from the GC-MS chromatograms (Fig. 4). Specifically, retention time (RT) and relative concentration (expressed as % of the total ion chromatogram, TIC area) enabled the identification of four distinct contaminant groups.

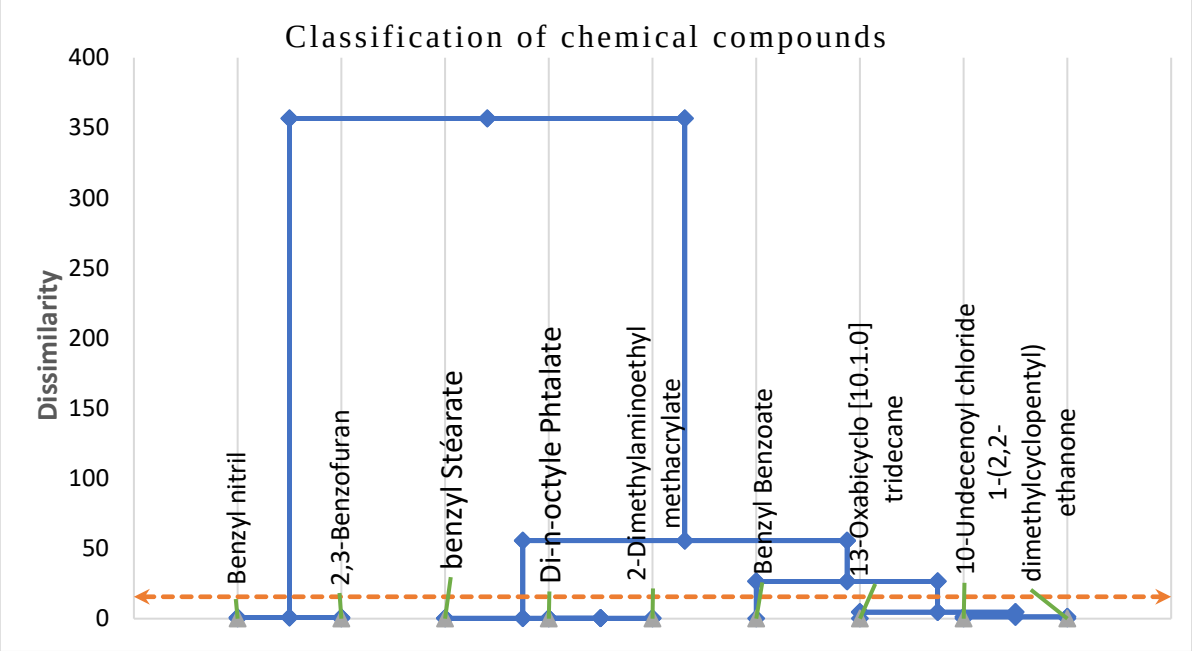

Fig. 4. Ascending Hierarchical Classification (AHC) of chemical compounds

Group 1: Characterized by RTs ranging from 15 to 25 minutes and relative concentrations between 1.68% and 2.5%. This group includes Benzyl stearate and Di-n-octyl phthalate (both found in room-dried MLE), as well as 2-Dimethylaminoethyl methacrylate (detected in Solar dryer-dried MLE).

Group 2: Composed solely of Benzyl benzoate (room dried MLE), with a retention time of 25 minutes and a relative concentration of 2.5%.

Group 3: Defined by short retention times (6.12–7.36 min) and low relative concentrations (0.18–3%). This group includes Benzyl nitrite and 2,3-benzofuran, both of which were identified in the control (market sample).

Group 4: Exhibits retention times between 20.19 and 21.55 minutes and higher relative concentrations ranging from 2.75% to 5.85%. The compounds in this group include 10-Undecenoyl chloride, 1-(2,2-dimethylcyclopentyl) ethenone, and 13-Oxabicyclo[10.1.0]tridecane.

A Hierarchical Ascending Clustering (HAC) analysis of the contamination marker compounds was performed based on their TIC and TR percentages. Thus, four clusters are well defined, with 97.27% of the total variance in the data explained by inter-cluster distances. The interclass variances (Between-class) are 54.27, and the intraclass variance (within-class) is 1.5. The high interclass variance confirms that the compounds within each

cluster are highly similar to one another and distinctly different from those in other clusters. The compounds are characterized by class. Class 1 consists of late-eluting chemical compounds with the highest retention times and medium abundance. The compounds in this class are: Di-n-octyl phthalate (MLE room drying), 2-dimethylaminoethyl methacrylate (MLE solar dryer), and benzyl stearate (MLE by room drying). Class 2 is composed of benzyl benzoate (MLE by room drying), the only compound in this class with a high mean abundance and a median TR that distinguishes it from other groups of compounds. Early-eluting, low-abundance compounds characterize class 3. The compounds that characterize this class are: benzyl nitrite and 2,3-benzofuran (control sample).

Late-eluting compounds and high abundance characterize class 4. The following compounds constitute this class: 10-undecenoyl chloride, 1-(2,2-dimethylcyclopentyl) ethanone, and 13-oxabicyclo[10.1.0]tridecane.

Discussion

A comparative analysis of the chemical profiles of *Moringa oleifera* leaves, based on the processing methods employed, clearly demonstrates that drying techniques exert a decisive influence on extract composition. Consistent with previous findings (Chong, Dibagar, Maulion, & Figiel, 2023; Bamisaye, Olasebikan, Asebioge, & Samson, 2025), this study demonstrates that drying conditions significantly impact the stability and concentration of bioactive compounds (Table 2). The abundance of essential fatty acids such as linoleic, palmitic, and oleic acids in the control, sun, and solar dryer extracts corroborates the results of Nakra, Tripathy, & Srivastav, (2024), who reported that drying is among the most widely used preservation techniques for medicinal plants, significantly shaping their physicochemical and functional properties. Thus, drying is a critical step for retaining bioactive molecules in Moringa leaves, while the variability observed across processing methods underscores the potential to tailor the levels of specific compounds of nutritional and pharmacological interest.

A notable finding is the exclusive detection of N,N-dimethyltryptamine (DMT) and 4-[5-dimethylamino-2-hydroxy-2-pentyl]-2-phenylquinonine in sun-dried extracts. This suggests that sun exposure may trigger photochemical transformations that lead to the synthesis of unique compounds with potential pharmacological applications, including antimalarial and anti-inflammatory effects (Konmy, Olounladé, Doko-Allou, & Azando, 2020). These results underscore the specificity of drying conditions in shaping chemical diversity.

Room-dried extracts were particularly enriched in esters (39.9%) and terpenes (18.8%), confirming earlier findings (Chukwu *et al*., 2024) that documented abundant methyl esters such as methyl palmitate, methyl stearate, and octadecenoic acid methyl ester in dried Moringa leaves. This preservation of esters highlights room-drying as a favorable technique for maintaining volatile lipid derivatives. Moreover, the distinctive terpene profiles obtained by room-drying and solar-drying demonstrate complementary outcomes: room-drying favors more volatile monoterpenes such as limonene, dihydrocarvyl acetate, and menthyl acetate, while solar-drying preserves less volatile sesquiterpenes such as α-cubebene, germacrene D, and β-bisabolene. These compounds are well-documented for their antioxidant, antimicrobial, and anti-inflammatory activities (Peixoto *et al*., 2015; Eddin *et al*., 2021, 2022). Such differentiation highlights the pharmacological significance of processing choices, as each method harnesses distinct therapeutic potentials.

The analysis of terpene alcohols further illustrates this specificity: sun-dried leaves contained the highest concentrations, while solar-dried extracts showed exclusive compounds, including τ-muurolol, α-cadinol, and δ-cadinol, which are recognized for their antioxidant and anti-inflammatory effects. In

contrast, room-drying favored the production of guaiol and farnesol. Similarly, aldehyde and ketone profiles varied with drying methods, with solar dryer drying yielding elevated levels of unsaturated aldehydes, such as (Z)-9,17-octadecadienal, a product of fatty acid oxidation (Ayseli & Ayseli, 2020; Codex Alimentarius, 2024).

In terms of lipid composition, the extracts revealed a predominance of unsaturated fatty acids, notably oleic acid (28.3%). However, these values differed from those reported for Moringa oil (Vergara-Jimenez, Almatrafi, & Fernandez, 2017), likely due to environmental and genetic variability (Anwar, Latif, Ashraf, & Gilani, 2007). This confirms that both growth conditions and processing protocols strongly modulate lipid composition. Notably, squalene was detected only in the cold extract, highlighting its thermo-sensitivity and confirming previous reports on its degradation under heat treatments (Kelly, 1999; Wiesner-Kiełczewska, Zagrodzki, Gawalska, & Paśko, 2025). The preservation of this valuable antioxidant underscores the importance of cold-extraction methods for maximizing its nutraceutical potential.

Overall, the differential chemical profiles obtained across drying and extraction methods reflect the high biochemical plasticity of Moringa leaves. Room-drying enhances the retention of esters and monoterpene, while solar-drying favors the retention of sesquiterpenes and aldehydes, and sun-drying induces the formation of unique photochemical compounds of pharmacological interest. These findings underscore the importance of carefully selecting processing techniques to optimize the preservation and functionality of bioactive compounds in Moringa leaves, depending on their intended nutritional or therapeutic application.

Conclusion

This study thoroughly characterized the phytochemical composition and contamination profile of dried leaf and seed oil extracts of Moringa. The results obtained conclusively demonstrate the decisive influence of processing methods on the types of bioactive compounds. GC-MS analysis revealed a diverse array of chemical compounds with distinct profiles, depending on the drying and extraction methods employed. Room and sun-dried extracts better preserve chemical qualities and functional properties. Cold extraction was found to be the most optimal method for preserving thermosensitive compounds. The detection of contaminants, including plastic residues and oxidation products, underscores the importance of selecting suitable packaging materials.

Acknowledgments

The authors would like to thank all those who, directly or indirectly, contributed to the completion of this work. Our sincere thanks go to the NGO Taimakon Manoma, HEKS-EPER, and the local communities who contributed to the completion of this work.

Funding Source

This research received no specific grant from any funding agency in the public, commercial, or not-for-profit sectors.

Author Contributions

Mr. Massaoudou Mahamane: conducted the literature review, sample collection for laboratory analysis, data analysis and interpretation, and drafted the initial version. **Dr. Issoufou Amadou:** conceptualized, supervised, validated, proofread, and edited the manuscript, and provided advice on structuring the data analyses and refining the manuscript. **Dr. Xiang-Rong Cheng**: provided technical support for data analysis and writing, and offered advice on structuring and refining the manuscript.

Availability of Data and Materials

The datasets generated and/or analyzed during the current study are available from the corresponding author on reasonable request.

Declarations

Ethics Approval and Consent to Participate

Not applicable.

Consent for Publication

Not applicable.

Competing Interests

The authors declare that they have no competing interests.

References

1. Adeyeye, E.I., Ibigbami, O.A., Akinsola, A.F., Akinwumi, O.A., Adubiaro, H.O., & Adesina, A.J. (2020). Assessment of pesticides residues in *Moringa oleifera* seed. *Indian Journal of Public Health Research & Development*, *11*(8), 261. https://doi.org/10.37506/ijphrd.v11i8.10932
2. Al-Maqtari, M.A., Al-Maydama, H., Bahadi, M., & Barfed, H. (2024). Extraction and comparative evaluation on the physicochemical characteristics of Yemeni *Moringa oleifera* seeds oil. *Sana'a University Journal*, *2*(1), 83–95. https://doi.org/10.59628/jast.v2i1.789
3. Anwar, F., Latif, S., Ashraf, M., & Gilani, A.H. (2007). *Moringa oleifera*: A food plant with multiple medicinal uses. *Phytotherapy Research*, *21*(1), 17-25. https://doi.org/10.1002/ptr.2023
4. Ayseli, M.T., & Ayseli, Y.İ. (2020). Volatile profiling and fingerprinting of *Moringa oleifera* Lam. leaves by headspace solid-phase microextraction coupled with gas chromatography-mass spectrometry (HS-SPME/GC-MS). *Journal of Essential Oil Research*, *32*(5), 406-417. https://doi.org/10.17504/protocols.io.81wgbwp9ngpk/v1
5. Bamisaye, V.J., Olasebikan, Y.O., Asebioge, O.O., & Samson, E.A. (2025). Effects of drying methods on phytochemical and antioxidant properties of *Ocimum gratissimum* (Lam.) leaves. *CABI Agriculture and Bioscience*, *6*(1), 0052. https://doi.org/10.1079/ab.2025.0052
6. Bhalla, N., Ingle, N., Patri, S.V., & Haranath, D. (2021). Phytochemical analysis of *Moringa oleifera* leaves extracts by GC-MS and free radical scavenging potency for industrial applications. *Saudi Journal of Biological Sciences*, *28*(12), 6915–6928. https://doi.org/10.1016/j.sjbs.2021.07.075
7. Chong, C.H., Dibagar, N., Maulion, R., & Figiel, A. (2023). Drying characteristics of herbs, spices, and medicinal plants. *Drying of Herbs, Spices, and Medicinal Plants*, 29–52. https://doi.org/10.1201/9781003269250-3
8. Chukwu, O.O., Iyare, C.O., Emelike, C.U., Ezimah, A.C.U., Asogwa, N.T., & Konyefom, N.G. (2024). GC-MS analysis of *Moringa oleifera* leaf extract and effects of administration on histology of reproductive organs and liver of female rats exposed to chronic unpredictable stress. *Journal of Ethnopharmacology*, *332*, 118345. https://doi.org/10.1016/j.focha.2024.100661
9. Codex Alimentarius. (2024). General standard for contaminants and toxins in food and feed. (CXS 193-1995). In Codex Alimentarius Commission Procedure Manual, 29th edition. Rome: FAO/WHO. https://doi.org/10.19103/as.2025.172.06
10. Djeneba, C., Dembélé, Y., Touré, O., & Iknane, A. (2023). Caractérisation et composition biochimique et nutritionnelle du *Moringa oleifera* récolté dans le district de Bamako, Mali en 2020. *Mali Santé Publique*, 5–13. https://doi.org/10.53318/msp.v12i01.2416
11. Eddin, L.B., Jha, N.K., Goyal, S.N., Agrawal, Y.O., Subramanya, S.B., Bastaki, S.M.A., & Ojha, S. (2022). Health benefits, pharmacological effects, molecular mechanisms, and therapeutic potential of α-bisabolol. *Nutrients*, *14*(7), 1370. https://doi.org/10.3390/nu14071370
12. El Bilali, H., Dan Guimbo, I., Nanema, R.K., Falalou, H., Kiebre, Z., Rokka, V.M., ... & Acasto, F. (2024). Research on moringa (*Moringa oleifera* Lam.) in Africa. *Plants*, *13*(12), 1613. https://doi.org/10.3390/plants13121613

13. Halket, J.M., Waterman, D., Przyborowska, A.M., Patel, R.K.P., Fraser, P.D., & Bramley, P.M. (2004). Chemical derivatization and mass spectral libraries in metabolic profiling by GC/MS and LC/MS/MS. *Journal of Experimental Botany, 56*(410), 219–243. https://doi.org/10.1093/jxb/eri069
14. Hassoumi, D. (2017). *Moringa oléfera* un outil de développement local : cas de la commune rurale de Liboré. *Revue des Etudes Multidsciplinaires en Sciences Economiques et Sociales, 2*(2), 55-68. https://doi.org/10.48375/IMIST.PRSM/remses-v2i2.7786
15. Kelly, G.S. (1999). Squalene and its potential clinical uses. *Alternative Medicine Review, 4*(1), 29-36. https://doi.org/10.1080/13590840050000954
16. Kind, T., & Fiehn, O. (2007). Seven golden rules for heuristic filtering of molecular formulas obtained by accurate mass spectrometry. *BMC Bioinformatics, 8*(105), 1-20. https://doi.org/10.1186/1471-2105-8-105
17. Konmy, B.B.S., Olounladé, P.A., Doko-Allou, S., & Azando, E.V.B. (2020). Evaluation of the activity of powder of leaves of *Moringa oleifera* on gastro intestinal parasites of the domestic rabbit (*Oryctolagus cuniculus*) in Southern Benin. *European Scientific Journal, 16*(30), 52. https://doi.org/10.19044/esj.2020.v16n30p51
18. Latla, S. (2020). Etude des fractions Lipidiques et Protéiques des extraits de quatre parties de *Moringa Oleifera* L (Feuilles, Fleurs, Gousses et Graines) Cultivée à Metlili (Ghardaïa) (*Doctoral dissertation*). dspace.univ-ghardaia.edu.dzdspace.univ-ghardaia.edu.dz
19. Li, A., Liu, C., Kang, L., Liu, K., & Wang, X. (2022). Chamber study on the migration of di-n-octyl phthalate (DNOP) between source surfaces and settled dust: Influence of temperature and dust loading. *Atmospheric Environment, 268*, 118789. https://doi.org/10.1016/j.atmosenv.2021.118789
20. Luoh, J.W., Sheu, A., Wu, W.J., & Yang, R.Y. (2015). Phytonutrient values of *Moringa oleifera* leaves. *In International Symposium on Moringa, 1158*, 341-348. https://doi.org/10.17660/actahortic.2017.1158.38
21. Mahamane, M., Amadou, I., & Moussa, M.R. (2025). Technical process and economic analyses of organic *Moringa oleifera* production in the Sahel region of Niger. *Journal of Food Research, 14*(2), 24. https://doi.org/10.5539/jfr.v14n2p24
22. Mahamane, M., Laminou, M.O., Amadou, I., & Hamadou, H.A. (2024). Effects of organic fertilization model on the growth of two *Moringa oleifera* Lam. Cultivars. *Journal of Applied Biosciences, 197*, 20826-20837. https://doi.org/10.35759/JABs.197.3
23. Moneim, S.A. (2024). Effect of moringa (*Moringa oleifera* Lam.) seed oil extraction methods on its physicochemical properties. *Sabrao Journal of Breeding and Genetics, 56*(5), 2143–2151. https://doi.org/10.1016/j.phyplu.2025.100762
24. Nakra, S., Tripathy, S., & Srivastav, P.P. (2024). Drying as a preservation strategy for medicinal plants: Physicochemical and functional outcomes for food and human health. *Food Chemistry Advances, 4*, 100727. https://doi.org/10.1016/j.focha.2024.100727
25. Ndong, M., Wade, S., Dossou, N., Guiro, A.T., & Gning, R.D. (2007). Valeur nutritionnelle du *Moringa oleifera*, Etude de la biodisponibilite du Fer, effet de L' Enrichissement de divers plats traditionnels Sénégalais avec la poudre des feuilles. *African Journal of Food, Agriculture, Nutrition and Développent, 7*(3), 1-17. https://doi.org/10.18697/ajfand.14.IPGRI1-8
26. Outani, B.A., Adamou, H., Mahamadou, A., & Delmas, P. (2023). Moringa (*Moringa oleifera* Lam): A Review on its importance worldwide. *East African Scholars Journal of Agriculture and Life Sciences, 6*(07), 112–120. https://doi.org/10.36349/easjals.2023.v06i07.01
27. Peixoto, M.G., Costa-Júnior, L.M., Blank, A.F., da Silva Lima, A., Menezes, T.S.A., de Alexandria Santos, D., Alves, P.B., de Holanda Cavalcanti, S.C., Bacci, L., & de Fátima

Arrigoni-Blank, M. (2015). Acaricidal activity of essential oils from *Lippia alba* genotypes and its major components carvone, limonene, and citral against *Rhipicephalus microplus*. *Veterinary Parasitology*, *210*(1-2), 118-122. https://doi.org/10.1016/j.vetpar.2015.03.010

28. Tamilselvi, N.A., & Arumugam, T. (2019). Health benefits, therapeutic and pharmacological properties of moringa- A Review. *Journal of Pharmaceutical Research International, 25*(1), 1–11. https://doi.org/10.9734/jpri/2018/37179
29. Uzair, Z. (2021). Physicochemical analysis and oil extraction yield of moringa (*Moringa oleifera*) seed. *Agricultural Sciences Journal, 3*(1), 72–78. https://doi.org/10.56520/asj.003.01.070
30. Vergara-Jimenez, M., Almatrafi, M.M., & Fernandez, M.L. (2017). Chemical profile of *Moringa oleifera* Lam. leaves, seeds and pods by gas chromatography-mass spectrometry (GC-MS) analysis. *International Journal of Food Properties, 20*(1), S1-S12. https://doi.org/10.3390/antiox6040091
31. Waring, R.H., Harris, R.M., & Mitchell, S.C. (2018). Plastic contamination of the food chain: A threat to human health? Maturitas, *115*, 64–68. https://doi.org/10.1016/j.maturitas.2018.06.010
32. Wiesner-Kiełczewska, A., Zagrodzki, P., Gawalska, A., & Paśko, P. (2025). Chemometric methods: A valuable tool for investigating the interactions between antifungal drugs (including antifungal antibiotics) and food. *Antibiotics*, *14*(1), 70. https://doi.org/10.3390/antibiotics14010070

نشریه پژوهشهای علوم و صنایع غذایی ایران
https://ifstrj.um.ac.ir

مقاله پژوهشی
جلد ۲۲، شماره ۳، مرداد- شهریور ۱۴۰۵، ص. ۲۴۰-۲۲۵

شناسایی فیتوشیمیایی و ارزیابی آلاینده‌ها در محصولات فرآوری شده *مورینگا اولیفرا* تولید شده به‌صورت ارگانیک از ساحل نیجر

ماسوئودو مهامانه[۱]- اسیوفو آمادو[۲*]- ژیانگ رانگ چنگ[۳]

تاریخ دریافت: ۱۴۰۴/۰۸/۰۴
تاریخ پذیرش: ۱۴۰۵/۰۲/۰۵

چکیده

در ساحل نیجر، فرآوری *مورینگا اولیفرا* یک فرصت اقتصادی ارزشمند برای جوامع محلی ارائه می‌دهد؛ با این حال، کیفیت و ایمنی محصول ارتباط نزدیکی با روش‌های فرآوری مورد استفاده دارد. این مطالعه با استفاده از آنالیز GC-MS، ترکیب فیتوشیمیایی و نشانگرهای آلودگی عصاره‌های برگ مورینگا (MLE) و روغن دانه مورینگا (MSO) را بررسی کرد. نتایج، تأثیر قابل توجه فرآوری بر پروفایل‌های شیمیایی را نشان داد. اسیدهای چرب در ترکیبات غالب بودند. MLE (۳۲/۹۳ ٪) خشک‌شده در اتاق غنی از استرها (۳۹/۹٪) و ترپن‌ها (۱۸/۸۴٪) بود، در حالی‌که نمونه‌های خشک‌شده در آفتاب، محتوای آلدهید بالایی (۲۵/۳٪) نشان دادند که نشان‌دهنده اکسیداسیون لیپید است. عصاره‌های خشک‌شده در آفتاب به‌طور منحصر به فردی حاوی N-، N-دی‌متیل‌تریپتامین و فنیل‌کینونین بودند که نشان‌دهنده وجود متابولیت‌های القا شده فتوشیمیایی است. در MSO، اسیدهای چرب غالب بودند (۷۲/۷۶٪) و شرایط استخراج بر پایداری ترکیبات زیست‌فعال تأثیر گذاشت. استخراج سرد، مولکول‌های حساس به حرارت مانند اسکوالن (۰/۲۹٪) را حفظ کرد که در نمونه‌های تیمار شده با حرارت وجود نداشتند. نشانگرهای آلودگی نیز شناسایی شدند، از جمله دی-ان-اکتیل فتالات (۱/۶۸٪) در MLE خشک شده در اتاق و ۲-دی متیل آمینو اتیل متاکریلات (۲٪) در عصاره‌های خشک شده در خشک‌کن خورشیدی. آلاینده‌های صنعتی، مانند ۱۰-آندسنوئیل کلرید (۳/۶۸٪) و ۱۳-اوکسابی‌سیکلو [۱۰.۱.۰] تری‌دکان (۵/۸۵٪)، در MSO کنترل شناسایی شدند. به‌طور کلی، پروفایل GC-MS نشان داد که هر روش فرایند، اثر انگشت فیتوشیمیایی متمایزی با پیامدهای تغذیه‌ای، دارویی و ایمنی خاص ارائه می‌دهد. این یافته‌ها بر نیاز به بهینه‌سازی فرایندها و بسته‌بندی برای افزایش کیفیت و ارزش بازار محصولات مبتنی بر مورینگا در ساحل تأکید می‌کند.

واژه‌های کلیدی: آلودگی، ساحل، فرآوری، کروماتوگرافی

۱- دانشکده تحصیلات تکمیلی (SISE)، دانشگاه مرادی، نیجر
۲- گروه تولید محصولات کشاورزی، دانشکده علوم زراعی و محیطی، دانشگاه مرادی، نیجر، دان دیکو دانکولودو
(*- نویسنده مسئول: Email: amadou.issoufou@uddm.edu.ne)
۳- دانشکده علوم و صنایع غذایی، دانشگاه جیانگنان، ووشی، چین

https://doi.org/10.22067/ifstrj.202696126.1498

Iranian Food Science and Technology Research Journal
Homepage: https://ifstrj.um.ac.ir

Research Article
Vol. 22, No. 3, July- August. 2026, p. 241-260

Response Surface Methodology– Driven Optimization of Pectin Extraction from Peels of an Indigenous *Musa acuminata*

E.J. Balaji[1], U. Shankar K[1*]

1- Department of Life Sciences, Christ University, Bengaluru, India
(*- Corresponding Author Email: uma.shankar@christuniversity.in)

Received: 02.12.2025
Revised: 19.03.2026
Accepted: 28.03.2026
Available Online: 19.05.2026

How to cite this article:
Balaji, E.J., & Shankar K, U. (2026). Response surface methodology–driven optimization of pectin extraction from peels of an indigenous *Musa acuminata*. *Iranian Food Science and Technology Research Journal*, *22*(3), 241-260. https://doi.org/10.22067/ifstrj.2026.96779.1526

Abstract

The current study aimed to optimize pectin extraction from the non-AIS (crude) sample variety of *Musa acuminata* (Yelakki) peel, which was conducted by applying Response Surface Methodology (RSM), using a citric acid-assisted extraction method. The study was conducted with RSM to systematically evaluate the individual, quadratic, and interactive effects of process variables (Citric acid concentration, extraction time, and temperature) on the pectin yield. It was carried out based on a three-factor design to determine optimal conditions and statistically significant factors. The optimum conditions for extraction were found to be a concentration of 1.5%, an extraction duration of 90 minutes, and a temperature of 61.59°C with a desirability value of 0.616. In these conditions, the yield of pectin of 2.025% was very lower, when compared with banana peel AIS (8-20%). Concentration, extraction time, and temperature showed a statistically significant effect ($p < 0.05$) on pectin yield. The extracted pectin was categorized as high methoxyl pectin, exhibiting a DE of 53.49%, which is slightly lower than values typically reported for conventional sources. The degree of esterification remains within the acceptable range for HM pectin and contains Methoxyl content of 4.75% and Anhydrouronic acid of 50.45%. Our findings suggest that non-AIS *Musa acuminata* (Yelakki) peel potentially considered as a low-cost raw material for pectin production. Future studies may focus on enhancing pectin yield by using alternative extraction methods and further refining process parameters through optimization techniques using RSM, ANN or other statistical models.

Keywords: Citric acid, Non-AIS, RSM, Statistical modelling, Yelakki banana

Introduction

The fruit processing industry produces significant amounts of by-products, particularly peels and seeds, which are mainly used for low-value applications such as animal feed. These by-products contain a high level of pectin and can serve as an alternative for traditional citrus peel, which has been utilized for the large-scale production of pectin (May, 1990; Min *et al.*, 2011). Pectin consists of a complex group of polysaccharides found in plant cell walls, composed of four structural domains homogalacturonan (HG), xylogalacturonan, rhamnogalacturonan I (RG-I), and rhamnogalacturonan II (RG-II). HG represents the linear chain of α-1,4-linked galacturonic acid units that could be partially methyl-esterified or acetylated, and intervened by rhamnose units (Baum *et al.*, 2017). The amount of galacturonic acid of pectin influences its physicochemical properties (Sundarraj, Thottiam Vasudevan, & Sriramulu,

https://doi.org/10.22067/ifstrj.2026.96779.1526

2018). Several studies have explored pectin extraction from a wide range of plant-based residues, including pumpkin, soy hulls, peach pomace, sugar beet, *Cissampelos pareira* (Krueo Ma Noy), apple pomace, mango, Ambarella, banana peel, cocoa husks, citrus peel, jackfruit waste, and Saba banana peel, highlighting the global interest in valorizing agro-industrial by-products as alternative pectin sources (Khamsucharit, Laohaphatanalert, Gavinlertvatana, Sriroth, & Sangseethong, 2018).

Bananas are largely consumed as raw or processed into value-added products such as flour, chips, crackers, and purées. The peel accounts for approximately 30% of the overall weight of the fruit and causes an environmental concern due to nitrogen, phosphorus content and a significant amount of water, making them very susceptible to microbial degradation (Aklilu, 2021). In India, which ranks among the top banana-producing countries, local cultivars like *Musa acuminata* (Yelakki) are particularly prominent in the southern regions of India. A study estimates that global pectin consumption is expected to reach approximately 48,735 metric tonnes, growing at a compound annual growth rate (CAGR) of 3.7%, showing increasing demand across food, pharmaceutical, and industrial applications (Sundarraj *et al*., 2018).

There are different methods proposed by different scientists for the extraction of pectin, extraction providing an environmentally sustainable and non-corrosive alternative to conventional strong acids, with improved suitability for food and pharmaceutical applications (Vriesmann, Teófilo, & Lúcia de Oliveira Petkowicz, 2012). The influence of extraction parameters on pectin recovery from banana peel has been widely investigated, however, to the best of our knowledge, no prior studies have reported the extraction and optimization of pectin yield specifically from *Musa acuminata* (Yelakki) peel using non-AIS crude material. Citric acid and Response Surface Methodology (RSM) was employed to model and optimize this process under such conditions. In many reported studies, pectin extraction was performed on Alcohol Insoluble Solids (AIS), which involves pre-treatment of the plant sample with alcohol to remove soluble impurities and enhance purity (Broxterman & Schols, 2018). However, AIS preparation adds cost and solvent usage, whereas a non-AIS crude sample provides a simpler and more economical alternative, though linked to reduced yield and purity due to residual enzymes.

In the current research, Response Surface Methodology (RSM) was used to model and analyze the impacts of multiple variables, in order to optimize responses by developing multivariate regression equations based on experimental data. According to Giovanni (Giovanni, 1983), the advantage of RSM is related to its ability to reduce the number of experimental trials required to evaluate multiple parameters and their interactions efficiently. Pectin is recognized as a food additive and value-added substance by the Joint FAO/WHO Expert Committee. According to the European Commission standards, pectin with at least 65% galacturonic acid is required to meet the food additive pectin (Müller-Maatsch *et al*., 2016). The level of esterification (DE) greater than 50% classifies pectin as high methoxyl (HM), while a DE below 50% indicates low methoxyl (LM) pectin (Einhorn-Stoll, 2018).

The current study focuses on evaluating the extraction efficiency and quality of pectin obtained directly from non-AIS crude *Musa acuminata* (Yelakki) peel samples, to determine its potential for pectin recovery under such conditions. The RSM model was developed to predict the relationship between input factors and response variable. A Central Composite Design (CCD) was adopted to systematically understand both linear and non-linear interactions among variables, and to create a predictive polynomial model for response optimization. The model was analyzed statistically using the coefficient of determination R^2 and the coefficient of variation (CV) to determine its strength. As a

result, this research was carried out to investigate the impacts of extraction parameters, namely, temperature, extraction time, and citric acid concentration, on both the yield of extracted pectin from non-AIS *Musa acuminata* (Yelakki) peel, and to enhance these conditions through the use of Response Surface Methodology (RSM).

Materials and Methods

Raw Materials

This study utilized ripe banana peels of Yelakki (*Musa acuminata)* as the primary source for pectin extraction. The fruit was acquired from local markets in Bengaluru, India. The peels were removed, thoroughly washed with tap water, and the samples were subsequently rinsed once with distilled water and sliced into pieces using a knife. The peels were subsequently oven-dried at 50°C for 24 h under controlled conditions to reduce residual moisture prior to grinding. Although moisture content was not quantified separately, identical drying conditions were applied to all samples to ensure consistency. The dried samples were then ground into a powder using a grinder, passed through a 1.0 mm mesh sieve, and stored in a polyethylene zip-seal pouch at -20°C in a laboratory freezer until further analysis. Solid-state parameters including drying temperature, particle size (1.0 mm), and solid-liquid ratio (1:20, w/v), were maintained constant throughout all experiments to eliminate their influence on variability and to reflect optimization on chemical and thermal extraction variables.

Pectin Extraction

The method for extracting pectin was carried out following the procedures from Rasco´n-Chu et al. (Rascón-Chu *et al*., 2009) and P. Khamsucharit et al. (Khamsucharit *et al*., 2018) with slight modification. The process of extracting pectin from powdered banana peels was conducted based on the specified parameters of citric acid concentration, time, and temperature outlined in the experimental design. For citric acid-assisted extraction, the Non-AIS crude sample was mixed and suspended in the citric acid solution in a proportion of 1:20 (solid-liquid, w/v). The acidity of the extraction medium was defined by the specified citric acid concentration (%w/v) according to the experimental design, and pH was not independently adjusted during the extraction process. After that, the mixture was heated in a water bath at the specified time and temperature as in the design, and the solution was left to cool down to room temperature. The mixture was then filtered with a muslin cloth and centrifuged at 8000 rpm for 10 minutes. The supernatant was collected and filtered through a muslin cloth to remove the impurities. The filtrate was mixed in an equal volume of 95% ethanol, stirred for 5 minutes to mix and allowed to stand for 24 h at 4°C. The white precipitates were then collected by centrifuging at 6000 rpm for 10 minutes and washed 2–3 times with 95% ethanol. The product obtained was dried at 40 °C in a hot air oven until it reached a stable weight, after which it was ground and stored at 4°C. Pectin yield was calculated as follows:

$$\text{Pectin yield (\%)} = \frac{\text{Amount of extracted pectin (g)}}{\text{Amount of dried peel powder (g)}} \times 100 \quad (1)$$

Experimental Strategies and Statistical Methodology

RSM is a set of mathematical and statistical techniques to identify optimum conditions that leverage data from systematically designed experiments. A Central Composite Design (CCD) under Response Surface Methodology (RSM) was employed to evaluate the individual and interactive effects of three independent variables, namely citric acid concentration (1.5-8.5%), extraction time (30-90 min), and temperature (60-105°C), on pectin extraction efficiency (Table 1). The upper temperature limit (105°C) was selected considering the use of non-AIS sample, which retains native soluble fractions and structural components (Khamsucharit *et al.*, 2018). Elevated temperatures enhance acid-mediated protopectin solubilization, whereas excessive

heating induces pectin depolymerization (De Roeck, Mols, Duvetter, Van Loey, & Hendrickx, 2010). Therefore, the selected range enabled evaluation of both enhanced extraction and potential thermal effects within the CCD framework.

The experimental matrix consisted of 20 runs, allowing for determining the best combination of parameters for the pectin extraction process. The independent variables were considered based on E. G. Aklilu, with some modification (Aklilu, 2021).

CCD of the model involves 3 numeric factors, 14 points at non-center, and 6 points at center, with an alpha factor of 1.68179, was conducted using Design Expert version 22 software (Stat-Ease Inc., Minneapolis, USA, Free trial version). The correlation between the process variables and the response was modelled using a second-order polynomial regression equation suitable for a three-factor system.

$$Y = b_0 + b_1x_1 + b_2x_2 + b_3x_3 + b_{11}x_1^2 + b_{22}x_2^2 + b_{33}x_3^2 + b_{12}x_1x_2 + b_{13}x_1x_3 + b_{23}x_2x_3 \quad (2)$$

Where **Y** is the predicted response, b_0 is the intercept, b_1, b_2, and b_3 are the linear coefficients, b_{11}, b_{22}, and b_{33} are the quadratic coefficients and b_{12}, b_{13} and b_{23} are the coefficients for the interaction terms x_1, x_2, and x_3 are the coded independent variables. The actual values of the independent variables were converted to coded values using the following standard transformation equation:

$$x = \frac{X_{actual} - X_{center}}{\Delta} \quad (3)$$

Where x is the coded value, X_{actual} is the actual value of the variable, X_{center} is the midpoint of the independent variable, and Δ is half the range of the variable (i.e., $\frac{X_{high}-X_{low}}{2}$). This transformation standardizes the variables and optimizes effective comparison and model fitting in RSM.

Analysis of variance (ANOVA) was conducted using the square root (Linear regression) to assess the statistical relevance of the regression model. The model's quality and predictive reliability were evaluated utilizing the coefficient of determination (R^2), adjusted R^2, and the lack-of-fit test.

Table 1- Values of coded variables

S. No.	Factors	-1	+1	- α	+ α
1	Conc.	1.5	8.5	0.05	9.95
2	Time	30	90	17.57	102.43
3	Temperature	60	105	50.68	114.32

Determination of Equivalent Weight (EW)

The method outlined by Ranganna (Ranganna, 1986) was followed to determine the equivalent weight of the extracted pectin with minor modifications. Extracted pectin of 0.2 g was dispersed in 5 mL of ethanol in a 150 mL conical flask, and dissolved in 40 mL of carbon dioxide-free water. 0.5g of sodium chloride was added to the solution to sharpen the endpoint, and three drops of phenol red indicator were added. The mixture was subsequently subjected to rapid stirring to dissolve the pectin completely. Titration was done with 0.2N sodium hydroxide until a pink coloration, indicative of a pH of 7.5, was observed for 30 s. The neutralized titrate was further used to analyze the Methoxyl Content of pectin. EW was calculated using the equation:

$$\text{EW (g/mol)} = \frac{\text{Weight of pectin (g)} \times 1000}{\text{Vol. of NaOH} \times \text{N of NaOH}} \quad (4)$$

Determination of Methoxyl Content (MC)

MC of extracted pectin was assessed using Ranganna's method (Ranganna, 1986). To the neutralized mixture obtained from the determination of EW, 10 mL of 0.25 N sodium hydroxide was added, following thorough stirring, the mixture was left undisturbed for 30

min at room temperature. After that, 10 mL of 0.25 N hydrochloric acid was added and titrated to the same endpoint as before against 0.2 N sodium hydroxide. MC was calculated using the equation:

$$\text{MC}\ (\%) = \frac{\text{Vol. of NaOH} \times \text{N of NaOH} \times 31 \times 100}{\text{Weight of pectin (g)} \times 1000} \quad (5)$$

Where 31 corresponds to the molecular mass of the methoxyl group.

Determination of Anhydrouronic Acid Content (AUA)

The total AUA value of pectin was estimated using the titration readings from the determination of equivalent weight and methoxyl content. It was obtained following a formula reported by Mohamed and Hasan (Mohamed & Hasan, 1995) as follows:

$$\text{AUA}\ (\%) = \frac{176 \times (0.2)\, z \times 100}{w \times 1000} + \frac{176 \times (0.2)\, y \times 100}{w \times 1000} \quad (6)$$

Where Molecular unit of AUA = 176, the Normality of sodium hydroxide = 0.2, z = mL (titre) of NaOH from EW determination, y = mL (titre) of NaOH from MC determination, w = weight of pectin.

Determination of Degree of Esterification (DE)

The DE of pectin was calculated following a formula reported previously by Lal et al. (Lal *et al*., 2021).

$$\text{DE}\ (\%) = \frac{176 \times \text{MC} \times 100}{31 \times \text{AUA}} \quad (7)$$

Fourier Transform Infrared Spectroscopy (FTIR)

The structural characteristics of Yelakki banana peel pectin, extracted under optimized conditions, were investigated using an FTIR Spectrometer. The pectin samples were kept in a hot air oven to remove moisture and processed into powder. The spectra were recorded within the wavelength range of 4000-400 cm^{-1}, and the resolution was measured at 4 cm^{-1} (Chua, Tang, Ali, & Chow, 2020). The FTIR spectra were analyzed to determine the surface functional groups present on the pectin. The spectra were designed using Origin Pro software (Version 10.25).

Scanning Electron Microscope (SEM)

To examine the morphological structure and elements of the extracted pectin under optimized conditions, SEM was used in conjunction with EDX. The pectin samples were mounted on double-sided carbon tape, secured onto a metal support, and subsequently coated with chromium using a sputter coater and then spotted under a Scanning Electron Microscope (Joel-JSM 6701-F). EDX was analyzed using Hitachi SU6600 FE-SEM. The SEM imaging was performed across a magnification range of 1000 to 35000X, utilizing an accelerating 2 kV voltage (Coimbra *et al*., 2011).

Results and Discussion

Extraction

Citric acid-assisted extraction of pectin from Yelakki banana peel powder (Non-AIS) yielded a range varied from 0.3% to 4.3% on a dry weight basis under various experimentally designed conditions. To elucidate the effects of several experimental factors on these responses within an experimental design, Response Surface Methodology (RSM) was adopted and utilized.

Temperature exhibited a significant influence on pectin recovery. Increasing temperature enhanced extraction efficiency up to an optimum level (82°C) (Chen *et al*., 2021), likely due to improved diffusional transport and enhanced acid-mediated protopectin solubilization. The use of non-AIS sample in the present study may have contributed to this behavior, as the material retains native soluble fractions and structural components unlike AIS-pretreated cell wall residues. The preserved matrix structure can influence mass transfer dynamics during extraction. However, a decline in yield at higher temperatures suggests possible thermally induced depolymerization. The thermal susceptibility of pectin is known to depend on intrinsic structural characteristics such as degree of methylation

(DM) (Fraeye *et al*., 2007), and individual chains may exhibit varying stability under elevated temperature.

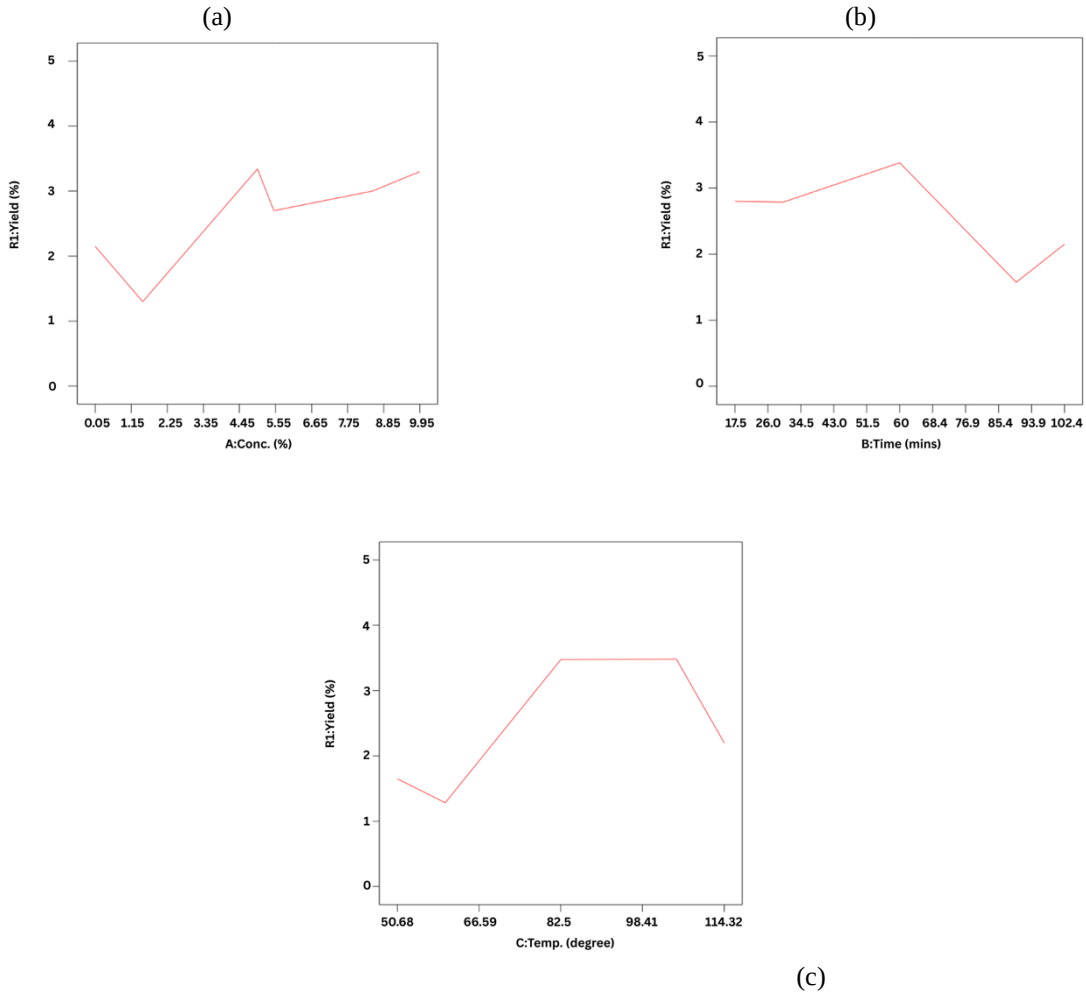

Fig. 1. Effect of citric acid concentration on pectin yield (a), effect of extraction time on pectin yield (b) and effect of temperature on pectin yield (c)

Table 2- Central composite design matrix and experimental yields

Run	Conc.	Time	Temp.	Response	Transformed Sqrt Actual value	Transformed Sqrt Predicted value
1	5	60	114.32	2.2	1.48	1.44
2	5	60	50.68	1.65	1.28	1.31
3	5	102.43	82.5	2.15	1.47	1.42
4	5	60	82.5	3.9	1.97	1.98
5	5	60	82.5	4.15	2.04	1.98
6	1.5	90	105	2.3	1.52	1.57
7	5	60	82.5	3.6	1.90	1.98
8	5.5	30	60	2.7	1.64	1.56
9	0.05	60	82.5	2.15	1.47	1.40
10	1.5	30	60	0.3	0.5477	0.5928
11	8.5	30	105	3.9	1.97	2.02
12	5	60	82.5	3.55	1.88	1.98

13	8.5	30	105	4.25	2.06	2.02
14	5	60	82.5	4.3	2.07	1.98
15	8.5	90	60	0.85	0.9220	0.9319
16	5	60	82.5	3.85	1.96	1.98
17	5	60	82.5	3.95	1.99	1.98
18	5	17.57	82.5	2.8	1.67	1.70
19	5	60	82.5	4	2.00	1.98
20	9.95	60	82.5	3.3	1.82	1.82

Preliminary Data Analysis and Experimental Observations

Following the execution of the Central Composite Design (CCD), a preliminary graphical evaluation of the non-transformed experimental data was performed to understand the underlying interactions among the independent variables concerning the pectin yield response prior to statistical modelling.

The observed pectin yield values across the 20 experimental runs ranged from 0.3% to 4.3% (Table 2). The pectin yield (%) (Fig. 1) presented a nonlinear relationship with rising concentration of citric acid. A decrease in yield was observed initially, followed by a progressive increase, suggesting that moderate to higher concentrations (above ~2.0%) enhance pectin extraction, with the maximum yield at ~5%. This suggests that sufficient acid strength facilitates efficient extraction of pectin. Extraction time (Fig. 1) demonstrated a nonlinear effect on pectin yield. The yield increased moderately up to 60 minutes but declined beyond 70 minutes, possibly resulting from thermal degradation of pectin. Yield (Fig. 1) increased with rising temperature up to ~82.5°C and stabilized between 82.5°C and ~101°C, beyond which a decline was observed. This pattern suggests that elevated temperatures enhance extraction efficiency up to a point; above this threshold, thermal degradation may reduce pectin integrity.

RSM Model Fitting

The statistical analyzes reveal that the quadratic model developed for the pectin yield is highly significant. A smaller p-value and a higher F-value indicate a more significant contribution from the corresponding coefficient in statistical modelling. The results of ANOVA (Table 3) showed that the developed quadratic regression model for pectin yield is highly significant, F-value = 63.94, ($p < 0.0001$); an F-value this large could only be the result of noise in 0.01% of occurrences. This extremely low p-value ($p < 0.0001$) implies that the developed model effectively explains the variability in pectin yield and is statistically significant beyond random chance. The quadratic model showed a statistically insignificant "Lack of Fit" (F-value = 2.63, p-value = 0.1327), relative to pure error. There is a 13.27% chance that a Lack of Fit F-value this large could occur due to noise. Thus, the developed regression model (Eqn. 8) demonstrated adequate predictive capability for pectin yield within the experimental domain, validating their effectiveness in representing the process dynamics over the investigated range of variables. The analysis shows that for pectin yield, A, B, AB, A^2, B^2, and C^2 were found to significantly influence the pectin yield, while C, AC, and BC did not significantly influence the pectin yield (Table 3).

The model's goodness-of-fit (Table 4) showed a strong coefficient of determination (R^2) of 0.9829 and an adjusted R^2 of 0.9675. These values suggest that approximately 98.3% of the total variability in the pectin yield can be linked to the fitted model, reflecting a satisfactory degree of model adequacy for the experimental data. The predicted R^2 of 0.7824 is in reasonable agreement with the Adjusted R^2 (difference < 0.2) as suggested by (Owolabi, Usman, & Kehinde, 2018), further confirming the good predictive potential of the model. An Adeq Precision value of 27.5 (Adeq Precision > 4) also validated the capacity of the model to navigate the design space effectively with a strong signal-to-noise ratio. The Coefficient of Variation (C.V.%) and standard

deviation (Table 4) were reasonably acceptable values for complex experimental systems, indicating good reliability and precision of the experimental data.

Table 3- ANOVA for the response surface quadratic model of pectin yield

Source	Sum of Squares	df	Mean Square	F-value	p-value	
Model	3.10	9	0.3448	63.94	< 0.0001	significant
A-Conc	0.1006	1	0.1006	18.65	0.0015	
B-Time	0.0433	1	0.0433	8.03	0.0178	
C-Temp.	0.0102	1	0.0102	1.89	0.1998	
AB	0.5308	1	0.5308	98.43	< 0.0001	
AC	0.0111	1	0.0111	2.05	0.1823	
BC	0.0070	1	0.0070	1.30	0.2806	
A^2	0.3001	1	0.3001	55.65	< 0.0001	
B^2	0.3918	1	0.3918	72.65	< 0.0001	
C^2	0.8099	1	0.8099	150.19	< 0.0001	
Residual	0.0539	10	0.0054			
Lack of Fit	0.0214	2	0.0107	2.63	0.1327	not significant
Pure Error	0.0325	8	0.0041			
Cor Total	3.16	19				

Table 4- Regression coefficients of the predicted second-order model

S.No.	Response Parameter	Values
1	Std. Dev.	0.0734
2	Mean	1.68
3	C.V. %	4.36
4	R^2	0.9829
5	Adjusted R^2	0.9675
6	Predicted R^2	0.7824
7	Adeq Precision	27.5458

Development of a Regression Model Equation

The regression model equation governing pectin yield was systematically constructed based on experimental data acquired through a Central Composite Design (CCD) under Response Surface Methodology (RSM). A second-order polynomial equation (2) was employed to capture the linear, interaction, and quadratic effects of the independent variables concentration, extraction time, and temperature on pectin yield. The final regression equation, formulated in terms of coded factors whose values are provided in the supplementary material and structured to retain model hierarchy, is presented below

$$\begin{aligned} Y = 1.98 &+ 0.1473x_1 - 0.0966x_2 \\ &+ 0.0468x_3 \\ &- 0.1866x^2{}_1 \\ &- 0.2123x^2{}_2 \\ &- 0.3053x^2{}_3 \\ &- 0.4711x_1x_2 \\ &- 0.0689x_1x_3 \\ &- 0.0499x_2x_3 \end{aligned} \quad (8)$$

In this model, positive coefficients indicate synergistic effects, whereas negative coefficients denote antagonistic effects on pectin yield. To further interpret the response surface geometry, the stationary point of the fitted second-order quadratic model was determined by equating the first-order partial derivatives of Eqn. 8 to zero in coded space. The stationary coordinates were obtained at x_1= 0.013, x_2= -0.104, and x_3= 0.102, which correspond in real units to 5.05% citric acid concentration, 56.9 min extraction time, and 84.8°C. Substitution of these values into the

regression equation predicted a pectin yield of 3.82%. Since all quadratic coefficients in the model are negative, the stationary point corresponds to a local maximum within the experimental domain. This mathematical maximum reflects the curvature of the fitted surface and is distinct from the numerically optimized solution obtained through desirability analysis.

The residuals versus predicted plot (Fig. 2) was evaluated to examine the assumptions of homoscedasticity and model adequacy. The externally studentized residuals exhibit a random distribution around the horizontal axis, with no discernible curvature, showing constant variance over the range of predicted values. This randomness supports the assumption of homoscedasticity. Moreover, all the residuals fell well within the critical bounds (±4.14579), confirming the absence of outliers. The result aligns with findings reported in similar studies (Pinheiro *et al.*, 2008).

The predicted versus actual response plot (Fig. 2) for square root-transformed yield values revealed a strong linear relationship, where all the data points were closely distributed along the 45° reference line. This indicates that the developed model is appropriate for accurately predicting pectin yield. The graphical alignment of experimental and predicted values further confirms the predictive reliability model. Similar findings have been reported in previous studies (Sundarraj *et al.*, 2018).

(a) (b)

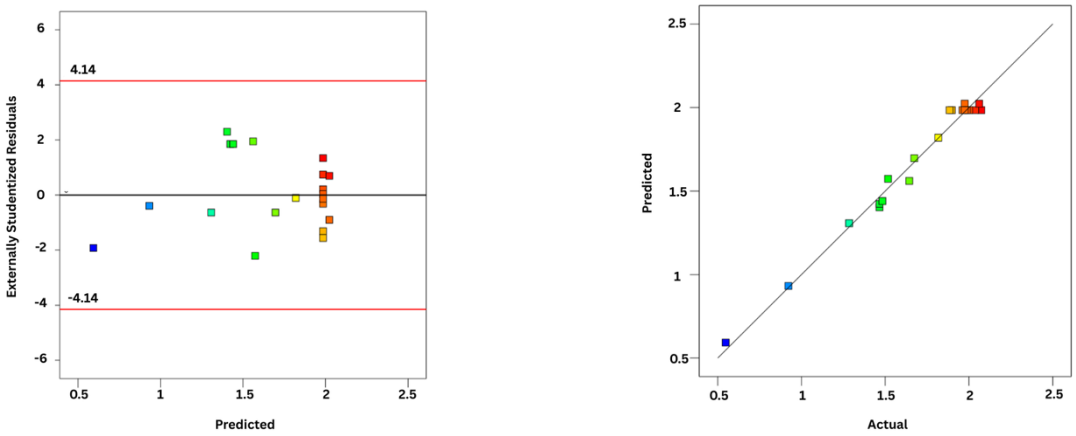

Fig. 2. Residuals versus Predicted (a) and Predicted versus Actual value (b)

Contour and Three-dimensional (3D) Response Surface Plot

To elucidate the effects of extraction parameters on pectin yield, two-dimensional contour and three-dimensional surface plots were constructed using the final regression model, Eqn. (8). Fig. 3 illustrates the contour and 3D surface plots of the effect of concentration and extraction time on pectin yield, with temperature held constant at its center point of 82.5 °C.

The contour plot (a) shows an elliptical pattern, indicating a significant interaction between concentration and time. As the concentration increased, pectin yield was improved consistently, especially at intermediate time durations. This is further supported by the corresponding 3D response surface plots (b). These results align well with previous studies (Pandit, Vijayanand, & Kulkarni, 2015; Vriesmann *et al.*, 2012).

(a) (b)

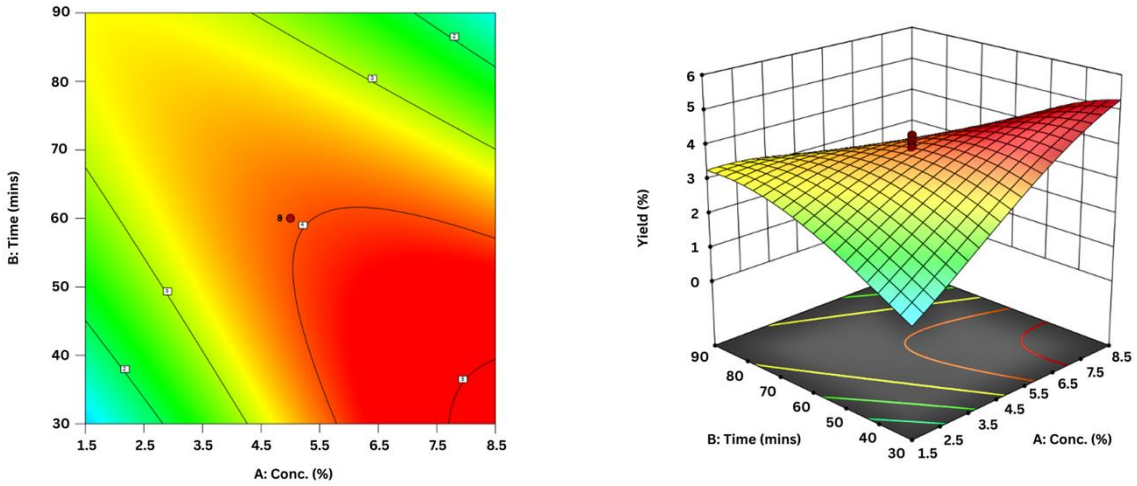

Fig. 3. Contour plot (a) and 3D response surface plot (b)

Analysis of Pectin Yield in Relation to Non-AIS Sample Preparation

The pectin yield obtained in the current research ranged from **0.3% to 4.3%**, which is within the lower to moderate range reported in the previous studies for banana peel and other fruit sources. Happi Emaga et al. (Happi Emaga, Ronkart, Robert, Wathelet, & Paquot, 2008) reported pectin yields from banana peel ranging from 2.4% to 21.7%, depending on the cultivar, pretreatment, and extraction conditions. Similarly, Oliveira et al. (Oliveira *et al.*, 2016) reported pectin yields ranging from 5.2% to 12.2% using citric acid extraction on AIS (Alcohol Insoluble Solids) banana peel samples, and another study (Maneerat, Tangsuphoom, & Nitithamyong, 2017) observed 7% to 11% of yield under optimized acid extraction conditions.

Notably, AIS-based extraction from unripe banana cultivars has demonstrated substantially higher yields. For instance, citric acid extraction of AIS-pretreated unripe banana peels resulted in yields ranging from 10.91% to 24.08%, with the highest yield reported for Kluai Leb Mu Nang (24.08%) (Khamsucharit *et al.*, 2018). Previous studies have indicated that pectin yield decreases with increasing fruit maturation (Azad, Ali, Akter, Rahman, & Ahmed, 2014); Castillo-Israel et al. (Castillo-Israel, Diasanta, Lizardo, Dizon, & Mejico, 2015) reported that unripe Saba banana peel yielded 16.54% pectin, whereas ripe peel yielded 11.87%. In the present study, ripe Yelakki banana peel was employed, which may partially explain the lower recovery efficiency observed relative to AIS unripe materials.

The lower yield in the current investigation can therefore be attributed to two primary factors: the use of non-AIS crude peel powder and the use of ripe fruit material. AIS preparation enriches the alcohol-insoluble cell wall fraction by removing soluble sugars, organic acids, pigments, and low-molecular-weight compounds, thereby increasing the relative concentration of protopectin in the matrix. In contrast, non-AIS material retains these soluble constituents, resulting in a diluted matrix and reduced apparent recovery on a dry weight basis. Furthermore, extraction efficiency is strongly influenced by temperature and acidity; previous studies have demonstrated that increased temperature and lower pH enhance pectin solubilization, although excessively harsh conditions may promote structural degradation. Residual enzymatic activity reported in untreated plant tissues (Broxterman & Schols, 2018) could also contribute to structural modification of pectin, thereby affecting recovery efficiency.

Despite the reduced yield, the observed values are consistent with other studies

Husnawati *et al*. **(**Husnawati, Astutik, & Ambarsari, 2020**)** reported banana peel pectin yields ranging from 1.92% to 3.68%, and *Durio zibethinus* peel has been shown to yield 2.27% - 9.35% pectin (Wai, Alkarkhi, & Easa, 2009). Extraction of pectin from passion fruit peels was also comparable, ranging from 2.25% to 14.60% (Liew, Chin, & Yusof, 2014), depending on acid strength and extraction time. Current findings are in reasonable agreement with published data for the non-AIS sample and demonstrate the feasibility of pectin recovery from crude materials, potentially representing a simplified processing alternative.

Validation of the Optimized Condition

Pectin extraction from non-AIS banana peel using citric acid was optimized using RSM in Design Expert version 22, applying numerical optimization to define the optimal levels of process variables. The optimization was based on statistically defined criteria for each independent variable and the response to identify process conditions that maximize pectin yield. Experimental validation was performed in duplicate under the model-predicted optimal conditions to confirm the statistical design approach.

To verify the stability and predictive accuracy of the model, a numerical optimization module was applied to generate 55 potential solutions based on their higher desirability values. Among these solutions, the condition that had the highest desirability (0.616) was selected as the optimal condition for experimental validation. Although the overall desirability value (0.616) was moderate, it reflects optimization strictly confined within the statistically validated boundaries of the Central Composite Design without extrapolation beyond coded factor limits. Given that only pectin yield was maximized within predefined experimental constraints, the obtained desirability represents the highest model-supported solution permitted by the quadratic response surface rather than an unconstrained theoretical maximum.

The optimal condition corresponding to 1.5% concentration, 90 min extraction time, and a temperature of 62 °C, with a higher predicted pectin yield of 2.219%. The experimental result was found to be 2.025% with a small difference from the predicted value, indicating strong correlation between them, which confirmed the validity of the model. The selected optimum corresponds to the highest composite desirability predicted by the fitted quadratic model within the experimental design space.

Physicochemical Characterization of Pectin

The physicochemical characterization of pectin was conducted under the model-optimized extraction conditions. The equivalent weight of extracted pectin from a non-AIS banana peel sample was determined to be 750.91 g/mol (Table 5), which was higher than the values reported for apple pomace (551g/mol) and citrus peel (577g/mol) but comparatively lower than pectin derived from other varieties of banana peels (943-1456 g/mol) (May, 1990). Methoxyl content of the extracted pectin was found to be 4.75% (Table 5), which is similar to the different varieties of banana peel (3.86%-5.97%) (May, 1990), but lower than citrus peel (9.06%) and apple pomace (7.92%).

The purity of pectin is determined by its total anhydrouronic acid (AUA) content, which, according to Food Chemical Codex (Kamble *et al*., 2017), should be at least 65% to be used as a food additive or for pharmaceutical purposes. In the current study, the Anhydrouronic acid content (AUA) of extracted pectin was found to be 50.45% (Table 5), this value is comparable to those reported for pectin extracted from various banana peel cultivars (34.56–66.67%) and Saba banana peel pectins 39.68 to 57.32% (Castillo-Israel *et al*., 2015), it remains below the threshold required for food or pharmaceutical use, while it is lower than the values observed for citrus peel and apple pomace (Aklilu, 2021; Khamsucharit *et al*., 2018). This limitation highlights the impact of raw material on the purity of the recovered

pectin and restricts its application in the food and pharma industry.

However, although the AUA content does not satisfy Food Chemical Codex specifications for direct food or pharmaceutical additive applications, pectin with moderate purity has been extensively reported for functional material applications where regulatory purity thresholds are not mandatory. Pectin-based biopolymer systems have demonstrated considerable potential in active and biodegradable packaging due to their film-forming capacity, barrier properties, and ability to retard lipid oxidation and microbial proliferation (Huang *et al*., 2021), and utilized in films, paper substitutes, foams, cosmetics and plasticizer formulations (Biswal, 2024; Thakur, Singh, & Handa, 1997). In addition, the presence of a carboxyl functional group enables effective coordination interactions with metal ions, supporting its application as a biosorbent for heavy metal remediation (Martínez-Sabando, Coin, Melillo, Goyanes, & Cerveny, 2023). Furthermore, pectin extracted from agro-industrial residues has been investigated for bioplastic synthesis and composite material development (Listyarini, Susilawati, Nukung, & Yua, 2020). Therefore, despite not fulfilling FCC purity requirements, the extracted pectin remains technically suitable for value-added non-food applications within sustainable biomaterials.

The degree of esterification classifies pectin as high methoxyl (HM, DE > 50%) and low methoxyl (LM, DE < 50%) (Mesbahi, Jamalian, & Farahnaky, 2005). The Degree of Esterification of extracted pectin was found to be 53.49% (Table 5), indicating that the extracted pectins were classified as high-methoxyl pectin. The observed DE value was lower than previously reported for citrus peel (62.83%) but comparable to apple pomace (58.44%), likely as a result of the depolymerization of pectin, which reduces the DE (Khamsucharit *et al.*, 2018) (Kumari, Singh, & Chauhan, 2023).

Table 5- Physicochemical charaterization of extracted pectin

Parameters	Values
Equivalent Weight	750.91 ± 31.76 g/mol
Methoxyl Content	4.75 ± 0.18%
Anhydrouronic Acid	50.45 ± 1.02%
Degree of Esterification	53.49 ± 1.73%

FTIR Analysis of Pectin

The chemical structure of the extracted pectin was characterized by FTIR to confirm its properties and to evaluate the impact of the extraction process on its functional groups, as presented in Fig. 4. The spectral region between 950 and 1200 cm^{-1} is considered as the carbohydrate fingerprint region, allows to identify key functional groups present within the polysaccharides (Fissore, Rojas, & Gerschenson, 2012).

Moisture content in pectin causes a broad absorption band between 3600-3000 cm^{-1}, due to stretching of the hydroxyl groups (O-H) associated with intra- and intermolecular hydrogen bonding within galacturonic acid in the pectin. Absorption bands in the 3000-2900 cm^{-1} region are attributed to aliphatic C-H stretching vibrations (Santos *et al.*, 2020). Although methoxy ($O-CH_3$) stretching within this region may theoretically enable differentiation between low- and high-methoxyl pectins, its diagnostic utility is limited due to overlap with the broad and intense O-H stretching band, which obscures the comparatively weaker methoxyl signals (Gnanasambandam, 2000).

The absorption band at 1760-1725 cm^{-1} was attributed to the stretching vibration of esterified carbonyl groups (C=O), and 1630-1600 cm^{-1} was attributed to carboxyl groups (COO^-). The carbonyl band at 1730cm^{-1} may be contributed from both methyl and acetyl ester groups; however, FTIR does not enable definitive discrimination between these functionalities due to spectral overlap. Hence,

the degree of acetylation was not quantified in the present study. Absorption bands in the 1220-1011 cm^{-1} region correspond to C–O–C stretching vibrations associated with glycosidic rings in the pectin (Khamsucharit *et al*., 2018; Kumari *et al*., 2023). High-degree esterified pectins are characterized by relatively greater intensity of the ester carbonyl (C=O) stretching band near (~1753 cm^{-1}) and comparatively reduced intensity of the carboxylate (COO^-) asymmetric stretching band near (~1640 cm^{-1}), whereas low-degree esterified pectins exhibit the inverse spectral profile (Fellah, Anjukandi, Waterland, & Williams, 2009; Santos *et al*., 2020).

In the present study (Fig. 4), a weak absorption band was observed at ~1730cm^{-1}, corresponding to esterified carbonyl stretching, while a comparatively more intense band was observed at ~1618 cm^{-1}, attributable to the asymmetric stretching of carboxylate groups. Although the carboxylate band appeared dominant, the titrimetric determination yielded a degree of esterification (DE) of 53.49 ± 1.73%, confirming its classification as high-degree esterified (HDE) pectin. This apparent spectral discrepancy may be attributed to the borderline nature of the carboxylate ion compared to the ester carbonyl. Furthermore, the intensity of the ~1618 cm^{-1} region can be influenced by residual moisture (O-H bending) or the ionization state of the pectin backbone (Fellah *et al*., 2009; Manrique & Lajolo, 2002). Consequently, when interpreted alongside chemical quantification, these spectral characteristics remain consistent with an HDE classification.

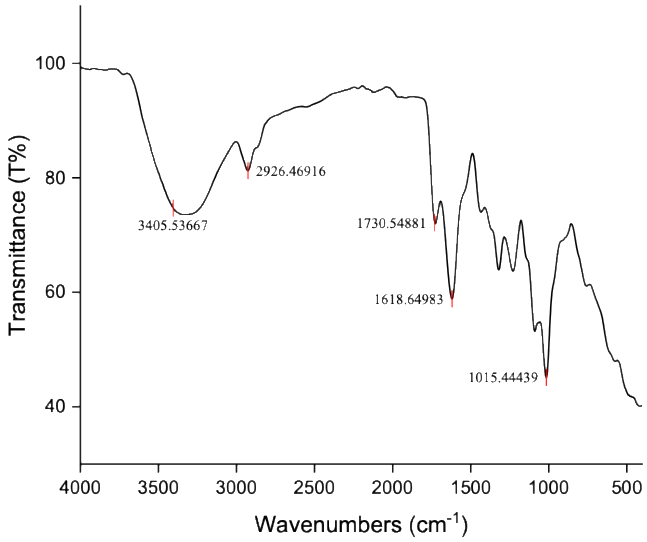

Fig. 4. FTIR analysis

(a)

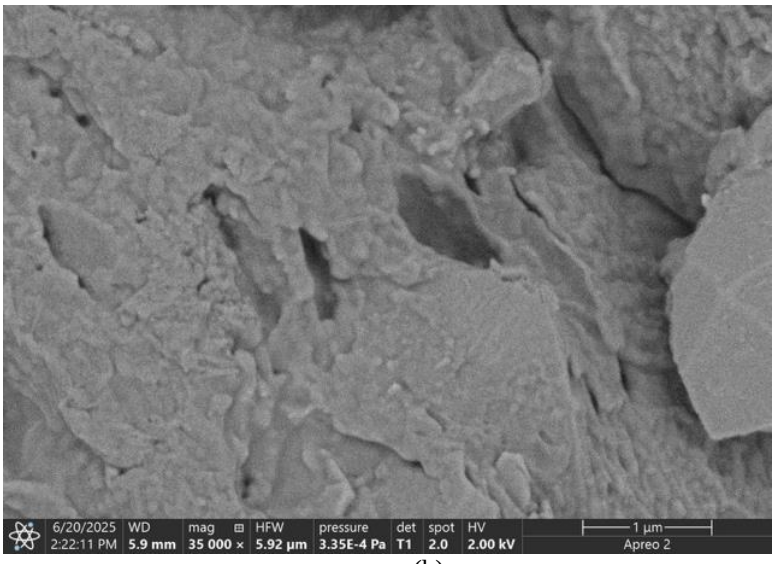

(b)

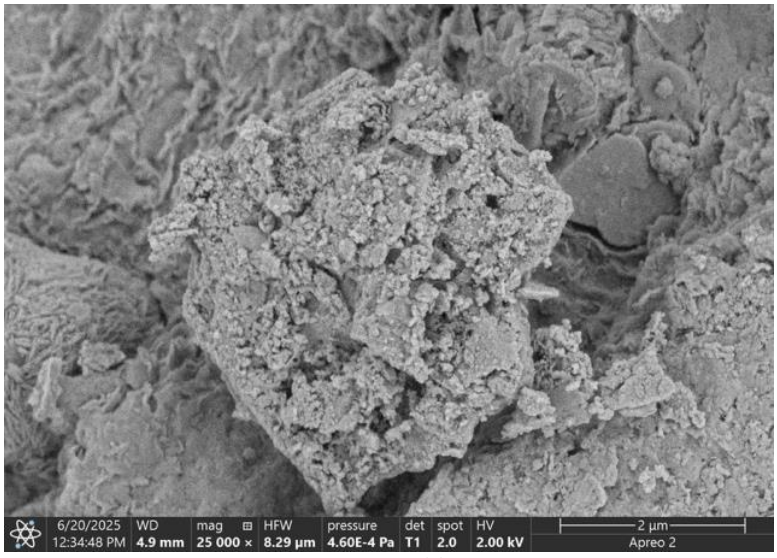

(c)

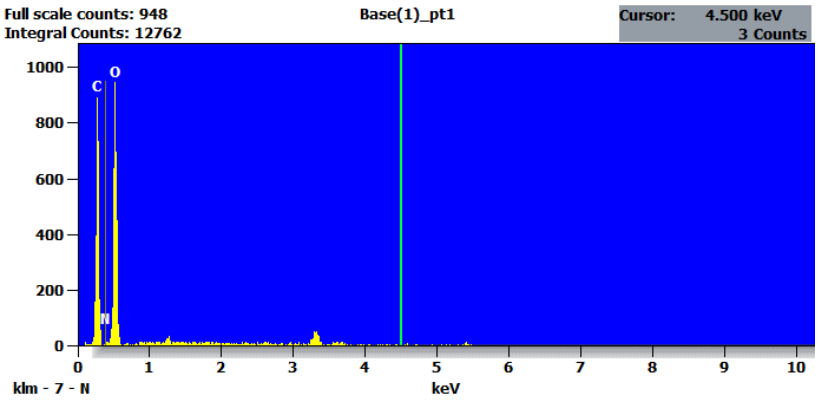

Element	Wt%
C	23.65
N	7.30
O	69.05

Fig. 5. SEM image of pectin at 35000x magnification (Scale bar-1 µm) (a), SEM image of pectin at 25000x magnification (Scale bar-2 µm) (b) and EDX spectrum (c)

Scanning Electron Microscopy

SEM micrographs (Fig. 5) of the pectin revealed uneven, compact, and irregularly aggregated particles with rough surfaces and porous microstructures, which are flaky, and this may be due to the high proportion of neutral sugar side chains in the pectin structure (Kumari *et al.*, 2023). Pectin obtained from apple waste by ultrasound-assisted extraction exhibited a compact, flaky, and rigid surface morphology, reported by Mahmoud et al. (Mahmoud, Abu-Salem, & Azab, 2022). Another investigation by Jiang et al. (Jiang *et al.*, 2012) on pectin also reported uneven and abrasive surface morphologies, highlighting the structural heterogeneity of plant-derived pectin. Chemical composition of the pectin was analyzed using Energy-Dispersive X-ray spectroscopy (EDX). The spectrum (Fig. 5) revealed the presence of elements such as carbon (C), oxygen (O), and minor traces of nitrogen (N), which are typical of polysaccharide structures.

Conclusion

The present study utilized Response Surface Methodology (RSM) to model and optimize the citric acid-assisted extraction of pectin from non-AIS *Musa acuminata* peel (Yelakki) indigenous to Karnataka. The study revealed that linear terms (A and B), their interaction (AB), and the quadratic terms (A^2, B^2, and C^2) significantly influence pectin yield, while other interaction effects were statistically non-significant. The RSM model showed strong predictive performance, which is supported by a high R^2 value, low CV, and adequate precision, indicating good model fit and a sufficient signal-to-noise ratio. The optimum condition of the pectin yield was achieved at conc., extraction time, and temp. of 1.5%, 90miin and 62°C respectively, with the desirability of 0.616 was 2.025%. In accordance with the determined DE value, the extracted pectin was categorized as high methoxyl pectin. The observed value of AUA was lower than the criteria for use as a food and pharmaceutical additive. Future studies may explore advanced extraction techniques such as enzymatic, microwave or ultrasound-assisted methods to enhance the AUA content of pectin extracted from *Musa acuminata* (Yelakki) peel and improve its applications in food and pharmaceutical formulations.

Abbreviations

CAE: Citric Acid-Assisted Extraction; Non-AIS: Non-Alcohol Insoluble Solids; RSM: Response Surface Method; CCD: Central Composite Design; EW: Equivalent Weight; MC: Methoxyl Content; AUA: Anhydrouronic acid; DE: Degree of Esterification; FTIR: Fourier transform infrared spectroscopy; SEM: Scanning Electron Microscope

Acknowlegement

We are very grateful to the Department of Life Sciences, Christ University, Bengaluru, for providing all the infrastructure and facilities to carry out this project.

Funding

The authors thank Christ University, Bangaluru, for the seed money project no. CU-ORS-SM-24/26

Data availability

The datasets obtained during the current study are available from the corresponding author on reasonable request. All the data analysed during this study are included in this research article and supplementary materials.

Declarations

Consent to Publish

Not applicable

Consent to Participate

Not applicable

Ethics declaration

Not applicable

Clinical Trial Registration

This study doesn't involve any clinical trial

Author Contribution

E.J.B. conducted the research, data collection, performed the statistical analysis and wrote the manuscript. **U.S.K.** Experimental design, formulated, and reviewed the manuscript.

Reference

1. Aklilu, E.G. (2021). Modeling and optimization of pectin extraction from banana peel using artificial neural networks (ANNs) and response surface methodology (RSM). *Journal of Food Measurement & Characterization*, *15*(3), 2759–2773. https://doi.org/10.1007/s11694-021-00852-7
2. Azad, A., Ali, M.A., Akter, M.S., Rahman, M.J., & Ahmed, M. (2014). Iso- lation and characterization of pectin extracted from lemon pomace during ripening. *Journal Food Nutrent Science*, *2*, 30–35. https://doi.org/10.11648/j.jfns.20140202.12
3. Baum, A., Dominiak, M., Vidal-Melgosa, S., Willats, W.G.T., Søndergaard, K.M., Hansen, P.W., Meyer, A.S., & Mikkelsen, J.D. (2017). Prediction of pectin yield and quality by FTIR and carbohydrate microarray analysis. *Food and Bioprocess Technology*, *10*(1), 143–154. https://doi.org/10.1007/s11947-016-1802-2
4. Biswal, T. (2024). Pectin-based biocomposite materials for biomedical and cosmetic applications. In *Biopolymers in Pharmaceutical and Food Applications* (pp. 471–495). Wiley. https://doi.org/10.1002/9783527848133.ch22
5. Broxterman, S.E., & Schols, H.A. (2018). Interactions between pectin and cellulose in primary plant cell walls. *Carbohydrate Polymers*, *192*, 263–272. https://doi.org/10.1016/j.carbpol.2018.03.070
6. Castillo-Israel, K., Diasanta, S.F., Lizardo, M., Dizon, R., & Mejico, M. (2015). Extraction and characterization of pectin from Saba banana [Musa 'saba' (*Musa acuminata* x *Musa balbisiana*)] peel wastes: A preliminary study. *International Food Research Journal*, *22*(1), 202–207. https://doi.org/10.26656/fr.2017.6(2).182
7. Chen, J., Cheng, H., Zhi, Z., Zhang, H., Linhardt, R.J., Zhang, F., Chen, S., & Ye, X. (2021). Extraction temperature is a decisive factor for the properties of pectin. *Food Hydrocolloids*, *112*(106160), 106160. https://doi.org/10.1016/j.foodhyd.2020.106160
8. Chua, B.L., Tang, S.F., Ali, A., & Chow, Y.H. (2020). Optimisation of pectin production from dragon fruit peels waste: drying, extraction and characterisation studies. *SN Applied Sciences*, *2*(4). https://doi.org/10.1007/s42452-020-2415-y
9. Coimbra, P., Ferreira, P., de Sousa, H.C., Batista, P., Rodrigues, M.A., Correia, I.J., & Gil, M.H. (2011). Preparation and chemical and biological characterization of a pectin/chitosan polyelectrolyte complex scaffold for possible bone tissue engineering applications. *International Journal of Biological Macromolecules*, *48*(1), 112–118. https://doi.org/10.1016/j.ijbiomac.2010.10.006
10. De Roeck, A., Mols, J., Duvetter, T., Van Loey, A., & Hendrickx, M. (2010). Carrot texture degradation kinetics and pectin changes during thermal versus high-pressure/high-temperature processing: A comparative study. *Food Chemistry*, *120*(4), 1104–1112. https://doi.org/10.1016/j.foodchem.2009.11.060
11. Einhorn-Stoll, U. (2018). Pectin-water interactions in foods– From powder to gel. *Food Hydrocolloids*, *78*, 109–119. https://doi.org/10.1016/j.foodhyd.2017.05.029
12. Fellah, A., Anjukandi, P., Waterland, M.R., & Williams, M.A.K. (2009). Determining the degree of methylesterification of pectin by ATR/FT-IR: Methodology optimisation and comparison with

theoretical calculations. *Carbohydrate Polymers*, *78*(4), 847–853. https://doi.org/10.1016/j.carbpol.2009.07.003

13. Fissore, E.N., Rojas, A.M., & Gerschenson, L.N. (2012). Rheological performance of pectin-enriched products isolated from red beet (*Beta vulgaris* L. var. conditiva) through alkaline and enzymatic treatments. *Food Hydrocolloids*, *26*(1), 249–260. https://doi.org/10.1016/j.foodhyd.2011.06.004
14. Fraeye, I., Deroeck, A., Duvetter, T., Verlent, I., Hendrickx, M., & Vanloey, A. (2007). Influence of pectin properties and processing conditions on thermal pectin degradation. *Food Chemistry*, *105*(2), 555–563. https://doi.org/10.1016/j.foodchem.2007.04.009
15. Giovanni, M. (1983). Response Surface Methodology and product Optimization. *Food Technology*, *37*, 41–45.
16. Gnanasambandam, R. (2000). Determination of pectin degree of esterification by diffuse reflectance Fourier transform infrared spectroscopy. *Food Chemistry*, *68*(3), 327–332. https://doi.org/10.1016/s0308-8146(99)00191-0
17. Happi Emaga, T., Ronkart, S.N., Robert, C., Wathelet, B., & Paquot, M. (2008). Characterisation of pectins extracted from banana peels (Musa AAA) under different conditions using an experimental design. *Food Chemistry*, *108*(2), 463–471. https://doi.org/10.1016/j.foodchem.2007.10.078
18. Huang, J., Hu, Z., Hu, L., Li, G., Yao, Q., & Hu, Y. (2021). Pectin-based active packaging: A critical review on preparation, physical properties and novel application in food preservation. *Trends in Food Science & Technology*, *118*, 167–178. https://doi.org/10.1016/j.tifs.2021.09.026
19. Husnawati, Astutik, I.Y., & Ambarsari, L. (2020). Characterization and bioactivity test of pectin from *Musa balbisiana* peel extracted using various acid solvents. *Current Biochemistry*, *6*(1). https://doi.org/10.29244/cb.6.1.1
20. Jiang, Y., Du, Y., Zhu, X., Xiong, H., Woo, M.W., & Hu, J. (2012). Physicochemical and comparative properties of pectins extracted from Akebia trifoliata var. australis peel. *Carbohydrate Polymers*, *87*(2), 1663–1669. https://doi.org/10.1016/j.carbpol.2011.09.064
21. Kamble, P.B., Gawande, S., Patil, T.S., Kamble, P.B., Gawande, S., & Patil, T.S. (2017). Extraction of pectin from unripe banana peel. *International Research Journal of Engineering and Technology*, *4*(7), 2259–2264.
22. Khamsucharit, P., Laohaphatanalert, K., Gavinlertvatana, P., Sriroth, K., & Sangseethong, K. (2018). Characterization of pectin extracted from banana peels of different varieties. *Food Science and Biotechnology*, *27*(3), 623–629. https://doi.org/10.1007/s10068-017-0302-0
23. Kumari, M., Singh, S., & Chauhan, A.K. (2023). A comparative study of the extraction of pectin from kinnow (*Citrus reticulata*) peel using different techniques. *Food and Bioprocess Technology*, *16*(10), 2272–2286. https://doi.org/10.1007/s11947-023-03059-4
24. Lal, A.M.N., Prince, M.V., Kothakota, A., Pandiselvam, R., Thirumdas, R., Mahanti, N.K., & Sreeja, R. (2021). Pulsed electric field combined with microwave-assisted extraction of pectin polysaccharide from jackfruit waste. *Innovative Food Science & Emerging Technologies: IFSET: The Official Scientific Journal of the European Federation of Food Science and Technology*, *74*(102844), 102844. https://doi.org/10.1016/j.ifset.2021.102844
25. Liew, S.Q., Chin, N.L., & Yusof, Y.A. (2014). Extraction and characterization of pectin from passion fruit peels. *Agriculture and Agricultural Science Procedia*, *2*, 231–236. https://doi.org/10.1016/j.aaspro.2014.11.033
26. Listyarini, R.V., Susilawati, P.R., Nukung, E.N., & Yua, M.A.T. (2020). Bioplastic from pectin of dragon fruit (*Hylocereus polyrhizus*) peel. *Jurnal Kimia Sains Dan Aplikasi*, *23*(6), 203–208. https://doi.org/10.14710/jksa.23.6.203-208

27. Mahmoud, M.H., Abu-Salem, F.M., & Azab, D.E.-S.H. (2022). A comparative study of pectin green extraction methods from apple waste: Characterization and functional properties. *International Journal of Food Science*, *2022*, 2865921. https://doi.org/10.1155/2022/2865921
28. Maneerat, N., Tangsuphoom, N., & Nitithamyong, A. (2017). Effect of extraction condition on properties of pectin from banana peels and its function as fat replacer in salad cream. *Journal of Food Science and Technology*, *54*(2), 386–397. https://doi.org/10.1007/s13197-016-2475-6
29. Manrique, G.D., & Lajolo, F.M. (2002). FT-IR spectroscopy as a tool for measuring degree of methyl esterification in pectins isolated from ripening papaya fruit. *Postharvest Biology and Technology*, *25*(1), 99–107. https://doi.org/10.1016/s0925-5214(01)00160-0
30. Martínez-Sabando, J., Coin, F., Melillo, J.H., Goyanes, S., & Cerveny, S. (2023). A review of pectin-based material for applications in water treatment. *Materials*, *16*(6), 2207. https://doi.org/10.3390/ma16062207
31. May, C.D. (1990). Industrial pectins: Sources, production and applications. *Carbohydrate Polymers*, *12*(1), 79–99. https://doi.org/10.1016/0144-8617(90)90105-2
32. Mesbahi, G., Jamalian, J., & Farahnaky, A. (2005). A comparative study on functional properties of beet and citrus pectins in food systems. *Food Hydrocolloids*, *19*(4), 731–738. https://doi.org/10.1016/j.foodhyd.2004.08.002
33. Min, B., Lim, J., Ko, S., Lee, K.-G., Lee, S. H., & Lee, S. (2011). Environmentally friendly preparation of pectins from agricultural byproducts and their structural/rheological characterization. *Bioresource Technology*, *102*(4), 3855–3860. https://doi.org/10.1016/j.biortech.2010.12.019
34. Mohamed, S., & Hasan, Z. (1995). Extraction and characterisation of pectin from various tropical agrowastes. *Asean Food Journal*, *10*(2), 43–50.
35. Müller-Maatsch, J., Bencivenni, M., Caligiani, A., Tedeschi, T., Bruggeman, G., Bosch, M., Petrusan, J., Van Droogenbroeck, B., Elst, K., & Sforza, S. (2016). Pectin content and composition from different food waste streams. *Food Chemistry*, *201*, 37–45. https://doi.org/10.1016/j.foodchem.2016.01.012
36. Oliveira, T.Í.S., Rosa, M.F., Cavalcante, F.L., Pereira, P.H.F., Moates, G.K., Wellner, N., Mazzetto, S.E., Waldron, K.W., & Azeredo, H.M.C. (2016). Optimization of pectin extraction from banana peels with citric acid by using response surface methodology. *Food Chemistry*, *198*, 113–118. https://doi.org/10.1016/j.foodchem.2015.08.080
37. Owolabi, R.U., Usman, M.A., & Kehinde, A.J. (2018). Modelling and optimization of process variables for the solution polymerization of styrene using response surface methodology. *Journal of King Saud University- Engineering Sciences*, *30*(1), 22–30. https://doi.org/10.1016/j.jksues.2015.12.005
38. Pandit, S.G., Vijayanand, P., & Kulkarni, S.G. (2015). Pectic principles of mango peel from mango processing waste as influenced by microwave energy. *Lebensmittel-Wissenschaft Und Technologie [Food Science and Technology]*, *64*(2), 1010–1014. https://doi.org/10.1016/j.lwt.2015.06.070
39. Pinheiro, E.S.R., Silva, I.M.D.A., Gonzaga, L.V., Amante, E.R., Teófilo, R.F., Ferreira, M.M.C., & Amboni, R.D.M.C. (2008). Optimization of extraction of high-ester pectin from passion fruit peel (*Passiflora edulis flavicarpa*) with citric acid by using response surface methodology. *Bioresource Technology*, *99*(13), 5561–5566. https://doi.org/10.1016/j.biortech.2007.10.058
40. Ranganna, S. (1986). *Handbook of Analysis and Quality Control of Fruit and Vegetable Products*. Tata McGrow-Hill Education.
41. Rascón-Chu, A., Martínez-López, A.L., Carvajal-Millán, E., Ponce de León-Renova, N.E., Márquez-Escalante, J.A., & Romo-Chacón, A. (2009). Pectin from low quality 'Golden

Delicious' apples: Composition and gelling capability. *Food Chemistry*, *116*(1), 101–103. https://doi.org/10.1016/j.foodchem.2009.02.016

42. Santos, E.E., Amaro, R.C., Bustamante, C.C.C., Guerra, M.H.A., Soares, L.C., & Froes, R.E.S. (2020). Extraction of pectin from agroindustrial residue with an ecofriendly solvent: use of FTIR and chemometrics to differentiate pectins according to degree of methyl esterification. *Food Hydrocolloids*, *107*(105921), 105921. https://doi.org/10.1016/j.foodhyd.2020.105921
43. Sundarraj, A.A., Thottiam Vasudevan, R., & Sriramulu, G. (2018). Optimized extraction and characterization of pectin from jackfruit (*Artocarpus integer*) wastes using response surface methodology. *International Journal of Biological Macromolecules*, *106*, 698–703. https://doi.org/10.1016/j.ijbiomac.2017.08.065
44. Thakur, B.R., Singh, R.K., & Handa, A.K. (1997). Chemistry and uses of pectin--a review. *Critical Reviews in Food Science and Nutrition*, *37*(1), 47–73. https://doi.org/10.1080/10408399709527767
45. Vriesmann, L.C., Teófilo, R.F., & Lúcia de Oliveira Petkowicz, C. (2012). Extraction and characterization of pectin from cacao pod husks (*Theobroma cacao* L.) with citric acid. *Lebensmittel-Wissenschaft Und Technologie [Food Science and Technology]*, *49*(1), 108–116. https://doi.org/10.1016/j.lwt.2012.04.018
46. Wai, W.W., Alkarkhi, A.F.M., & Easa, A.M. (2009). Optimization of pectin extraction from durian rind (*Durio zibethinus*) using response surface methodology. *Journal of Food Science*, *74*(8), C637-41. https://doi.org/10.1111/j.1750-3841.2009.01331.x

نشریه پژوهشهای علوم و صنایع غذایی ایران
https://ifstrj.um.ac.ir

مقاله پژوهشی

جلد ۲۲، شماره ۳، مرداد- شهریور ۱۴۰۵، ص. ۲۶۰-۲۴۱

روش‌شناسی سطح پاسخ- بهینه‌سازی مبتنی بر استخراج پکتین از پوست یک موز بومی

ایژیلاراسان جی بلاجی[۱]- اوما شانکار کی[۱*]

تاریخ دریافت: ۱۴۰۴/۰۹/۱۱
تاریخ پذیرش: ۱۴۰۵/۰۱/۰۸

چکیده

مطالعه حاضر با هدف بهینه‌سازی استخراج پکتین از نمونه غیر AIS (خام) پوست موز آکومیناتا (Yelakki) انجام شد که با استفاده از روش استخراج به کمک اسیدسیتریک و با استفاده از روش سطح پاسخ (RSM) انجام شد. این مطالعه با استفاده از RSM انجام شد تا اثرات فردی، درجه دوم و تعاملی متغیرهای فرآیند (غلظت اسیدسیتریک، زمان استخراج و دما) بر بازده پکتین به‌طور سیستماتیک ارزیابی شود. این مطالعه بر اساس یک طرح سه عاملی برای تعیین شرایط بهینه و عوامل آماری معنی‌دار انجام شد. شرایط بهینه برای استخراج، غلظت ۱/۵٪، مدت زمان استخراج ۹۰ دقیقه و دمای ۶۱/۵۹ درجه سانتی‌گراد با مقدار مطلوبیت۰/۶۱۶ بود. در این شرایط، بازده پکتین ۲/۰۲۵٪ در مقایسه با پوست موز (AIS 8-20 ٪) بسیار کمتر بود. غلظت، زمان استخراج و دما اثر آماری معنی‌داری ($p < 0.05$) بر بازده پکتین نشان دادند. پکتین استخراج‌شده به‌عنوان پکتین با متوکسیل بالا طبقه‌بندی شد و DE آن ۵۳/۴۹٪ بود که کمی کمتر از مقادیری است که معمولاً برای منابع متعارف گزارش می‌شود. درجه استری شدن در محدوده قابل قبول برای پکتین HM باقی می‌ماند و حاوی محتوای متوکسیل ۴/۷۵٪ و اسید آنهیدرورونیک ۵۰/۴۵٪ است. یافته‌های ما نشان می‌دهد که پوست موز آکومیناتا (Yelakki) بدون AIS به‌طور بالقوه به‌عنوان یک ماده اولیه کم‌هزینه برای تولید پکتین در نظر گرفته می‌شود. مطالعات آینده ممکن است بر افزایش بازده پکتین با استفاده از روش‌های استخراج جایگزین و اصلاح بیشتر پارامترهای فرآیند از طریق تکنیک‌های بهینه‌سازی با استفاده از RSM، ANN یا سایر مدل‌های آماری تمرکز کنند.

واژه‌های کلیدی: اسید سیتریک، غیر AIS، مدل‌سازی آماری، موز یلاکی، RSM

۱- گروه علوم زیستی، دانشگاه مسیح، بنگلور، هند
(*- نویسنده مسئول: Email: uma.shankar@christuniversity.in)

https://doi.org/10.22067/ifstrj.2026.96779.1526

Iranian Food Science and Technology Research Journal
Homepage: https://ifstrj.um.ac.ir

Research Article
Vol. 22, No. 3, July- August. 2026, p. 261-283

Ethanolic Propolis Extract as a Natural Antifungal Preservative: Impact on the Physicochemical, Microbial, and Sensory Properties of Cupcakes

N. Adelipour[1], M. Mehraban Sang Atash[2]*, H. Yarabbi[3], B. Sahraiyan[2]

1- Department of Food Science and Technology, ACECR Kashmar Higher Education Institute, Kashmar, Iran
2- Food Science and Technology Research Institute, ACECR Khorasan Razavi Branch, Mashhad, Iran
(*- Corresponding Author Email: mehraban@acecr.ac.ir)
3- Department of Food Science and Technology, Faculty of Agriculture, Ferdowsi University of Mashhad, Mashhad, Iran

Received: 17.12.2025
Revised: 05.02.2026
Accepted: 22.02.2026
Available Online: 19.05.2026

How to cite this article:
Adelipour, N., Mehraban Sang Atash, M., Yarabbi, H., & Sahraiyan, B. (2026). Ethanolic propolis extract as a natural antifungal preservative: Impact on the physicochemical, microbial, and sensory properties of cupcakes. *Iranian Food Science and Technology Research Journal, 22*(3), 261-283. https://doi.org/10.22067/ifstrj.2026.97040.1533

Abstract

The widespread use of food additives worldwide has raised concerns regarding their potential adverse effects. Given the increasing demand for natural antimicrobial compounds, propolis extract can serve as a safer alternative to synthetic preservatives. This study aimed to investigate the effect of ethanolic propolis extract (EPE), a natural antimicrobial agent, on the physicochemical, microbial, and sensory properties of cake. For this purpose, EPE at concentrations of 0.15%, 0.30%, 0.45%, and 0.60% was incorporated into cake batters, and the quality characteristics of the cakes were evaluated. The results indicated that incorporating EPE at levels above 0.30% increased batter density. Additionally, the presence of EPE and its increased concentration resulted in greater batter consistency. The inclusion of EPE in the cake formulation also contributed to moisture retention during baking and storage (two weeks). However, all cake samples exhibited a decline in moisture content over the storage period, with the control sample (without EPE) experiencing the most significant moisture loss. The cakes containing 0.15% and 0.30% EPE demonstrated the highest specific volume and porosity, as well as the lowest firmness (measured two hours after baking) compared to other formulations. Notably, all EPE-containing samples maintained a softer texture than the control throughout storage. The presence of EPE also influenced the crust color of the cakes, as higher EPE concentrations resulted in decreased L^* and a^* value and an increased b^* value, leading to a darker appearance. Sensory evaluation revealed that cakes with 0.15% and 0.30% EPE exhibited similar characteristics in terms of shape, form, hardness, softness, chewability, upper surface properties, and porosity. Although their flavor and aroma scores were deemed acceptable by sensory panelists, they were slightly lower than those of the control sample. Overall, cupcakes containing 0.15% and 0.30% ethanolic propolis extract were identified as the optimal formulations, with 0.30% EPE offering the best balance between antifungal efficacy, physicochemical quality, and sensory acceptability, making it a promising natural preservative for bakery products. Therefore, EPE has the potential to be utilized as a natural additive with antifungal properties in cake formulations.

Keywords: Antifungal effect, Cake, Natural preservative, Propolis extract

https://doi.org/10.22067/ifstrj.2026.97040.1533

Introduction

In 2023, Ireland led the European cake and pastry market with a per capita consumption of 24.52 kg, followed by France at 17.67 kg and the United Kingdom at 17.15 kg. Countries such as Spain, Slovakia, and Italy also showed significant consumption levels, exceeding 16 kg per capita. Meanwhile, Poland, the Czech Republic, and Scandinavian countries like Sweden and Denmark had lower consumption volumes, ranging between 6 and 7 kg per capita. In the United States, the per capita volume in the *Preserved Pastry Goods & Cakes* segment of the food market was projected to increase steadily between 2025 and 2030, rising by a total of 1.5 kilograms (+18.09%). After eight consecutive years of growth, the average per capita volume is expected to reach 9.8 kilograms by 2030, marking a new peak. In 2022, the annual per capita consumption of biscuits and industrial sweets (including cakes, muffins, cookies, and wafers) by Iranians was 10 kg per person (reportlinker).

Microbial spoilage is the primary limiting factor affecting the shelf life of bakery products with medium to high moisture content. Therefore, controlling microbial spoilage, particularly mold growth, is crucial for the economic sustainability of the flour and bakery industry. The most practical, common, and cost-effective approach is the use of chemical preservatives such as propionates and sorbates, which are directly incorporated into product formulations (Pyrgioti, Graikou, Cheilari, & Chinou, 2022). The rising incidence of foodborne diseases, along with the associated social and economic challenges, has highlighted the need for healthier food production and the use of novel antimicrobial compounds. Concerns regarding certain chemical preservatives and negative consumer reactions toward their use have led to an increased interest in natural preservatives as an alternatives. Consequently, both manufacturers and consumers have turned their attention towards plant essential oils. The antimicrobial properties of these substances against a wide range of bacteria, yeasts, and fungi have been well documented (Tajik, Nateghi, & Berenji, 2017). The significance of essential oils lies not only in their ability to impart aroma and flavor to food but also in their phenolic compounds, such as eugenol, carvacrol, and thymol, which exhibit antimicrobial effects. The higher the phenolic content in essential oils, the stronger their antimicrobial properties (Hosseinzadeh & Shirazinejad, 2019). Essential oils and extracts derived from medicinal plants are emerging as new natural preservatives with potent antimicrobial, anticancer, and antioxidant properties, making them highly effective in protecting both raw and processed foods (Ike, Emeka-Ike, & Ogwuegbu, 2020). Propolis, one of the most important bee products, is recognized as a natural antibiotic and a potential alternative to industrial antibiotics, contributing to the reduction of unnecessary antibiotic use. Flavonoids constitute the majority of the resinous fraction of propolis and are primarily responsible for its antioxidant, antibacterial, antiviral, antifungal, anticancer, and anti-inflammatory properties (Garzoli *et al*., 2023).

The main components of propolis include aromatic acids (such as cinnamic acid, caffeic acid, and ferulic acid), aromatic esters (e.g., ether esters of cinnamic and caffeic acids), and volatile compounds (such as geraniol, nerol, farnesol, and beta-eudesmol) (Abtahi, Mehraban, Bagheri, Fathi Najafi, & Islami, 2022). Additionally, it contains aromatic compounds (e.g., vanillin), hydrocarbons (such as eicosane, tricosane, and pentacosane), steroids (e.g., cholestanol, fucosterol, and stigmasterol), enzymes (such as α-amylase and β-amylase), flavonoids (e.g., pinocembrin, chrysin, galangin, apigenin, and kaempferol), acids (such as palmitic acid, melissic acid, and cerotic acids), as well as micro- and macronutrients (e.g., calcium, potassium, magnesium, sodium, zinc, iron, manganese, aluminum, and chlorine). Furthermore, it contains vitamins (such as B1, B2, B6, C, and E) and essential oils, which are primarily represented by monoterpenes and

sesquiterpenes (Garzoli *et al*., 2023). However, limited research has been conducted on the impact of propolis on the physicochemical, sensory, and microbial properties of bakery products, particularly cakes. Therefore, this study aims to investigate the effects of ethanolic propolis extract (EPE) on the quality characteristics of cakes and explore its potential as a natural preservative. The results of this research could contribute to enhancing the quality and safety of bakery products and offer a practical alternative to synthetic preservatives in the industry.

Materials and Methods

The raw materials, including wheat flour, white sugar, liquid vegetable oil, fresh eggs, vanilla, and baking powder, were purchased from the local market. Propolis powder and chemicals required for the cake tests were purchased from reputable Iranian companies.

Lyophilized strains of *Aspergillus niger* (ATCC 9142), *Rhizopus stolonifer* (ATCC 14037), and *Penicillium expansum* (ATCC 58619)—the primary molds responsible for spoilage in cakes and bakery products—were purchased from the Regional Center for Bacteria and Industrial Fungi Collection of Iran. The lyophilized strains were inoculated into Potato Dextrose Broth (PDB) and then surface-cultured on Potato Dextrose Agar (PDA). The cultures were then incubated at 25°C for three days and stored at 4°C until use. Molds were cultured on slanted PDA medium at 25°C for 4–7 days until sporulation occurred. The spores were then collected from the surface of the PDA medium by adding sterile Ringer's solution. Finally, the spore count was determined using a hemocytometer under a microscope, and a suspension containing 10^5 spores/ml was prepared (Rezaei Boroojerdi, Habibi Najafi, Hosseini, & Karazhyan, 2018).

The MIC and MFC of propolis extract were determined using the microdilution method. Serial dilutions of propolis extract were prepared in PDB medium, starting from an initial concentration of 300 mg/ml. Then, 100 µL of each dilution was added to a 96-well microplate, followed by adding 95 µL of PDB medium and 5 µL of the mold spore suspension. A negative control contained only PDB medium and the mold strain. A positive control included PDB medium, the mold strain, and potassium sorbate as antifungal agent. The microplates were incubated at 25°C for 72 hours. The lowest concentration of propolis extract that completely inhibited mold growth (showing no turbidity) was recorded as the MIC. To determine the MFC, 100 µL from wells where no mold growth was observed was plated onto PDA medium. The plates were incubated at 25°C for 3–5 days, and the lowest concentration of propolis extract that resulted in 99.9% inhibition of mold growth was recorded as the MFC (Olamaeian, Kouhdar, & Hosseini, 2022).

The cake batter was prepared using 312 g wheat flour, 233 g water, 242 g sugar, 112 g oil, 6.7 g baking powder, 1.1 g vanilla, 140 g eggs, and propolis extract at concentrations of 0, 0.15, 0.30, 0.45, and 0.60% (based on flour weight). Oil, powdered sugar, and eggs were mixed using an electric mixer at 128 rpm for 6 minutes to form a creamy, aerated mixture. Water was then added, and mixing continued for 4 minutes. Baking powder and vanilla were combined with the flour and gradually incorporated into the batter, followed by the addition of propolis extract. The final batter was poured into cupcake molds and baked at 170°C for 20 minutes. After cooling, the cakes were packaged and stored at room temperature for subsequent physicochemical and microbiological analyses (Tajik *et al*., 2017).

Evaluation of Physicochemical Properties of Wheat Flour

The chemical composition of wheat flour was measured based on standard methods outlined by the American Association of Cereal Chemists (AACC, 2005).

Dough Density and Consistency

The specific weight of the dough was measured according to the method of Pasukamonset *et al.* (2018). In this method, the

weight of a specific volume of dough was measured in a designated container, and then the weight of an equal volume of water at the same temperature was used to divide the dough weight. The dough consistency was measured using a Bostwick consistency meter. This device consists of a rectangular or semi-cylindrical chamber with two compartments (small and large). Dough is placed in the small compartment, and after releasing a specialized blade between the two compartments, the distance traveled by the dough during 30 seconds was recorded as the consistency (Aleman, Morris, Prinyawiwatkul, Moncada, & King, 2022).

Evaluation of Physicochemical, Sensory, and Microbiological Properties of Oil Cake

According to the method of Pasukamonset *et al*. (2018), the moisture content of powdered samples was measured at 2 hours, 1 week, and 2 weeks after baking using a moisture analyzer. To measure the specific volume of the cake, the canola seed displacement method was used, following AACC Standard 72-10 (AACC, 2005). The color analysis of the cake crust was conducted 2 hours after baking using a colorimeter (Minolta CR-400, Konica Minolta, Japan), determining the three-color indices: L*, a*, and b* (Hassan, Fahmy, Magdy, & Hassan, 2020). Texture evaluation was performed using a texture analyzer (TA Plus, UK) at 2 hours, 1 week, and 2 weeks after baking. The maximum force required to penetrate a cylindrical probe (2 cm diameter and 3/2 cm height) at a speed of 60 mm/min from the center of the muffin was calculated as the firmness index (Salem, El-Zayet, Rayan, & Shatta, 2024). The sensory characteristics of the product were evaluated by 12 trained panelists, based on attributes such as form and shape, upper surface (crust), lower surface, porosity and crumb structure, texture firmness and softness, chewability, and taste (smell and flavor) using a 5-point hedonic scale. In this test, the ratings were: 5 (excellent), 4 (good), 3 (average), 2 (bad), and 1 (very bad) (Ahmed, Ragab, Gadallah, Alhomaid, & Almujaydil, 2024). The enumeration of mold and yeast, as well as the total mesophilic microorganism count, were performed according to the international standard ISO 4833-1, at time intervals of 1, 7, 14, and 21 days after baking.

Statistical Design

The experiments were conducted using a completely randomized design with different concentrations of ethanolic propolis extract (0, 0.15, 0.30, 0.45, and 0.60%). For variables affected by storage time, a separate statistical analysis was carried out to evaluate differences among storage days within each treatment as well as differences among treatments at each storage day. Mean comparisons were performed using Tukey's multiple range test ($P < 0.05$).

Results and Discussion

Antifungal Properties of Propolis Against mold spoilage of Cake in Laboratory Conditions

In this study, the antifungal activity of ethanolic propolis extract was evaluated against *Aspergillus niger*, *Rhizopus stolonifer*, and *Penicillium expansum*, which are the primary molds responsible for spoilage in cakes. The microdilution method was used to assess the antifungal properties. The minimum inhibitory concentration (MIC) of the ethanolic propolis extract against *Aspergillus niger*, *Rhizopus stolonifer*, *and Penicillium expansum* was 125 µg/ml, 62.5 µg/ml, and 62.5 µg/ml, respectively. The minimum fungicidal concentration (MFC) was 250 µg/ml, 125 µg/ml, and 125 µg/ml, respectively (Table 1). Ethanol 80% was used as a control solvent and did not affect the fungi studied. The minimum inhibitory concentration of ethanol 80% was higher than 8000 µg/ml. Shokri, Katiraee, Fatahinia, & Minooeianhaghighi, (2017) examined the chemical composition and antifungal potential of Iranian propolis against *Candida krusei* strains. They reported that the minimum inhibitory concentration (MIC) and minimum fungicidal concentration (MFC) of Iranian propolis were 2-20 mg/ml and 4-25 mg/ml,

respectively. Gucwa, Kusznierewicz, Milewski, Van Dijck, & Szweda, (2018) reported the minimum fungicidal concentration (MFC) of ethanolic propolis extract from Poland against a group of 69 clinical *Candida albicans* isolates was in the range of 1.25% to 0.08% (v/v). The results of Fernández-Calderón *et al.* (2021) showed that the ethanolic propolis extract from Spain exhibited antifungal activity against *Candida glabrata* isolates, with a minimum inhibitory concentration (MIC) of approximately 0.2% (v/v) and a minimum fungicidal concentration (MFC) of 0.4% (v/v). Papp *et al.* (2021) collected propolis samples from four regions in Hungary: Csikóstőttős, Héhalom, Somogybabod, and Szolnok. The Szolnok, Héhalom, and Csikóstőttős samples exhibited stronger antifungal activity, with their minimum inhibitory concentration (MIC) and IC50 values reported ranged between 100-200 µg/ml and 72-134 µg/ml, respectively. Although the Somogybabod sample was significantly weaker than the other propolis samples, its inhibitory effect on fungal cell growth at 400 µg/ml was not less than 18%. The results of these researchers are consistent with our findings. Zampini, Salas, Maldonado, Simirgiotis, & Isla, (2021) showed that these extracts exhibited significant antibacterial effects, particularly against Gram-positive bacteria such as *Staphylococcus aureus*, with minimum inhibitory concentration (MIC) values ranging from 10 to 100 µg/mL. In contrast, the extracts were less effective against Gram-negative bacteria, showing MIC values between 400 and 1600 µg/mL. Additionally, the propolis extracts demonstrated antifungal activity against dermatophytes like *Microsporum gypseum*, *Trichophyton mentagrophytes*, and *Trichophyton rubrum*, with MIC values between 16 and 125 µg/mL. The primary compounds responsible for this antifungal activity were identified as two chalcones, DHC and DHMC, which exhibited MIC values between 1.9 and 2.9 µg/mL. Vică *et al.* (2022) reported that the minimum inhibitory concentration (MIC) of ethanolic propolis extracts from the Romanian against *Candida albicans*, *Candida krusei*, *Candida tropicalis*, *Candida glabrata*, and *Aspergillus fumigatus* ranged from 1.56 mg/mL to 3.12 mg/mL. The antimicrobial activity of nine aqueous propolis extracts from various Romanian regions reported by Heghedűş-Mîndru *et al.* (2023) was evaluated against six bacterial strains commonly associated with cereals. They employed the disk diffusion method to measure the diameters of inhibition zones, which ranged from 16 to 29 mm, indicating varying degrees of antimicrobial efficacy. Notably, sample S1 from Transylvania exhibited the most potent inhibitory effect, particularly against *Bacillus cereus*.

Table 1- Minimum Inhibitory Concentration (MIC) and Minimum Bactericidal Concentration (MBC) of ethanolic propolis extract against the main spoilage molds in cakes (µg/ml)

Mold	MIC	MFC
Aspergillus niger	125	250
Rhizopus stolonifer	62.5	125
Penicillium expansum	62.5	125

Physical and Chemical Properties of Wheat Flour

Table 2 presents the physical and chemical properties of wheat flour with an extraction rate of 75%. According to the results, the flour used in the cake formulation contained 9.84% moisture, 8.58% protein, 1.42% fat, 0.49% ash, and 29.71% wet gluten.

Table 2- Physical and chemical properties of wheat flour

Properties	Value (%)
Moisture	9.84
Protein	8.58
Fat	1.42
Ash	0.49
Wet Gluten	29.71

Dough Characteristics

Density

With an increase of more than 0.30% propolis extract in the cake dough formulation, the density significantly increased ($P<0.05$) (Fig. 1). The highest value for this parameter was observed in the samples containing 0.45% and 0.60% propolis extract, while the lowest value was found in both the control sample and the samples containing 0.15% and 0.30% propolis extract.

The density of cake dough and similar products indicates the presence of air bubbles in the dough and its proper aeration, as well as the retention of gas bubbles during the dough preparation process, particularly in the mixing stage. In this way, the more efficiently air bubbles are incorporated into the dough, the lower the density, resulting in a lighter dough (Salem *et al.*, 2024). Scanlon & Koksel (2024) reported that proper processing and aeration of cake dough led to the better incorporation and distribution of air bubbles, which in turn results in a reduction in dough density. The decrease in dough density plays a crucial role in increasing the volume, porosity and reducing the firmness of the internal texture of cakes. As the results of this study showed, at higher levels of propolis extract (0.45% and 0.60%), the dough density increased. It is likely that the use of propolis or bee pollen, by reinforcing the gluten network of the dough and strengthening this network, causes an increase in dough density through disruption of the aeration process. Tahmouzi *et al.* (2023) stated that when biopolymer compounds, such as various gums, are used in food formulations at appropriate levels, they can improve dough aeration by preventing the aggregation of gas bubbles. This is due to the formation of a thick layer on the surface of the bubbles, which stabilizes the gas bubbles and keeps them separated, ultimately increasing dough density and, consequently, volume and porosity. Milinčić, Kostić, Stanojević, & Pešić, (2024) reported that the inclusion of propolis or bee pollen extract in the formulation of oil-based cakes led to a reduction in the spreadability of air bubbles during the mixing process and the air bubbles generated from the activity of baking powder. As a result, dough density increased, and cake volume decreased.

Consistency

Incorporation of propolis extract at all levels in the cake dough formulation increased consistency. An upward trend in consistency was observed from the control sample to the sample containing 0.60% propolis extract. The Bostwick value is inversely related to dough consistency, with a decrease in this value indicating an increase in dough consistency. The control sample had the lowest consistency, while the sample containing 0.60% propolis extract exhibited the highest consistency compared to the other treatments (Fig. 2). Dough consistency refers to the time it takes for fluids to flow. It directly impacts product properties such as moisture content, texture firmness, porosity, and shelf life. Low dough viscosity allows air bubbles to easily rise to the surface and burst. Additionally, air bubbles trapped in the dough may not remain during baking, leading to the collapse of the cake structure in the oven. Several factors, including increased water absorption, gel formation, the strengthening of the three-dimensional network of the dough, and emulsion stability, contribute to enhancing the consistency of cake dough. Milinčić *et al.* (2024) reported that the inclusion of propolis in cupcake formulations helped strengthen the

gluten network in the dough. At higher concentrations of propolis, both dough consistency and viscosity increased significantly, which, however, had technologically destructive effects on the texture of both the dough and the resulting cake.

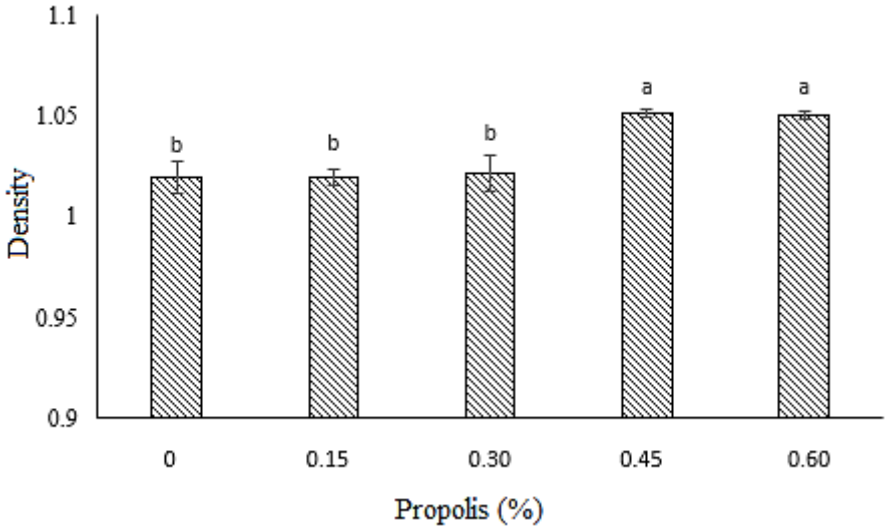

Fig. 1. Effect of different levels of propolis extract on the density of cake dough
Like letters are not statistically significant at the P<0.05 level.

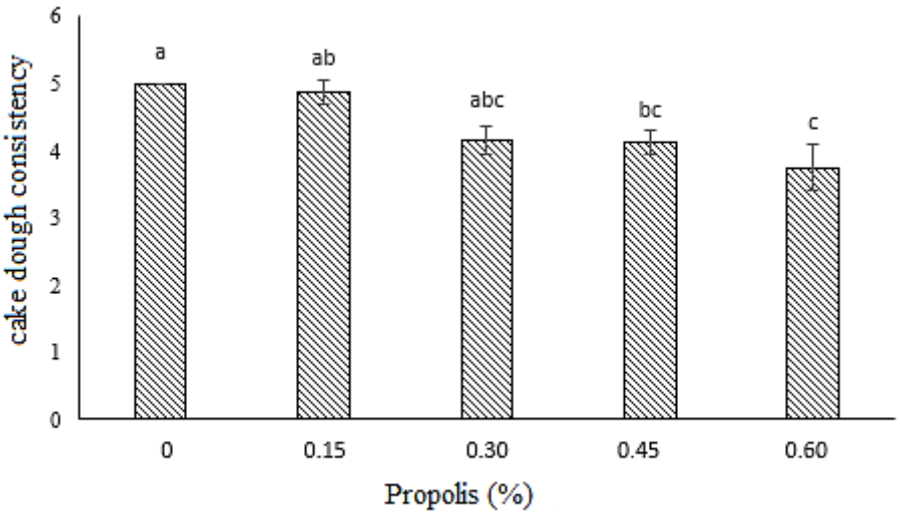

Fig. 2. Effect of different levels of propolis extract on cake dough consistency
Like letters are not statistically significant at the P<0.05 level.

Physical and Chemical Properties of Cake

Moisture

The moisture content of cake samples containing more than 0.15% propolis extract was significantly higher (P<0.05) than that of the control sample within 2 hours after baking. The lowest moisture content was observed in the control sample, while the highest moisture content was found in the sample containing 0.60% propolis extract. The results indicated that the samples containing 0.45% and 0.60% propolis extract had the highest moisture

content, both at 1 and 2 weeks after baking (Fig. 3). Moisture content in all cake samples decreased over the 2-week storage period, with the control sample showing the greatest moisture loss compared to the other formulations. The optimal consumption time for baked products is within 3 days after production; however, the shelf life of baked goods can be extended by using moisture-absorbing compounds (Pyrgioti *et al*., 2022). Based on the results, propolis extract and its increased concentration helped retain moisture in the samples compared to the control sample, both during the baking process and throughout the 2-week storage period. This highlights the hygroscopic properties of propolis extract. Tahmouzi *et al*. (2023) also reported that hydrocolloid compounds have a gelling property and can trap free water in the environment, thereby increasing the moisture content of the sample and preserving it during storage. Compounds with the ability to form gels create a three-dimensional network by forming a series of cross-links that connect polymer chains. This network traps water in its gaps, thereby helping to retain the product's moisture during storage. The baking temperature reduces chain interactions, allowing for the formation of water bonds with the polysaccharide chains. Milinčić *et al.* (2024) reported that the addition of propolis extract to the formulation of oil cake resulted in higher moisture content in the samples containing this additive compared to the control sample. The researchers stated that some compounds in propolis likely contain a large number of hydroxyl groups, which help trap and encapsulate water, thereby enhancing its retention. Consequently, the propolis extract in the cake formulation was effective in retaining moisture during the baking process and afterward.

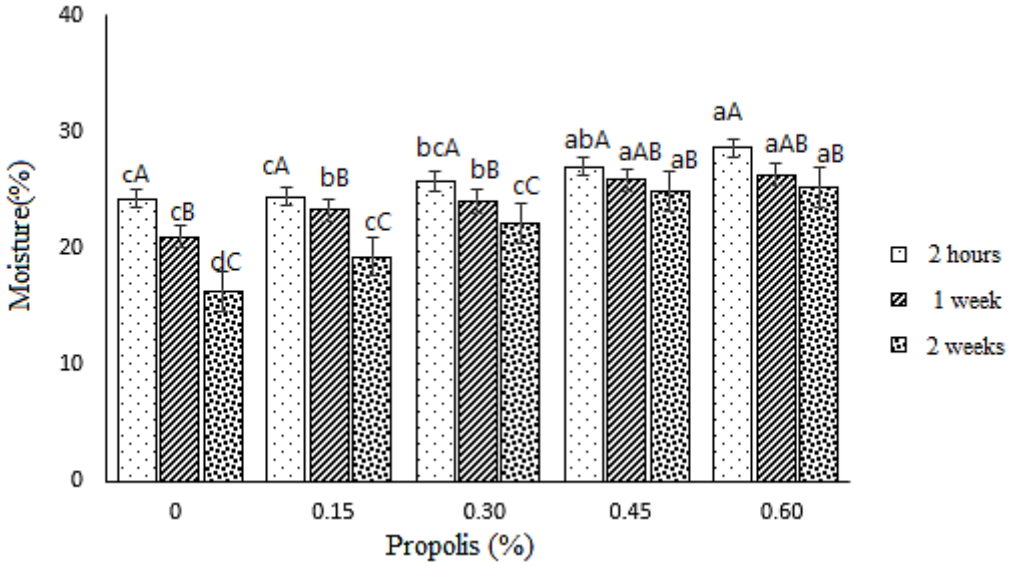

Fig. 3. Effect of different concentrations of ethanolic propolis extract on the moisture content (%) of cupcakes during storage

Different lowercase letters indicate significant differences among treatments at the same storage time, while different uppercase letters indicate significant differences among storage times within the same treatment ($P < 0.05$)

Specific Volume

Cake samples containing 0.15% and 0.30% propolis extract had the highest specific volume compared to the other samples. In contrast, the lowest specific volume was observed in the samples containing 0.45% and 0.60% propolis extract (Fig. 4). These two samples had a lower specific volume than the control sample (the sample without propolis extract). Therefore, adding more than 0.30%

propolis extract not only failed to improve the specific volume of the cake samples but also resulted in a downward trend in specific volume (reduced specific volume compared to the control sample).

The volume of bakery products is influenced by various factors, such as the number of air bubbles entering or leaving the dough (during the mechanical mixing process, air bubbles are incorporated, and during kneading, molding, and dividing, some air bubbles escape), air bubbles produced by biological activity (yeast activity) and chemical activity (such as baking powder and baking soda), their retention in the dough during baking, and proper water evaporation. The presence of additives, such as biopolymers (gums, emulsifiers, proteins, etc.), is also crucial, and if any disturbance occurs in one of these factors, the volume decreases (Scanlon & Koksel, 2024). Based on the results in this section, high levels of propolis extract caused a reduction in the specific volume of the produced samples. The high concentration of this additive in the cake formulation, which was not needed for reinforcing the gluten network or improving the cake texture structure, led to a competition for water absorption between this hydrophilic propolis and the starch in the flour. Since biopolymeric compounds have a higher water absorption capacity than starch, sufficient water was not available for the starch. As a result, starch did not gelatinize properly during baking, leading to a sticky dough with excessive shrinkage and a reduced specific volume of the cake. Additionally, the excessive moisture absorption by the hydrophilic compound negatively impacted volume reduction. By absorbing too much water and preventing the evaporation of some water during the baking process, it hinders the volume expansion related to evaporation, thus reducing the specific volume of the cake. On the other hand, intense water evaporation during the heat transfer process in baking leads to the formation of abnormal holes and pores in the cake. Hydrocolloid compounds, by reducing the heat transfer coefficient and water retention capacity, affect the intensity of water evaporation. Intense evaporation also causes shrinkage and the development of surface roughness and porosity. Excessive evaporation can also lead to the formation of larger holes on the surface of the product. Nasirzadeh Dizaji, Rofehgarinezhad, Tabibiazar, & Alizadeh, (2022) reported that the use of an oleogel containing propolis wax in cake formulation negatively affected the volume and symmetry index of the produced samples compared to the control sample. However, the destructive effects of this compound on the texture properties were not observed in the optimized sample containing 4% propolis wax oleogel (bee propolis). Basturk, Badem, & Ceylan, (2023) also reported that using propolis oleogel in cakes resulted in decreased acceptance of textural properties. Hosseini Khabbazi, Mansouripour, & Saremnezhad, (2023) used propolis extract in toast bread formulation and observed a reduction in the specific volume of the toast bread due to the presence of this additive. However, this reduction was not significant, and considering the positive physicochemical and antimicrobial effects of propolis, the use of this extract up to 2% in toast bread formulations is recommended.

Porosity

Cakes containing 0.15% and 0.30% propolis extract had the highest porosity compared to the control sample. The porosity of sample containing 0.45% propolis and the control sample were statistically similar at a 95% confidence level. The lowest porosity was observed in the sample containing 0.60% propolis extract (Fig. 5). Porosity refers to the number of air-filled cavities within the product, and it is calculated by dividing the total volume of pores by the total volume of the sample. Baking temperature and time affect the porosity of bakery products. As baking begins, the volume and, consequently, the porosity of the product change (Ahmed *et al*., 2024).

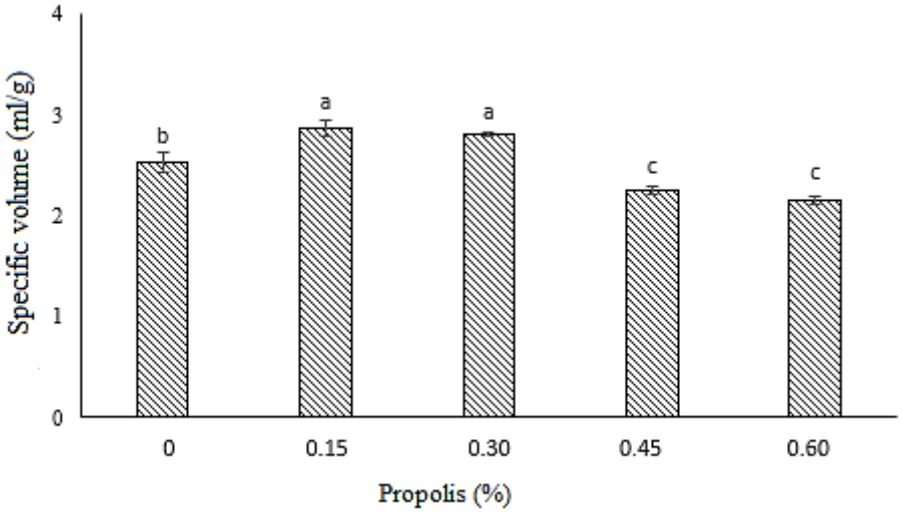

Fig. 4. Effect of different levels of propolis extract on the specific volume of cake
Like letters are not statistically significant at the P<0.05 level.

At the beginning of the baking process, the volume of the product increases due to the expansion of gases. During baking, the heat transferred into the product also causes moisture evaporation. The steam produced may become trapped in the cavities within the product's structure, enlarging these pores and increasing porosity. Towards the end of the baking process, significant changes in volume are less noticeable. In the final minutes of baking, due to the formation of a crust and the release of steam, the product may shrink, resulting in a decrease in volume. As the baking temperature increases, volume changes occur more rapidly, which may be due to faster heat transfer into the product and a quicker increase in the temperature of water (Aleman *et al*., 2022). On the other hand, the porosity of the inner texture is influenced by the number of cavities present in the core and how evenly these cavities are distributed. The higher the number of cavities and gas cells and the more uniform their distribution, the higher the porosity of the final product (Scanlon & Koksel, 2024). Tahmouzi *et al*. (2023) stated that if hydrocolloid compounds are used in food formulations at appropriate levels, without disrupting the distribution of air bubbles in the sample, they can help stabilize gas cells by reducing the coalescence of gas cells through the formation of a thick layer on the surface of the cells. As a result, each cell remains separate, and its size is smaller, which significantly impacts increasing porosity. Sahraiyan, Pourhaji, & Alizadeh Behbahani, (2021) used different ingredients as gluten-free dough binders. Their results showed that samples containing hydrocolloids had the highest specific volume and porosity compared to those containing water, cheese powder, oil, etc., because they were more successful in dispersing and maintaining the air bubbles in the dough during both dough preparation and baking. Bozdogan, Ormanli, Kumcuoglu, & Tavman, (2022) explored the combined use of pear pomace powder and xanthan gum in gluten-free cake formulations. The inclusion of xanthan gum was found to increase cake volume and decrease crumb hardness, while pear pomace powder contributed to enhanced water retention. Notably, when used together, pear pomace powder and xanthan gum improved the porosity of the cakes, leading to a softer texture.

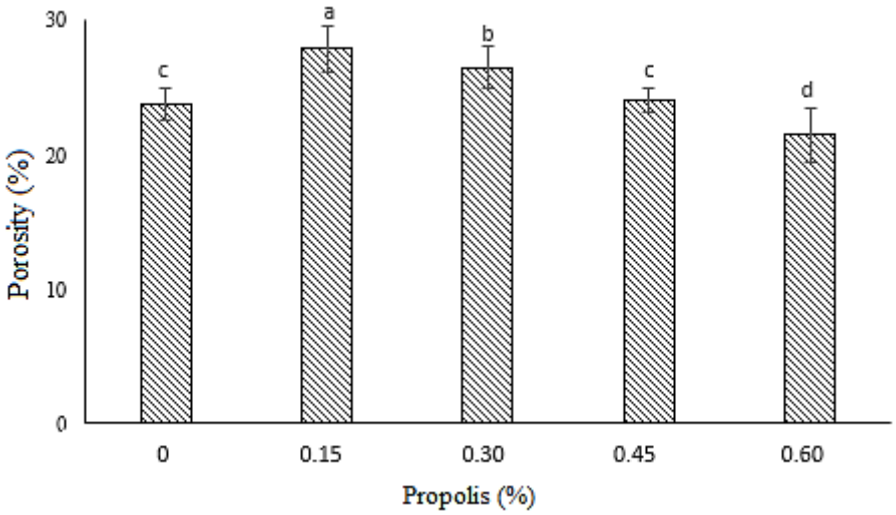

Fig. 5. Effect of different levels of propolis extract on cake porosity
Like letters are not statistically significant at the P<0.05 level.

Texture Firmness

Although specific volume and porosity increased in cakes containing 0.15% and 0.30% propolis extract compared to the control, this trend did not always result in a proportional reduction in firmness. Texture firmness is influenced not only by volume and porosity but also by moisture distribution, starch gelatinization, and interactions between propolis compounds and the gluten–starch matrix. At low propolis concentrations (0.15% and 0.30%), the improvement in volume and porosity contributed to a softer texture shortly after baking. However, propolis is a highly hydrophilic compound, and its interaction with water and gluten proteins may partially limit starch gelatinization. This effect can counterbalance the softening impact of increased porosity, resulting in firmness values that are not strictly inversely correlated with volume. As a result, the increase in firmness observed at certain propolis concentrations does not contradict the higher specific volume and porosity but rather reflects the dominance of water competition and matrix reinforcement effects over structural expansion.

Therefore, the observed firmness behavior at these concentrations reflects the combined effects of structural expansion, moisture retention, and biopolymer interactions rather than being solely dependent on specific volume or porosity. Similar inconsistencies between volume-related parameters and firmness have also been reported in cake systems containing hydrocolloids or phenolic-rich additives, where water competition and matrix reinforcement alter the expected structure–texture relationship.

Samples containing 0.15% and 0.30% propolis extract exhibited lower firmness compared to the control sample within 2 hours after baking. In the same period, samples containing 0.45% and 0.60% propolis extract had the highest firmness among all cake samples. However, after 1 and 2 weeks of storage, all samples had a softer texture than the control. Specifically, the sample with 0.30% propolis extract had the lowest firmness after 1 week, while after 2 weeks, the samples containing 0.30% and 0.45% propolis exhibited the lowest firmness. Over 2-week storage period, the firmness of all cake samples increased, with the control sample showing the most significant increase in firmness compared to the other treatments (Table 3). The firmness of baked products immediately after production is mainly influenced by moisture retention during baking and key technological properties such as specific volume and porosity. Higher moisture

retention helps prevent excessive crust hardening, resulting in a softer texture, while increased volume and porosity—associated with a greater number and more uniform distribution of air cells—reduce crumb compactness and contribute to lower firmness. Therefore, samples with higher volume and porosity are generally expected to exhibit softer textures immediately after baking.

Moreover, it was expected that samples with higher moisture retention during storage would maintain a softer texture. This is because the moisture-absorbing components in their formulation help slow down the migration of moisture from the inner texture to the crust. Essentially, the loss of moisture, which is the main cause of staling and firmness decrease in baked goods during storage, occurs at a much slower rate.

If the number of hydrophilic compounds exceeds the formulation's requirements, these additives will absorb more water than starch. This can prevent the complete gelatinization of starch during baking, ultimately accelerating the staling process and increasing the firmness of the stored samples (Sahraiyan *et al*., 2021). Nasirzadeh Dizaji *et al.* (2022) utilized wax extracted from propolis as a substitute for shortening in cake formulation. Their findings indicated that incorporating oleogel into the cake formulation had a significant impact on the texture and symmetry index of the cake samples. The use of 20% and 40% oleogel containing 4% propolis wax did not have any adverse effects on the texture or overall quality attributes of the cake. Similarly, Hosseinizadeh, Pedram Nia, Saeidi Asl, & Dovlat Abadi, (2020) and Basturk *et al.* (2023) reported that while propolis extract exhibited a positive effect on the texture of oil-based cakes at low concentrations, it led to increased firmness at higher concentrations immediately after baking. Limited studies have investigated the effects of propolis extract on the textural properties of baked products. The majority of research has focused on its application as a natural preservative to extend the shelf life of fruits and vegetables. de Queiroz, Ramos, Armond, Felipini, & Di Piero, (2024) investigated the efficacy of ethanolic extracts of brown and green propolis, along with their homeopathic preparations, against *Colletotrichum scovillei*. The results demonstrated that these propolis extracts possess antifungal properties, effectively inhibiting the pathogen responsible for anthracnose. When incorporated into gelatin-based coatings, propolis not only enhanced the antimicrobial activity but also contributed to the preservation of bell pepper quality during storage.

Table 3- Effect of different levels of propolis extract on the firmness of cake texture over 2 weeks after baking

Treatments	Propolis extract (%)	Tissue stiffness		
		2 hours	1 week	2 weeks
1	0	2.31±0.21 ^{bA}	714±0.19 ^{aB}	15.62±0.22 ^{aC}
2	0.15	2.48±0.17 ^{bA}	4.30±0.06 ^{cB}	8.41±0.47 ^{bC}
3	0.30	2.51±0.04 ^{bA}	3.81±0.02 ^{dB}	5.32±0.63 ^{cC}
4	0.45	2.79±1.11 ^{aA}	4.32±0.10 ^{cB}	5.39±0.27 ^{cC}
5	0.60	2.86±2.09 ^{aA}	4.96±0.14 ^{bB}	7.21±0.06 ^{bC}

Different lowercase letters in each column indicate significant differences among treatments at the same storage time (P<0.05). Different uppercase letters in each row indicate significant differences among storage times within the same treatment (P<0.05).

Crust Color (L*, *a, b*)**

The results indicated that incorporating propolis extract into the cake formulation significantly ($P < 0.05$) reduced the L* and a* color components. However, when the propolis extract level exceeded 0.30%, the b* color component exhibited an increasing trend. The lowest b* value was observed in the control sample and in the samples containing 0.15% and 0.30% propolis extract, while the

highest b* value was recorded in the samples with 0.45% and 0.60% propolis extract (Table 4). The addition of high concentration of propolis extract in the cake formulation resulted in a darker color of the final product. Color changes in food products depend on multiple factors, with baking temperature and time being among the most influential. These changes are primarily attributed to non-enzymatic browning reactions occurring in the food matrix. Consequently, the addition of ingredients that contain substrates affecting these reactions can intensify color changes (Hassan *et al*., 2020). According to Hoseinzadeh & Shirazinejad (2019), crust surface characteristics significantly influence brightness, with smoother surfaces exhibiting better color uniformity compared to wrinkled ones. However, beyond enzymatic and non-enzymatic reactions and the physical nature of the surface (smooth vs. wrinkled), pigments present in additives and the intrinsic color properties of the formulation ingredients can also have a considerable impact on the final product's color. Propolis extract, due to its distinct hue (ranging from light brown to olive green), alters the cake's coloration. The a* color component was found within the negative range (green), whereas baked goods typically exhibit a positive a* value (red spectrum). Nasirzadeh Dizaji *et al*. (2022) reported that the propolis wax in cake formulations led to darkening of the color. The phenolic compounds present in the extracts also contribute to the darkening and opacity of food products, significantly altering both the surface and internal texture color components. Since propolis extract contains significant amounts of phenolic compounds (Refaat, Mady, Sarhan, Rateb, & Alaaeldin, 2021), it is likely that part of the color change in the samples containing this additive, compared to the control, is influenced by polyphenols.

Table 4– Effect of different levels of propolis extract on the amount of color components (L*a*b*) of cake crust

Treatments	Propolis extract (%)	Color components		
		b*	a*	L*
1	0	22.69±0.31 b	-0.07±0.01 a	74.53±0.86 a
2	0.15	23.49±0.25 b	-0.51±0.03 b	72.63±0.34 ab
3	0.30	23.26±0.30 b	-1.29±0.04 c	70.46±0.30 abc
4	0.45	24.76±0.15 a	-1.36±0.07 c	68.47±1.21 bc
5	0.60	25.04±0.03 a	-1.71±0.08 d	66.80±2.07 c

Similar letters in each column are not statistically significant at the P<0.05 level.

Sensory Characteristics of Cake

Form and Shape

The results indicated that samples containing 0.15% and 0.30% propolis extract had superior scores for form and shape compared to the control sample. The form and shape score of 0.15% propolis extract sample was higher than that of 0.30% propolis extract sample, earning the highest score among all the produced samples. Additionally, the findings showed that higher levels of propolis extract (0.45% and 0.60%) had negative effect on the form and shape scores of the samples (Fig. 6)

Surface Characteristics (Crust)

The results indicated that the samples containing 0.15% and 0.30% propolis extract showed similar surface characteristics to the control sample. No significant difference (P<0.05) was observed between these three samples. In contrast, cake samples containing 0.45% and 0.60% propolis extract had the lowest surface characteristic scores compared to the other samples. No significant difference was observed between these two samples at 95% confidence level (Fig. 6).

Lower Surface Characteristics

As a result of the presence of propolis extract and its high concentration in the cake

formulation, the lower surface characteristics score of the produced samples significantly decreased (P<0.05). The highest score for lower surface characteristics was observed in the control sample (propolis-free sample), while the lowest score for this parameter was recorded in the two samples containing 0.45% and 0.60% propolis extract (Fig. 6). Samples containing 0.15% and 0.30% propolis extract ranked second in terms of lower surface characteristics scores. All the produced samples, even those with the lowest surface characteristics scores, received an acceptable sensory score from panelists (above 2.5).

Porosity and Pore Structure

The results showed that samples containing 0.15% and 0.30% propolis extract had porosity and pore structure characteristics similar to the control sample (propolis-free sample). No significant difference (P<0.05) was observed between these three samples. In contrast, cake samples containing 0.45% and 0.60% propolis extract exhibited the lowest porosity scores compared to the other samples (Fig. 6).

Texture Firmness and Softness

Sample containing 0.15% propolis extract exhibited superior texture firmness and softness scores compared to the other samples (Fig. 6). The texture firmness and softness score of sample containing 0.30% propolis extract was similar to that of the control sample. No significant difference (P<0.05) was observed between these two samples. Both the control sample and the sample with 0.30% propolis extract ranked second in terms of texture firmness and softness, after the sample containing 0.15% propolis extract. Furthermore, the results indicated that higher levels of propolis extract (0.45% and 0.60%) negatively affected the texture firmness and softness scores of the samples. The lowest texture firmness and softness score was observed in the sample containing 0.60% propolis extract.

Chewability

Sample containing 0.15% propolis extract exhibited superior chewability scores compared to the other produced samples, achieving the highest chewability score. The chewability score of sample containing 0.30% propolis extract was similar to that of the control sample, and no significant difference (P<0.05) was observed between these two samples (Fig. 6). Both the control sample and the sample with 0.30% propolis extract ranked second in terms of chewability, after the sample containing 0.15% propolis extract. Higher levels of propolis extract (0.45% and 0.60%) negatively affected the chewability scores of the samples. The lowest chewability score was observed in the sample containing 0.60% propolis extract. Cake sample containing 0.60% propolis extract was considered unacceptable by the panelists, as it received a chewability score lower than 2.5 in the sensory evaluation.

Smell and Taste

The presence of propolis extract at different concentration from 0.15% to 0.60% in the cake formulation significantly (P<0.05) decreased the smell and taste scores of the samples. The highest smell and taste scores among the cake samples were observed in the control sample, while the lowest score was recorded for the sample containing 0.60% propolis extract. In the sensory evaluation, the smell and taste scores of the cake samples containing 0.15% and 0.30% propolis extract, ranked second and third, respectively, received acceptable scores (greater than 2.5). On the other hand, the samples containing 0.45% and 0.60% propolis extract were deemed unacceptable by the panelists, as they received scores lower than 2.5 (Fig. 6).

To provide an overall comparison of sensory quality, a radar plot (Fig. 6) was used to simultaneously evaluate the main sensory attributes of the control cake and cakes containing 0.15% and 0.30% propolis extract. The radar plot clearly showed that the cake containing 0.15% propolis extract achieved the

highest and most balanced sensory scores across most attributes, particularly in form and shape, surface characteristics, texture, and aroma and taste. The 0.30% propolis sample exhibited sensory properties comparable to the control, while higher propolis concentrations were excluded from the radar plot due to their lower sensory acceptance.

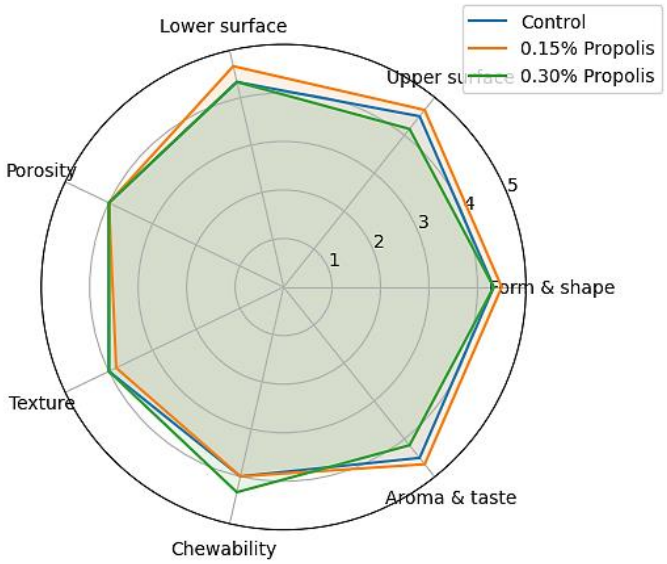

Fig. 6. Radar plot of sensory attributes of cakes containing different levels of propolis extract (control, 0.15%, and 0.30%)

Values represent the mean scores of sensory panelists for form and shape, upper and lower surface characteristics, porosity and crumb structure, texture firmness and softness, chewability, and aroma and taste.

Overall Acceptance

The overall acceptance score is the average of various sensory parameters (shape and form, characteristics of the upper and lower surfaces, porosity and crumb structure, texture firmness and softness, chewability, and smell and taste), calculated after applying the relevant weighting factors.

Sample containing 0.15% propolis extract achieved the highest overall acceptance score compared to the other samples, and this was the only sample with a higher overall acceptance score than the control sample. The overall acceptance scores of samples containing 0.30%, 0.45%, and 0.60% propolis extract were also above 2.5% (Fig. 7). The smell and taste scores of the cakes containing 0.45% and 0.60% propolis extract were below 2.5 and deemed unacceptable. Although these two samples had acceptable overall acceptance scores, they are not recommended.

Cake samples containing 0.15% and 0.30% propolis extract scored higher in terms of shape and form compared to the control sample. The 0.15% propolis extract sample also outperformed the control in terms of texture firmness and softness as well as chewability, while the 0.30% sample showed similar results to the control for these two attributes. Findings also indicated that the upper surface characteristics (crust) and crumb porosity of both propolis-containing samples were comparable to the control. However, all samples received lower scores for lower surface characteristics, aroma, and taste than control. The 0.15% and 0.30% propolis extract samples ranked second and third, respectively, in aroma and taste, following the control sample. Nonetheless, panelists considered the aroma and taste of these two samples acceptable, as their scores exceeded 2.5. There are varying results regarding the effects of propolis on the sensory characteristics of

cakes. Nasirzadeh Dizaji *et al*. (2022) reported that incorporating propolis-containing oleogel into cake formulations had no significant impact on the color and texture of the samples and did not affect their overall quality attributes. In contrast, Basturk *et al*. (2023) found that cakes made with propolis oleogel were less acceptable than the control sample. According to their findings, the most negative impact of propolis was on the aroma and taste of the cakes. Similarly, Hosseinizadeh *et al*. (2020) reported comparable results, stating that propolis extract and its increased levels in oil cakes did not negatively affect sensory attributes such as color, texture, and chewability. However, the addition of propolis extract led to a significant decrease in aroma and taste scores.

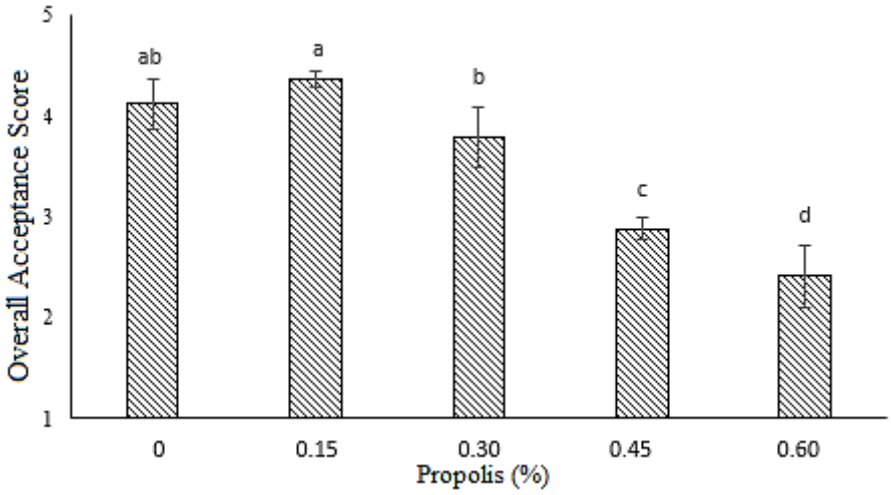

Fig. 7. Effect of different levels of propolis extract on overall cake acceptance score
Like letters are not statistically significant at the P<0.05 level.

Microbial Properties of Propolis-Containing Cake Samples

The results of the study on the antimicrobial effects of propolis in oil cakes showed that after 7 days of storage, all propolis-containing cake samples remained free of mold. From day 14 onward, the mold levels in these samples remained within the acceptable microbial load limits. In contrast, mold growth in the control sample was detected after 7 days, exceeding the permissible standard limits. Additionally, cakes containing 0.45% and 0.6% propolis showed no mold growth even after 12 days of storage (Table 6). These findings indicated that propolis enhances the shelf life of oil cakes due to its antimicrobial properties. Researchers suggest that natural antimicrobial compounds, due to their bioactive components, penetrate the lipid membranes of cells and mitochondria, leading to the leakage of cellular contents and, ultimately, microbial cell death (Bouchelaghem, 2022). Propolis significantly reduced mold growth at a 5% significance level compared to the control sample. Afsharian Torghabeh, Sheikholeslami, & Ataye Salehi, (2016) conducted a study to compare the antimicrobial properties of orange peel essential oil with potassium sorbate, a common chemical preservative, in oil cakes. Their findings revealed that the lowest levels of mold and yeast were observed in samples containing orange essential oil extracted using ultrasound waves at 90% intensity for 5 minutes, as well as in samples containing potassium sorbate. This suggests that orange essential oil can effectively compete with potassium sorbate as a preservative. Similarly, Tajik *et al*. (2017) investigated the effects of green tea and lime essential oils on the physicochemical, microbial, and sensory properties of oil cakes over 28 days of storage.

Their results showed that no mold or yeast growth was detected in samples containing 0.2% and 0.3% lime and green tea essential oils throughout the storage period. Kringel *et al*. (2021) evaluated the antifungal activity of free and encapsulated orange essential oil against Aspergillus spp. The study found that orange essential oil inhibited the growth of all tested Aspergillus species, with minimum inhibitory concentration values ranging from 45.24 to 90.47 mg/mL. Incorporating the essential oil into cakes delayed fungal spoilage from 30 to 150 days, highlighting its effectiveness as a natural antifungal agent in bakery products. Sharayei and Azarpazhooh (2022) optimized the microencapsulation of apple pomace extract and examined its antimicrobial effects in oil cakes. Their findings indicated that the optimal wall composition for microencapsulation included 33.41% maltodextrin (DE 7), 35.384% pectin, and 30.75% maltodextrin (DE 20). The encapsulated apple pomace extracts effectively controlled mold and yeast growth while maintaining the sensory properties of the cake. The lowest mold and yeast growth after 9 days of storage at room temperature was observed in samples containing 4500 mg/L of microencapsulated extract, which was comparable to the effect of 100 mg/L potassium sorbate.

Table 5- Effect of different concentrations of propolis on total mesophilic microorganisms count (Log cfu/g) during 21-day storage

Sample	Production day	7th day	14th day	21st day
Control	0.00 ^{dA}	3.00 ^{aB}	4.30 ^{aC}	4.50 ^{aD}
0.15%	0.00 ^{cA}	0.00 ^{bA}	1.68 ^{bB}	1.75 ^{bC}
0.30%	0.00 ^{cA}	0.00 ^{bA}	1.30 ^{cB}	1.48 ^{cC}
0.45%	0.00 ^{cA}	0.00 ^{bA}	1.00 ^{dB}	1.30 ^{cC}
0.60%	0.00 ^{cA}	0.00 ^{bA}	1.00 ^{dB}	1.18 ^{cC}

Different lowercase letters in each column indicate significant differences among treatments at the same storage time ($P < 0.05$). Different uppercase letters in each row indicate significant differences among storage times within the same treatment ($P < 0.05$).

Table 6- Effect of different concentrations of propolis on mold count (Log cfu/g) during 21-day storage

Sample	Production day	7th day	14th day	21st day
Control	0.00 ^{aA}	2.79 ^{aB}	4.23 ^{aC}	4.38 ^{aD}
0.15%	0.00 ^{bA}	0.00 ^{bA}	1.40 ^{bB}	1.60 ^{bC}
0.30%	0.00 ^{bA}	0.00 ^{bA}	1.00 ^{cB}	1.17 ^{cC}
0.45%	0.00 ^{bA}	0.00 ^{bA}	0.00 ^{dA}	0.00 ^{dA}
0.60%	0.00 ^{bA}	0.00 ^{bA}	0.00 ^{dA}	0.00 ^{dA}

Different lowercase letters in each column indicate significant differences among treatments at the same storage time ($P < 0.05$). Different uppercase letters in each row indicate significant differences among storage times within the same treatment ($P < 0.05$).

Both total mesophilic microorganisms and mold counts were significantly affected by propolis concentration and storage time ($P < 0.05$). In all samples, microbial counts increased significantly during storage; however, at each storage time, cakes containing propolis showed significantly lower microbial growth compared to the control. The highest inhibitory effect was observed in samples containing 0.45% and 0.60% propolis, in which mold growth was completely inhibited throughout storage. The total mesophilic microorganism count increased in all cake samples over time, reaching its highest level by the end of the third week of storage (Table 5). The highest microbial count was observed in the control sample, which showed a statistically significant difference from other samples ($p < 0.05$). However, on the production day, there was no significant difference in microbial count among the samples ($p > 0.05$). Increasing the amount of

propolis in the cake formulation resulted in a lower microbial count. Furthermore, no significant statistical difference ($p > 0.05$) was observed in the total microbial count of propolis-containing samples on days 14 and 21. Research on the antimicrobial activity of medicinal plants and bee-derived products indicates a growing preference for natural preservatives over chemical ones. Propolis, due to its flavonoid content, exhibits antioxidant activity. Its medicinal effects include hepatoprotective and anticancer properties, anti-inflammatory and cytostatic effects, immune system enhancement, and anti-allergenic benefits (Fernández-Calderón *et al*., 2021). Baghbani and Shirazi Nejad (2019) investigated the antioxidant and antimicrobial properties of date seed extract and its effects on the physicochemical, microbial, and sensory properties of cupcakes. All cakes containing different concentrations of date seed extract met standard physicochemical criteria. Sample containing 0.2% date seed extract had the lowest microbial count among the tested samples and received the highest sensory evaluation score. Similarly, Hosseinizadeh and Shirazi Nejad (2019) studied the antioxidant and antimicrobial effects of grape seed extract in sponge cakes. Their results showed that increasing the extract concentration led to a reduction in the total microbial count, confirming the extract's effectiveness in controlling microbial growth and proliferation.

Conclusion

The findings of this study indicate that incorporating propolis extract at levels exceeding 0.30% in cake formulation led to an increase in batter density. Additionally, the presence of this extract at higher concentrations contributed to improved batter consistency. Including propolis extract in the formulation enhanced moisture retention in the cake samples during baking and throughout the storage period (two weeks). However, all cake samples exhibited a reduction in moisture content over time, with the control sample experiencing the highest moisture loss compared to the other formulations. Samples containing 0.15% and 0.30% propolis extract exhibited the highest specific volume and porosity, along with the lowest firmness, within two hours post-baking. Cake formulated with 0.30% propolis extract maintained the lowest firmness after one week, whereas samples containing 0.30% and 0.45% propolis extract exhibited the lowest firmness levels after two weeks of storage. Notably, all cake samples remained softer than the control sample throughout the storage period. Furthermore, the inclusion of propolis extract affected the color of the crust of the cakes. As the concentration of propolis extract increased, the L* and a* color parameters decreased, while the b* parameter increased, resulting in a darker overall appearance of the cake samples. Sensory evaluation results indicated that cakes containing 0.15% and 0.30% propolis extract received comparable or superior scores relative to the control sample in terms of shape, texture firmness and softness, chewability, upper surface characteristics (crust), and porosity. However, the lower surface characteristics, aroma, and taste of these two formulations (0.15% and 0.30%) received slightly lower scores than the control sample, though they remained within the acceptable range according to the sensory panel. Overall, cakes formulated with 0.15% and 0.30% propolis extract were identified as the most promising samples in this study, demonstrating optimal technological and sensory properties. Among the tested formulations, the incorporation of 0.30% ethanolic propolis extract was determined to be the most effective treatment, providing optimal antifungal activity while maintaining desirable physicochemical properties and acceptable sensory characteristics. Therefore, this concentration can be recommended as a natural antifungal preservative for cake formulations.

Author Contributions

Najmeh Adelipour: investigation (equal); software (supporting); writing – original draft (lead). **Masoomeh Mehraban Sang Atash**: Conceptualization (lead); methodology (lead); resources (lead); visualization (equal); writing–review, and editing (equal). **Hanieh Yarabbi**: Formal analysis (equal); methodology (equal); project administration (equal); software (lead); supervision (lead); writing, review, and editing (lead). **Bahareh Sahraiyan**: Formal analysis (equal); methodology (equal); project administration (equal); software (lead); supervision (lead).

Founding Source

This research was supported by the Food Science and Technology Department of the Kashmar Jihad University Institute of Higher Education under grant number 3/1283.

Conflicts of Interest Statement

None declared.

Data Availability Statement

Our research data is available and can be easily accessed. Details of the data and how to request access are available by emailing the corresponding author.

References

1. American Association of Cereal Chemists. Approved Methods Committee. (2000). *Approved methods of the American association of cereal chemists* (Vol. 1). American Association of Cereal Chemists. https://doi.org/10.1002/star.19890411114
2. Abtahi, S.M., Mehraban, R., Bagheri, H., Fathi Najafi, M., & Islami, N. (2022). Antibacterial and mechanical properties of glass ionomer cement containing Iranian propolis. *Journal of Mashhad Dental School*, *46*(3), 188-198. https://doi.org/10.22038/jmds.2022.59140.2073
3. Afsharian Torghabe, S.A., Sheikholeslami, Z., & Ataye Salehi, E. (2016). Effect of orange peel essential oils as a natural preservative on rheological, sensory and microbial properties of cupcake. *Journal of Food Science & Technology*, *12(50)*, 1-12.
4. Ahmed, W.E., Ragab, I., Gadallah, M.G., Alhomaid, R.M., & Almujaydil, M.S. (2024). Effect of sprouting whole wheat grain on the sensory quality, physicochemical properties, and antioxidant activity of cupcakes. *Applied Food Research*, *4*(1), 100412. https://doi.org/10.1016/j.afres.2024.100412
5. Aleman, R.S., Morris, A., Prinyawiwatkul, W., Moncada, M., & King, J.M. (2022). Physicochemical properties of Frontière rice flour and its application in a gluten-free cupcake. *Cereal Chemistry*, *99*(2), 303-315. https://doi.org/10.1002/cche.10484
6. Baghbani, F., & Shirazinejad, A. (2019). Study of antioxidant and antimicrobial activity of date seed extract and its effects on physicochemical, microbial and sensory properties of cupcake. *Journal of Food Science and Technology (Iran)*, *16*(88), 327-342.
7. Basturk, A., Badem, S., & Ceylan, M.M. (2023). Propolis and carnauba wax-based safflower oil oleogels as fat substitutes in cakes: Production, oxidative stability, and characterization. *European Journal of Lipid Science and Technology*, 200-213. https://doi.org/10.1002/ejlt.202200213
8. Bouchelaghem, S. (2022). Propolis characterization and antimicrobial activities against *Staphylococcus aureus* and *Candida albicans*: A review. *Saudi Journal of Biological Sciences*, *29*(4), 1936-1946. https://doi.org/10.1016/j.sjbs.2021.11.063
9. Bozdogan, N., Ormanli, E., Kumcuoglu, S., & Tavman, S. (2022). Pear pomace powder added quinoa-based gluten-free cake formulations: effect on pasting properties, rheology, and product quality. *Food Science and Technology*, *42*, e39121. https://doi.org/10.1590/fst.39121

10. de Queiroz, A.G., Ramos, E.G., Armond, C., Felipini, R.B., & Di Piero, R.M. (2024). Coating based on gelatin and propolis for the control of anthracnose in postharvest of bell pepper. *Food Control*, *166*, 110689. https://doi.org/10.1016/j.foodcont.2024.110689
11. Fernández-Calderón, M.C., Hernández-González, L., Gómez-Navia, C., Blanco-Blanco, M.T., Sánchez-Silos, R., Lucio, L., & Pérez-Giraldo, C. (2021). Antifungal and anti-biofilm activity of a new Spanish extract of propolis against *Candida glabrata*. *BMC Complementary Medicine and Therapies*, *21(1)*, 1-10. https://doi.org/10.1186/s12906-021-03323-0
12. Garzoli, S., Maggio, F., Vinciguerra, V., Rossi, C., Donadu, M.G., & Serio, A. (2023). Chemical characterization and antimicrobial properties of the hydroalcoholic solution of *Echinacea purpurea* (L.) Moench. and propolis from Northern Italy. *Molecules*, *28*(3), 1380. https://doi.org/10.3390/molecules28031380
13. Gucwa, K., Kusznierewicz, B., Milewski, S., Van Dijck, P., & Szweda, P. (2018). Antifungal activity and synergism with azoles of polish propolis. *Pathogens*, 7(2), 56-63. https://doi.org/10.3390/pathogens7020056
14. Hassan, E.M., Fahmy, H.A., Magdy, S., & Hassan, M.I. (2020). Physicochemical and sensorial characterization of gluten-free cupcakes. *Egyptian Journal of Nutrition*, *35*(1), 33-64. https://doi.org/10.21608/ENJ.2020.144755
15. Heghedűş-Mîndru, R.C., Glevitzky, M., Heghedűş-Mîndru, G., Dumitrel, G.A., Popa, M., Popa, D.M., & Vică, M.L. (2023). Applications of Romanian propolis in phyto-inhibitory activity and antimicrobial protection: A comparative study. *Antibiotics*, *12*(12), 1682. https://doi.org/10.3390/antibiotics12121682
16. Hoseinizadeh, Z., Pedram Nia, A., Saeidi Asl, M.R., & Dovlat Abadi, Z. (2020). Optimization of the cupcake formulation with lamb wax extract and guar gum. *Journal of Innovation in Food Science and Technology*, *12(4)*, 31-40.
17. Hoseinzadeh, F., & Shirazinejad, A. (2019). Study of antioxidant and antimicrobial properties of grape seed extract and evaluation of its sensory characteristics in sponge cake. *Journal of Food Science and Technology (Iran)*, *15*(85), 165-178.
18. Hosseini Khabbazi, S., Mansouripour, S., & Saremnezhad, S. (2023). The effect of propolis extract as a vaaluable natural additive on the quality characteristics of toast bread. *Food Science & Nutrition*, *11*(9), 5438-5445. https://doi.org/10.1002/fsn3.3500
19. HTTPS://www.reportlinker.com/dataset/8ae025c2298d3358a3f31f7f1a50337df1655a81.
20. Ike, C.C., Emeka-Ike, P.C., & Ogwuegbu, H.O. (2020). Sensory properties, physical and microbiological studies of pumpkin seed (*Cucurbita pepo*) blended cakes. *GSC Biological and Pharmaceutical Sciences*, *12*(3), 073-081. https://doi.org/10.30574/gscbps.2020.12.3.0224
21. ISO 4833-1. (2013). Microbiology of the food chain- Horizontal method for the enumeration of microorganisms- Part 1: Colony count at 30 °C by the pour plate technique. https://doi.org/10.3403/30229853u
22. Kringel, D.H., Lang, G.H., Dias, Á.R.G., Gandra, E.A., Valente Gandra, T.K., & da Rosa Zavareze, E. (2021). Impact of encapsulated orange essential oil with β-cyclodextrin on technological, digestibility, sensory properties of wheat cakes as well as *Aspergillus flavus* spoilage. *Journal of the Science of Food and Agriculture*, *101*(13), 5599-5607. https://doi.org/10.1002/jsfa.11211
23. Milinčić, D.D., Kostić, A.Ž., Stanojević, S.P., & Pešić, M.B. (2024). Techno-functional properties of pollen. In *Pollen Chemistry & Biotechnology*, 291-318. Cham: Springer International Publishing. https://doi.org/10.1007/978-3-031-47563-4_14
24. Nasirzadeh Dizaji, R., Rofehgarinezhad, L., Tabibiazar, M., & Alizadeh, A. (2022). Preparation of the soybean structured oil based on propolis wax and its feasibility as shortening

replacer in cakes. *Iranian Journal of Nutrition Sciences & Food Technology*, *17*(3), 67-76. https://doi.org/10.1007/s11694-024-02840-z

25. Olamaeian, N., Kouhdar, V., & Hosseini, H. (2022). Assessment of the antimicrobial effects of propolis from Taleghan region on foodborne pathogenic bacteria. *Iranian Journal of Nutrition Sciences & Food Technology*, *17*(2), 99-107.
26. Papp, Z., Bouchelaghem, S., Szekeres, A., Meszéna, R., Gyöngyi, Z., & Papp, G. (2021). The scent of antifungal propolis. *Sensors, 21(7),* 23-34. https://doi.org/10.3390/s21072334
27. Pasukamonset, P., Pumalee, T., Sanguansuk, N., Chumyen, C., Wongvasu, P., Adisakwattana, S., & Ngamukote, S. (2018). Physicochemical, antioxidant and sensory characteristics of sponge cakes fortified with *Clitoria ternatea* extract. *Journal of Food Science and Technology*, *55*(8), 2881-2889. https://doi.org/10.1007/s13197-018-3204-0
28. Pyrgioti, E., Graikou, K., Cheilari, A., & Chinou, I. (2022). Assessment of antioxidant and antimicrobial properties of selected greek propolis samples (North East Aegean Region Islands). *Molecules*, *27*(23), 8198. https://doi.org/10.3390/molecules27238198
29. Refaat, H., Mady, F.M., Sarhan, H.A., Rateb, H.S., & Alaaeldin, E. (2021). Optimization and evaluation of propolis liposomes as a promising therapeutic approach for COVID-19. *International Journal of Pharmaceutics*, *592*, 120028. https://doi.org/10.1016/j.ijpharm.2020.120028
30. Rezaei Boroojerdi, S., Habibi Najafi, M.B., Hosseini, F., & Karazhyan, R. (2018). In vitro evaluation of anti-mold activity of annatto natural dye. *Iranian Food Science and Technology Research Journal*, *14(4)*, 533-541. https://doi.org/10.4315/0362-028x.jfp-17-533
31. Sahraiyan, B., Pourhaji, F., & Alizadeh Behbahani, B. (2021). Evaluation of the effect of cheese powder and ultrasonic wave on physicochemical and sensory properties of gluten-free oil cake. *Iranian Food Science & Technology Research Journal/Majallah-i Pizhūhishhā-yi ʿUlūm va Sanāyiʿ-i Ghaẕāyī-i Īrān*, *17*(4). https://doi.org/10.22067/ifstrj.v17i4.86707
32. Salem, M., El-Zayet, F., Rayan, A., & Shatta, A. (2024). Physicochemical and sensory properties of gluten-free cupcakes produced with pearl millet flour and cactus mucilage powder as a new natural hydrocolloid. *Journal of Chemistry and Nutritional Biochemistry*, *5(1)*, 25-36. https://doi.org/10.48185/jcnb.v5i1.1090
33. Scanlon, M.G., & Koksel, F. (2024). The role of bubbles and interfaces in the quality of foamed cereal products. *Current Opinion in Colloid & Interface Science*, *73*, 101843. https://doi.org/10.1016/j.cocis.2024.101843
34. Sharayei, P., & Azarpazhooh, E. (2022). Optimization of microencapsulation of pomace apple extract and evaluation of its antimicrobial properties in the food model (oily cake). *Food Engineering Research*, *20(2)*, 31-48.
35. Shokri, H., Katiraee, F., Fatahinia, M., & Minooeianhaghighi, M.H. (2017). Chemical composition and antifungal potential of Iranian propolis against Candida krusei strains. *Journal of Apicultural Research*, *56(5)*, 581-587. https://doi.org/10.1080/00218839.2017.1371534
36. Tahmouzi, S., Meftahizadeh, H., Eyshi, S., Mahmoudzadeh, A., Alizadeh, B., Mollakhalili-Meybodi, N., & Hatami, M. (2023). Application of guar (*Cyamopsis tetragonoloba* L.) gum in food technologies: A review of properties and mechanisms of action. *Food Science & Nutrition*, *11*(9), 4869-4897. https://doi.org/10.1002/fsn3.3383
37. Tajik, Z., Nateghi, L., & Berenji, S. (2017). The effect of green tea and lemon essential oils on the physicochemical, microbial, and sensory properties of oily cake. *Journal of Food Industry Research (Iran)*, *27(3)*, 113-125.
38. Vică, M.L., Glevitzky, M., Dumitrel, G.A., Bostan, R., Matei, H.V., Kartalska, Y., & Popa, M. (2022). Qualitative characterization and antifungal activity of Romanian honey and propolis. *Antibiotics*, *11(11)*, 1552. https://doi.org/10.3390/antibiotics11111552

39. Zampini, I.C., Salas, A.L., Maldonado, L.M., Simirgiotis, M.J., & Isla, M.I. (2021). Propolis from the Monte region in Argentina: A potential phytotherapic and food functional ingredient. *Metabolites*, *11*(2), 76. https://doi.org/10.3390/metabo11020076

نشریه پژوهشهای علوم و صنایع غذایی ایران
https://ifstrj.um.ac.ir

مقاله پژوهشی

جلد ۲۲، شماره ۳، مرداد- شهریور ۱۴۰۵، ص. ۲۸۳-۲۶۱

کاربرد عصاره اتانولی بره‌موم به‌عنوان نگهدارنده طبیعی ضدقارچ: تأثیر بر ویژگی‌های فیزیکوشیمیایی، میکروبی و حسی کیک فنجانی

نجمه عادلی‌پور[۱]- معصومه مهربان سنگ آتش[۲*]- هانیه یاربی[۳]- بهاره صحراییان[۲]

تاریخ دریافت: ۱۴۰۴/۰۹/۲۶
تاریخ پذیرش: ۱۴۰۴/۱۲/۰۳

چکیده

استفاده گسترده از افزودنی‌های غذایی شیمیایی موجب افزایش نگرانی‌ها در خصوص اثرات نامطلوب احتمالی آن‌ها بر سلامت مصرف‌کنندگان شده است. در این راستا، گرایش روزافزون به سوی ترکیبات ضدمیکروبی طبیعی، زمینه‌ساز معرفی بره‌موم به‌عنوان جایگزینی مناسب برای نگهدارنده‌های سنتتیک گردیده است. هدف از این پژوهش بررسی تأثیر عصاره اتانولی بره‌موم (EPE) به‌عنوان یک عامل ضدقارچ طبیعی بر ویژگی‌های فیزیکوشیمیایی، میکروبی و حسی کیک فنجانی بود. بدین منظور، عصاره اتانولی بره‌موم در سطوح ۰/۱۵، ۰/۳، ۰/۴۵ و ۰/۶ درصد به فرمولاسیون خمیر کیک افزوده شد و خصوصیات کیفی نمونه‌ها مورد ارزیابی قرار گرفت. نتایج نشان داد افزودن EPE در سطوح بالاتر از ۰/۳ درصد موجب افزایش دانسیته و قوام خمیر کیک گردید. همچنین حضور عصاره بره‌موم سبب بهبود نگهداشت رطوبت در طول فرآیند پخت و دوره نگهداری دو هفته‌ای شد، به‌طوری‌که نمونه شاهد بیشترین کاهش رطوبت را نشان داد. کیک‌های حاوی ۰/۱۵ و ۰/۳ درصد EPE بیشترین حجم ویژه و تخلخل و کمترین سفتی (دو ساعت پس از پخت) را در مقایسه با سایر تیمارها دارا بودند. تمامی نمونه‌های حاوی EPE در طول دوره نگهداری بافت نرم‌تری نسبت به شاهد حفظ کردند. از نظر رنگ پوسته، افزایش غلظت EPE موجب کاهش مقادیر L* و a* و افزایش مقدار b* شد که بیانگر تیره‌تر شدن رنگ کیک‌ها بود. ارزیابی حسی نشان داد نمونه‌های حاوی ۰/۱۵ و ۰/۳ درصد عصاره بره‌موم از نظر شکل، بافت، نرمی، جویدگی، ویژگی‌های سطحی و تخلخل تفاوت معنی‌داری با یکدیگر نداشتند و اگرچه امتیاز طعم و عطر آن‌ها اندکی کمتر از نمونه شاهد بود، اما همچنان در محدوده قابل قبول قرار داشت. به‌طور کلی، کاپ‌کیک‌های حاوی ۰/۱۵٪ و ۰/۳۰٪ عصاره پروپولیس الکلی به‌عنوان فرمولاسیون‌های بهینه شناسایی شدند، که در میان آن‌ها، ۰/۳۰٪ EPE بهترین تعادل را بین اثربخشی ضدقارچی، کیفیت فیزیکوشیمیایی و پذیرش حسی ارائه می‌دهد و آن را به یک نگهدارنده طبیعی امیدوارکننده برای محصولات نانوایی تبدیل می‌کند. نتایج حاکی از آن است که عصاره اتانولی بره‌موم پتانسیل بالایی برای استفاده به‌عنوان نگهدارنده طبیعی با خاصیت ضدقارچی در فرمولاسیون کیک دارد.

واژه‌های کلیدی: اثر ضدقارچی، پایداری میکروبی، عصاره بره‌موم، کیک فنجانی، نگهدارنده طبیعی، ویژگی‌های حسی

۱- گروه علوم و صنایع غذایی، مؤسسه آموزش عالی جهاد دانشگاهی کاشمر، کاشمر، ایران
۲- پژوهشکده علوم و صنایع غذایی، جهاد دانشگاهی واحد خراسان رضوی، مشهد، ایران
(*- نویسنده مسئول: Email: mehraban@acecr.ac.ir)
۳- گروه علوم و صنایع غذایی، دانشکده کشاورزی، دانشگاه فردوسی مشهد، مشهد، ایران

https://doi.org/10.22067/ifstrj.2026.97040.1533

Iranian Food Science and Technology Research Journal
Homepage: https://ifstrj.um.ac.ir

Research Article
Vol. 22, No. 3, July- August. 2026, p. 285-302

Optimization of Conventional and Superheated Solvent Extraction Methods for Extracting Polyphenolic Compounds from *Salvia leriifolia* Leaves

M. Sarabi-Jamab[1*], E. Mansouri[1], A. Bostan[2]

1- Department of Food Biotechnology, Research Institute of Food Science and Technology, Mashhad, Iran
(*- Corresponding Author Email: m.sarabi@rifst.ac.ir)
2- Department of Food Nanotechnology, Research Institute of Food Science and Technology, Mashhad, Iran

Received:	26.12.2025
Revised:	21.03.2026
Accepted:	12.04.2026
Available Online:	19.05.2026

How to cite this article:
Sarabi-Jamab, M., Mansouri, E., & Bostan, A. (2026). Optimization of conventional and superheated solvent extraction methods for extracting polyphenolic compounds from *Salvia leriifolia* leaves. *Iranian Food Science and Technology Research Journal*, *22*(3), 285-302. https://doi.org/10.22067/ifstrj.2026.97188.1537

Abstract

The efficiency of an extraction procedure in recovering bioactive phenolic compounds is highly dependent on its mechanism and operating conditions. Polyphenols were extracted from *Salvia leriifolia* leaves using conventional solvent extraction and also superheated extraction techniques. The faced central composite experimental design of response surface methodology (RSM) applied to evaluate the effects of the solvent ratio, temperature, and time on both the process yield and total phenolic content. Optimization revealed that the modification in the extraction technology greatly affected the procedure. According to the results, the superheated solvent method was significantly more efficient compared to the conventional solvent extraction, and the highest yield of 53.29 % and total phenolic content of 737.21 mg GAE/g E were obtained under the optimal conditions (25.17 % ethanolic solvent at the extraction temperature of 160 °C for 28.97 min). In contrast, the optimization of conventional solvent extraction method revealed a maximum extraction yield and total phenolics of 30.96 % and 693.23 mg GAE/g E, respectively (using 50 % ethanolic solvent at the extraction temperature of 82.57 °C for 103.31 min). This is the first report on optimizing the superheated solvent extraction of phenolic compounds from *Salvia leriifolia* leaves.

Keywords: Conventional extraction, Polyphenols, Response surface methodology (RSM), *Salvia leriifolia*, Superheated solvent extraction

https://doi.org/10.22067/ifstrj.2026.97188.1537

Introduction

The *Salvia* genus is part of the Nepetoideae subfamily within the Mentheae tribe of the Lamiaceae family. Various *Salvia* species are recognized for their high polyphenol levels and medicinal uses (Jia *et al*., 2019; Loizzo *et al*., 2010; Tepe *et al*., 2004). *Salvia leriifolia* is an endemic perennial herbaceous plant native to the south-tropical areas of Khorasan and Semnan provinces in Iran (Hosseinzadeh, Sadeghnia, Imenshahidi, & Fazly Bazzaz, 2009; Shahi, Abrishamchi, Radjabian, & Salami, 2025). The plant was included in Florica Iranica in 1982 and is known by several local names (Nouroozak, Jobleh, etc.) (Modarres *et al*., 2014). Recently, many pharmacological and preservative properties of this plant—including hypoglycemic, analgesic, anti-inflammatory, anticonvulsant, anti-ulcer, antioxidant, and antibacterial effects—have been successfully assessed (Farhoush, Rahimzadeh, Pourazarang, & Seyedi, 2004; Hosseinzadeh *et al*., 2009; Loizzo *et al*., 2010; Modarres & Yazdi, 2021; Shahi *et al*., 2025). Plant extraction is a complex procedure designed to isolate high-quality active compounds from plant tissues. Nowadays, enzymatic, mechanical, and thermal extraction methods have been improved or customized based on the chemical nature and amount of bioactive compounds (such as polyphenols) and also available facilities (Patel, Dave, & Patel, 2021). Conventional extraction methods primarily rely on solvent-based extraction techniques (Alara, Abdurahman, & Ukaegbu, 2021; Adamez, Samino, Sanchez, & Gonzalez-Gomez, 2012; Hayrapetyan, Hazeleger, & Beumer, 2012; Sagdic, Ozturk, & Kisi, 2012). In this method, the crude powder is soaked in a specific solvent and agitated frequently for a set period to dissolve the soluble bioactive material (Patel *et al*., 2021). Despite being simple and widely applied, conventional extraction methods require long processing times, high solvent volumes, and may co-extract unwanted constituents. These drawbacks have led to the adoption of modern instrumentation techniques, resulting in remarkable progress in making the extraction process more efficient and precise (Da Porto, Porretto, & Decorti, 2013; Wijngaard, Ballay, & Brunton, 2012). Superheated solvent extraction is an eco-friendly technique that may serve as an alternative to traditional solvent extraction. In this method, an aqueous or organic solvent is heated and pressurized below its critical point, making it suitable for extracting a broad range of analytes in both polar and non-polar forms. The basis of the superheated solvent extraction method is the application of high pressure (between 4 and 20 MPa) to keep the solvent in a liquid state at temperatures above its normal boiling point. Under these conditions, the solvent penetration in the solid matrix, the diffusivity of analytes to the outer space, and the solubility of the analytes in the solvent are enhanced, which facilitates the extraction process. The use of a combination of temperature and pressure allows the extraction to be carried out quickly and in a short time. (Azmir *et al*., 2013; Morales-Munoz, Luque-Garcıa, & de Castro, 2003; Wijngaard *et al*., 2012). Based on the literature review, superheated extraction overcomes several drawbacks of conventional solvent extraction, thereby improving both selectivity and extraction efficiency. By lowering solvent viscosity and surface tension, this technique enhances extraction rate and decreases solvent consumption (Alupului, Calinescu, & Lavric, 2012). Performing the process without exposure to air or light substantially reduces oxidation and degradation of phenolic compounds (Oubannin *et al*., 2024; Japon-Lujan & de Castro, 2006; Luque-Rodríguez, de Castro, & Pérez-Juan, 2007). Also, the elevated temperature in a relatively short time employed in such extraction method enhances the solubility of certain fractions and mass transfer rates, while weakening and disrupting the matrix-analyte interactions (Wong, Khoiroh, Gan, & Croft, 2025). This extraction method has previously been employed to recover phenolic bio actives from numerous plant and fruit sources (e.g., red grape stems (Wenzel *et al*., 2015), citrus

fruits (Ledesma-Escobar, Priego-Capote, & de Castro, 2015), olive leaves and pomace (Cea Pavez *et al*., 2019; Japon-Lujan & de Castro, 2006), pomegranate peel (Rahnemoon, Sarabi Jamab, Javanmard Dakheli, Bostan, & Safari, 2018)). Based on our knowledge, this is the first application of this technique for extracting phenols from *Salvia leriifolia* leaves. This study focused on optimizing superheated solvent extraction for isolating phenolic compounds from *Salvia leriifolia* leaves. The effects of extraction condition (solvent ratio, time and temperature) upon the process yield and total phenolic content were determined and compared with those obtained using the conventional extraction method. As this species is endemic to the Khorasan region of Iran, optimization of the extraction conditions offers considerable potential for providing a variety of polyphenolic compounds.

Materials and Methods

Materials

Salvia leriifolia leaves were collected from Mashhad surrounding highlands, Iran; and the samples botanical type were confirmed. The gallic acid, $CaCl_2$, Na_2Co_3, and Folin–Ciocalteu reagent were prepared from Sigma-Aldrich (USA). Deionized water, methanol, Ethanol, and all other chemicals applied in this research were of analytical grade.

Preparation of Fresh *Salvia leriifolia* Leaves for Extraction

In brief, fresh *Salvia leriifolia* leaves were cleaned and air dried to the moisture content of 9.94±0.05 % (based on dry matter content) at room temperature. The dried leaves were then powdered and sieved using a 35-mesh sieve to obtain a fine powder. Then they were placed in sealed jars and stored in a dry and dark place until use.

Conventional Solvent Extraction

For conventional extraction of phenols, ethanol and water were utilized as solvents. The ratio of leave powder to the solvent was 10% w/v. Different levels of ethanol: water ratios (50:50, 40:60, and 30:70), temperatures (70, 80, and 90 °C), and times (30, 75, and 120 min) were examined to modify the extraction procedure. The solvents and the process conditions were chosen based on pre-experiments. After extraction, the mixture was filtered and centrifuged (3000×g / 10 min); then dried at 40 °C under the pressure of 0.8 bar in a vacuum oven (Gallenkamp, UK) for 5-8 h (based on the solvent ratios). In our study, the dry matter content of the powder obtained after extractions was 95%, so 5% of the solvent still remained in the powder (Hayrapetyan *et al*., 2012).

Superheated Solvent Extraction

Based on pre-treatments, the leaves powder was extracted with a mixture of water and ethanol in the ratios of 60:40, 80:20 and 100:0. Three extraction times (10, 20 and 30 min) were used at three different temperatures (130, 145 and 160 °C), and the extraction solid: liquid ratio (leaves powder to the solvent) was 10% w/v. The procedure was carried out using a laboratory-built extraction apparatus (RIFST, Iran) equipped with a sample cell and a high-pressure pump. The schematic of superheated solvent extraction device is shown in Fig. 1. The design of the extractor is such that it is capable enough to withstand high pressures, helps to maintain the solvent in a liquid state at a high temperature. In the heater, the solvent is heated to the desired temperature and introduced to the extractor contacting takes place between the substance and the solvent to dissolve the constituents in the fluid. The system pressure was maintained at a range of 5 to 15 bar during the process given by a nitrogen tank (based on the other extraction parameters). The fluid leaving the extractor is then cooled in a cooler. Finally, fresh extract is filtered, centrifuged and then dried (40 °C/0.8 bar (Aliakbarian, Fathi, Perego, & Dehghani, 2012; Garcia-Marino, Rivas-Gonzalo, Ibanez, & Garcia-Moreno, 2006).

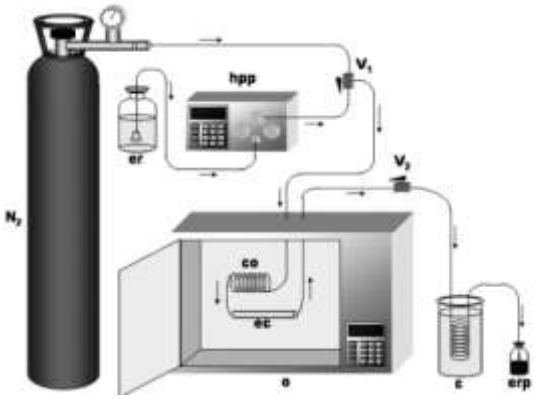

Fig. 1. Schematic of superheated solvent extraction device (Rodrıguez et al, 2007).
er: solvent vessel; hpp: high pressure pump; co:heating coil; ec: extraction cell; o: oven; c: chiller, erp; extract collection vessel, v1; selection valve, v2; restrictor valve.

The Extraction Yield

The yield of extractions was calculated using following equation:

$$\text{Yield (g/100 g)} = (W_1/W_2) \times 100 \quad \text{(Equation 1)}$$

Where W_1 is the weight of dried extract after the solvent removal and W_2 is the weight of *Salvia leriifolia* leaves powder.

Total Phenolic Content

Modified Folin–Ciocalteu method was used to determine the total phenols (Singleton & Stikeleather, 1999). According to the method, 1 g of sample powder was dissolved in 10 ml solvent (water/ethanol), and diluted in 1:10 ratio. Then the obtained filtered solution (100 µl), and aqueous Folin-Ciocalteu solution (10% v/v / 1 ml) were mixed in a volumetric flask. The mixture final volume was adjusted to 10 ml using distilled water. After 3 min, 1 ml of NaHCO3 solution (7.5% w/v) was added to the mixture and the sample incubated in the dark (25 °C/ 1 h). Finally, the absorbance was measured at 760 nm by UV-Vis spectrophotometer (Cecil CE 2040, cecil instruments, Cambridge, England). The calibration curve was created by measuring the light absorption of the solutions at various known concentrations of gallic acid (0.1, 0.2, 0.3, 0.4, 0.5, 0.6, 0.7, 0.8 and 0.9 ml of the standard gallic acid stock solution (1000 g/ml of gallic acid)). The perfect fit established with the R^2 of 0.995 in a linear regression model. Total phenolic content was expressed as milligrams of gallic acid equivalents per gram of dried extract (mg GAE/g E).

HPLC Analysis of the Extract Phenolic Compounds

Three main phenolic compounds in *Salvia leriifolia* plant (rosmarinic acid, salvianolic acid, caffeic acid) were used as the respective reference compounds (Modarres, Esmaeilzadeh Bahabadi, & Taghavizadeh Yazdi, 2018; Vishwakarma, Singh, Shukla, Singh, & Singh, 2013). By a Smartline HPLC (Kenuer, Germany), phenolic compounds were quantified. This instrument equipped with a pump (S2100) and a UV-Vis detector (UV (2489)). The selected wavelength was 330 nm and the samples were filtered (0.45 µm) before injection to the system. For the analysis, C18 column (5 µm × 150 mm × 4.6 mm) was used at room temperature (20 ˚C) with phosphoric acid (1%) and methanol as the mobile phase (60:40 v/v). The flow rate was 1.8 mL/min and the injection volume was 20 µL. The extract samples were injected three times to HPLC and for each phenolic compound, the determination was done using the corresponding calibration curve (1-100 µg/ml).

Statistical Analysis

To determine the relationship between the variable factors and responses and also

optimize the extraction methods, faced central composite design (faced-CCD) with the six replicates of a central point were applied using Version 7 of Design-Expert software (Stat-Ease, Inc., Minneapolis, USA). Temperature (X_1), time (X_2) and the ratio of solvents (water to ethanol) (X_3) were chosen as three independent variables for both extraction methods (conventional extraction with solvent and superheated solvent extraction) with two dependent variables (responses) including yield as Y1 and Y3 and total phenolic content as Y_2 and Y_4 for conventional and superheated extraction respectively. There was a total of 20 runs for optimizing the parameters. The stepwise regression model was developed to optimize the favorable process factors and suitable equation was fitted for obtained response in each analysis; in which, β_0 was constant and β_i (β_1, β_2 and β_3), β_{ii} (β_{11}, β_{22} and β_{33}) and β_{ij} (β_{12}, β_{13} and β_{23}) were linear, quadratic and interaction coefficients, respectively. To evaluate the accuracy of the optimized model, P-value, Lack of fit, R^2, Adjusted-R^2, and CV were calculated.

Results and Discussion

Optimization of *Salvia leriifolia* Leaves Extraction

Conventional Solvent Extraction

The experimental design with encoded values and the responses for each analysis were presented in Table 1. To determine the optimal conditions of the three factors (temperature, time, and water: ethanol ratio) towards conventional solvent extraction method, three levels of time (30, 75 and 120 min), temperature (70, 80 and 90 ˚C) and water: ethanol ratio (50:50, 60:40 and 70:30) were chosen based on our pre-experiments (Table 1).

Table 1- Design matrix for three independent variables in conventional solvent extraction method

Run	Variables			Run	Variables		
	Temperature (˚C)	Time (min)	Water: Ethanol ratio		Temperature (˚C)	Time (min)	Water: Ethanol ratio
1	80	30	60:40	11	80	75	60:40
2	80	75	60:40	12	70	30	50:50
3	70	120	50:50	13	70	120	70:30
4	90	120	50:50	14	80	120	60:40
5	90	30	50:50	15	70	30	70:30
6	70	75	60:40	16	80	75	60:40
7	80	75	50:50	17	80	75	70:30
8	90	75	60:40	18	80	75	60:40
9	80	75	60:40	19	90	30	70:30
10	90	120	70:30	20	80	75	60:40

According to the results (Table 2), the linear model was found to be a good fitting model for the efficiency of extraction; and the evaluation of the coefficients in various terms indicated that the changes in the levels of time and temperature had significant effects on EY % ($p<0.05$).

The analysis of the data showed that the Lack of fit value was not significant, and the high amounts of R^2 (0.991), and Adj-R^2 (0.989) indicated that the linear model was properly accurate for predicting the efficiency of the yield of conventional extraction process. The obtained R^2 and Adj-R^2 values implied a strong relationship, explaining about 99% of the variance in the dependent variable. The EY % was calculated using the following equation:

$$Y_1 = -13.327 + 0.475\ X_1 + 0.053\ X_2 - 0.008\ X_3 \quad \text{(Equation 2)}$$

Where Y_1 is EY % response and X_1, X_2 and X_3 are temperature, time and water: ethanol ratio, respectively.

As shown in Fig. 2, temperature changes, compared to the other independent variables, had the greatest effect on the EY %. With an increase in level of this factor, from 70 to 90 ˚C, EY % increased by 10 %.

Table 2- Results of regression analysis for extraction yield and total phenolic content in conventional solvent extraction

Source	df	Extraction yield			df	Total phenolic content		
		Equation coefficient	Sum of squares	p-value		Equation coefficient	Sum of squares	p-value
Linear model	3	-13.327	282.53	0.000	9	-17648.632	707600.5	0.000
X_1	1	0.475	226.29	0.000	1	468.810	474.86	0.000
X_2	1	0.053	56.17	0.000	1	19.627	125000.5	0.000
X_3	1	-0.008	0.074	0.501	1	-44.155	471.14	0.767
Quadratic model								
X_1X_1					1	-2.751	208200.5	0.000
X_2X_2					1	-0.067	50539.38	0.010
X_3X_3					1	0.620	10536.82	0.183
Interaction model								
X_1X_2					1	-0.076	9314.08	0.209
X_1X_3					1	-0.037	10890.67	0.177
X_2X_3					1	0.017	481.90	0.766
Residual	16		2.50		10		51651.15	
Lack of Fit	11		1.90	0.364	5		40728.16	0.087
Total	19		285.04		19		759300.5	
R^2		0.991				0.932		
Adj-R^2		0.989				0.871		
CV		1.40				9.30		

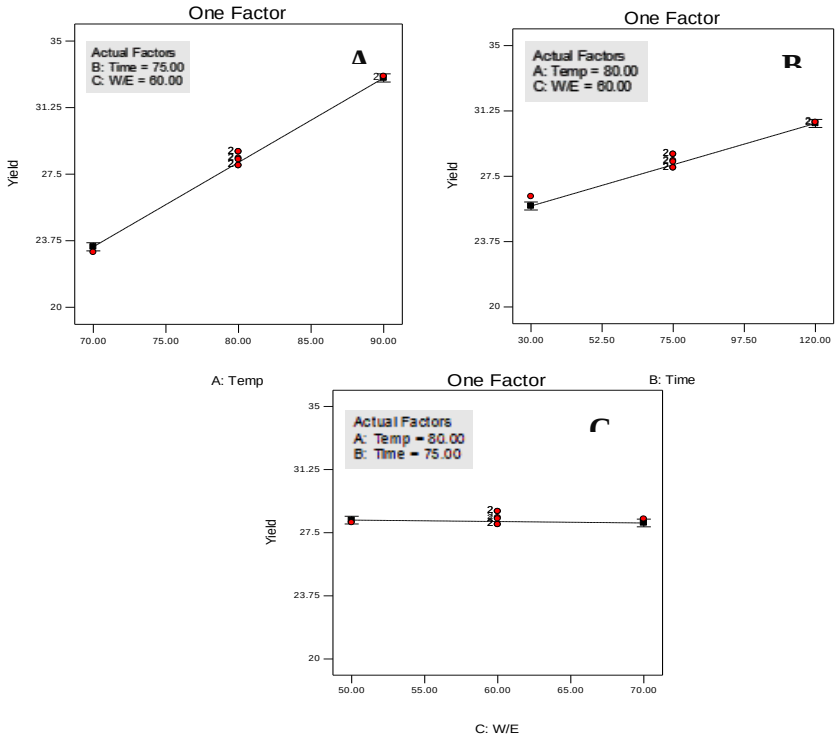

Fig. 2. The Scatter plot of extraction yield (EY) vs. predicted level of Temperature (A), Time (B) and water:ethanol ratio (C) in conventional extraction method

*Temp= temperature; W/E= water:ethanol ratio.

Design and data of optimal experiments (Table 2) showed that the time factor at the linear level as well as the temperature factor at both linear and quadratic levels affect significantly ($p<0.05$) on the amount of total phenolic content.

The coefficients of the independent variables are displayed in an equation as follows:

$$Y_2 = -17648.632 + 468.810\ X_1 + 19.627\ X_2 - 44.155\ X_3 + 0.076\ X_1X_2 - 0.037\ X_2X_3 + 0.017\ X_2X_3 - 2.751\ X_1^2 - 0.067\ X_2^2 + 0.620\ X_3^2 \quad \text{(Equation 3)}$$

where Y_2 is the total phenol (mg GAE/g extract) and X_1, X_2 and X_3 are temperature, time and water: ethanol ratio, respectively.

The 3D response surface graphs of the combined effects of time, temperature and the solvent ratio on the extracted phenolic compounds are shown in Fig. 3. Based on the results, increasing the extraction time to 120 min had a positive effect on the total phenolic content, with a greater effect in the range of 30-75 min compared to 75-120 min (Fig. 3-A and 3-C). The figure illustrated that as the temperature increased from 70 to 80 ˚C, the total phenols increased along with the temperature; whereas in the range of 80 to 90 ˚C, the extract total phenols decreased (Fig. 3-A and 3-B). As the data showed, the extraction solvent ratio did not have a significant effect ($p\geq0.05$) on the total phenols (Fig. 3-B and 3-C).

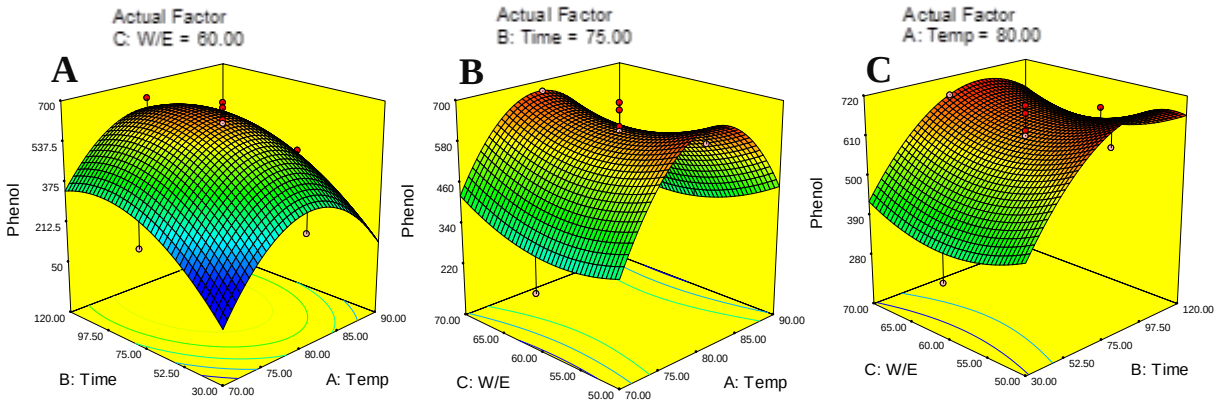

Fig. 3. Response surface for the effect of independent variables including temperature to time (A), temperature to the solvents ratio (B) and time to the solvents ratio (C) on the total phenolic content in Conventional extraction method

*Temp= temperature; W/E= water:ethanol ratio.

In a study, Tan, Tan, & Ho (2013) optimized the conditions used for extracting total phenolic compounds from the Henna plant. They reported that prolonging the extraction time increased significantly the total phenolic yield up to 270 min, after which it gradually decreased and reached its lowest level at 360 min. They suggested that after some time, an equilibrium may form between the solute level in the plant matrix and the solvent that slows down the extraction yield. Moreover, the extended extraction periods may enhance the degradation or oxidation of phenolic compounds because of prolonged exposure to environmental elements such as light. Wang *et al*. (2011) examined how variations in solvent type and temperature affect the extraction of total phenolics from pomegranate peel. In mentioned research, by boosting the temperature from 25 to 95 ˚C, the amount of phenolic compounds was increased. Tomsik *et al*. (2017) noted that elevating the temperature alters the physicochemical behavior of water, making its characteristics more like organic solvents and thereby improving extraction yield. During the

extraction procedure, polyphenols and other bioactive compounds in the matrix will be dissolved by the solvent (based on their polarities). The extraction solvent can affect the release of the target compound into the solution. The present study used ethanol and water, both of which are polar, food-grade solvents suitable for extracting phenolic compounds. Our results indicated a significant interaction between the extraction parameters and the amount of phenolic compounds obtained from *Salvia leriifolia* leaves. Different levels of the extraction yield were typically obtained due to the differences in the solvent polarity and the process parameters, which affect the solubility of the sample's chemical constituents and their extraction (Butsat & Siriamornpun, 2016). Throughout the process, the changes in the process parameters, such as temperature, time, type of solvent, etc., affect the phenolic extraction by changing both the diffusion coefficient and solubility (Al-Farsi & Lee, 2008; Chew, Ng, Thoo, & Khoo, 2011; Li, Wong, Cheng, & Chen, 2008). However, temperature exerts a stronger influence on polyphenol extraction yield compared to other variables (solvents ratio and time). This is primarily because elevated temperatures simultaneously reduce solvent viscosity and surface tension, enhance solute solubility, accelerate mass transfer and diffusion rates, and improve penetration into the plant matrix as well as desorption kinetics. While solvent ratio mainly affects equilibrium partitioning and time influences diffusion duration (after a certain point), temperature directly impacts multiple physicochemical processes simultaneously, leading to more pronounced yield increases. This dominant role of temperature is well-supported in the literature on various extraction techniques, including ultrasound-assisted, microwave-assisted, and pressurized liquid extraction methods (Lopez-Salas, Exposito-Almellon, Borras-Linares, Lozano-Sanchez, & Segura-Carretero, 2024; Osorio-Tobón, 2020; Tomasi, Santos, Boaventura, & Botelho, 2023).

Superheated Solvent Extraction

Three variables of extraction: temperature (130, 145 and 160 C), time (10, 20 and 30 min) and water: ethanol ratio (60:40, 80:20 and 100:0), were chosen (Table 3) to determine the optimal conditions for the extraction efficiency and total phenolic content towards superheated solvent extraction method.

Table 3- Design matrix for three independent variables in superheated solvent extraction method

Run	Variables			Run	Variables		
	Temperature (˚C)	Time (min)	Water: Ethanol ratio		Temperature (˚C)	Time (min)	Water: Ethanol ratio
1	160	10	60:40	11	145	30	80:20
2	145	20	80:20	12	130	10	60:40
3	130	20	80:20	13	145	20	80:20
4	145	20	80:20	14	145	20	80:20
5	130	30	100:0	15	160	30	100:0
6	160	30	60:40	16	145	20	80:20
7	145	20	100:0	17	130	30	60:40
8	145	20	60:40	18	160	20	80:20
9	145	20	80:20	19	145	10	80:20
10	160	10	100:0	20	130	10	100:0

Table 4 shows the analysis of variance for extraction efficiency and total phenolic content in superheated solvent extraction technique. Considering the EY % and phenolic compounds experimental results, the non-linear quadratic multivariate model was the predictor model for independent variables, and their interaction and quadratic effects (equation 4 and equation 5).

The calculated R^2 and CV values were 0.980 and 1.47 for the EY % and 0.991 and 5.40 for the total phenolic content, respectively. The results for each of the response factor were described by the following non-linear equations:

$Y_3 = 135.127 -1.788 X_1 -0.0323 X_2 +0.438 X_3 -1.867 X_1X_2 -1.308 X_1X_3 +7.610 X_1^2 +0.013 X_2^2 –1.594 X_3^2$ (Equation 4)

Where Y_3 is EY % the response for three independent variables (X_1= temperature, X_2 = time and X_3 = water: ethanol ratio).

$Y_4 = 11158.175 -184.060 X_1 +20.238 X_2 +16.265 X_3 -0.043 X_1X_2 -0.031 X_1X_3 +0.014 X_2X_3 +0.664 X_1^2 -0.307 X_2^2 –0.078 X_3^2$ (Equation 5)

Where Y_4 is the total phenolic content response and X_1, X_2 and X_3 are the temperature, time and water: ethanol ratio, respectively.

Table 4- Results of regression analysis for extraction yield and total phenolic content in superheated solvent extraction method

Source	Extraction yield				Total phenolic content			
	df	Equation coefficient	Sum of squares	p-value	df	Equation coefficient	Sum of squares	p-value
Linear model	8	135.127	274.05	0.000	9	-11158.184	574869	0.000
X_1	1	-1.788	172.39	0.000	1	-175.060	466923	0.000
X_2	1	-0.032	45.80	0.000	1	20.238	7678	0.003
X_3	1	0.438	0.18	0.535	1	16.265	602	0.304
Quadratic model								
X_1X_1	1	7.610	8.06	0.001	1	0.664	63141	0.000
X_2X_2	1	0.013	4.59	0.008	1	-0.307	5774	0.048
X_3X_3	1	-1.595	1.12	0.144	1	-0.078	2680	0.045
Interaction model								
X_1X_2	1	-1.867	0.63	0.263	1	-0.043	335	0.438
X_1X_3	1	-1.308	1.23	0.127	1	-0.031	685	0.278
X_2X_3					1	0.014	60	0.739
Residual	11		4.98		10		5128	
Lack of Fit	6		4.25	0.051	5		3982	0.099
Total	19		252.03		19		552997	
R^2		0.980				0.991		
Adj-R^2		0.966				0.982		
CV		1.47				5.40		

As shown in Table 4, superheated solvent extraction revealed significant effects of the linear and quadratic terms of time and temperature on the extraction yield ($p<0.05$). For total phenolic content, the linear and quadratic terms of time and temperature, along with the quadratic term of the water: ethanol ratio, were significant ($p<0.05$).

Fig. 4 (4-A and 4-B) illustrates the effects of process time and temperature on the extraction yield. The change in temperature from 130 ˚C to 160 ˚C caused a sharp increase in the value of EY %. The changes in the extraction time (from 10 to 30 min) had similar effects on the EY %, although the rate of increase was lower (Fig. 4-A).

The effects of temperature and solvent ratio at the fixed extraction time (20 min) were shown in Fig. 4-B. As the temperature increased, the level of EY % also increased, while increasing the water: ethanol ratio had no significant effect ($p\geq0.05$) on EY %. Observing the effects of various levels of water: ethanol ratio, the highest yield was obtained in the 80:20 ratio of water to ethanol.

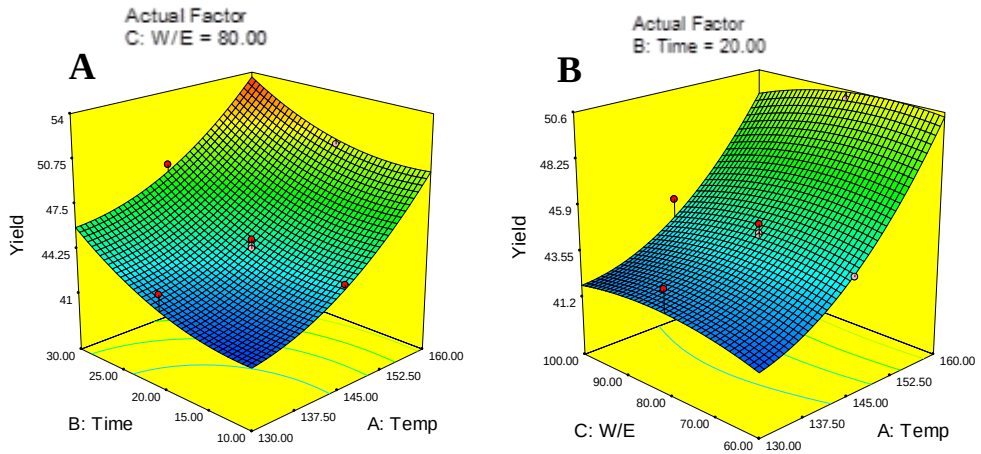

Fig. 4. Response surface for the effect of independent variables including temperature to time (A), temperature to the solvents ratio (B) on the extraction yield (EY %) in superheated solvent extraction method
*Temp= temperature; W/E= water:ethanol ratio.

Fig. 5 (5-A, 5-B and 5-C) illustrates the effects of three independent variables on the total phenolic content. The maximum level of phenols was found when the temperature increased to 160 ˚C. Treatments with water to solvent ratio ranging from 60 % to 80 %, increased total phenolic content ($p<0.05$), whereas the higher ratios (ranging from 80 % to 100 %) decreased the level of total phenols. As a result, it could be concluded that increasing the water concentration in the solvent (to an optimum level) enhanced the phenolic extraction, and the combination of organic solvent and water portions can improve the extraction of both components that are soluble in water or organic solvent (Cavalcanti *et al*., 2021; Oubannin *et al*., 2024). As illustrated in Fig. 5-A and 5-C, increasing the process time from 10 min to 20 min led to a significant increase ($p<0.05$) in the total phenolic content. This result is consistent with existing literature on plant extraction optimization, which have demonstrated that the extraction time significantly affects the total phenolic content of the extract (Hamad & Hartanti, 2023; Malenica, Kass, & Bhat, 2025).

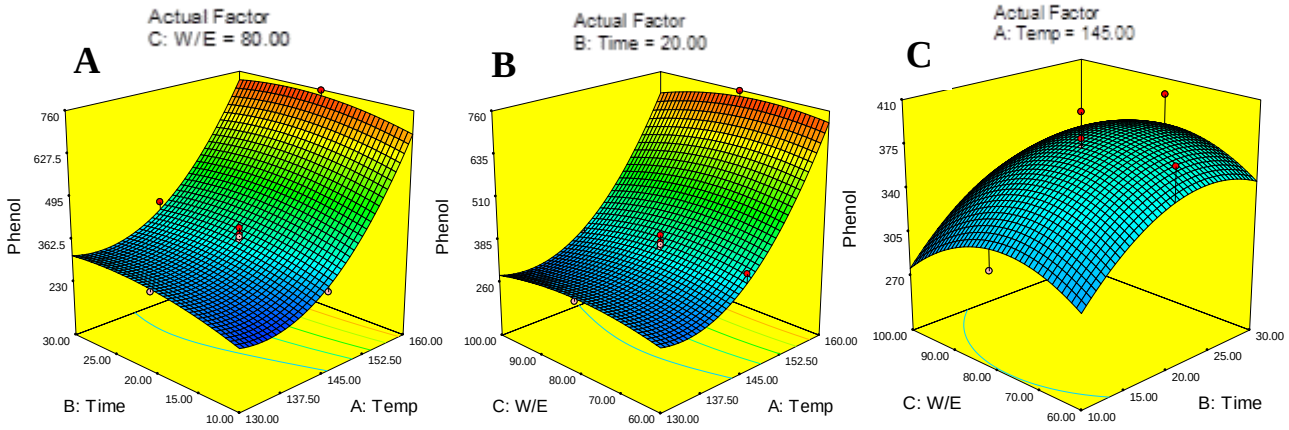

Fig. 5. Response surface for the effect of independent variables including temperature to time (A), temperature to the solvents ratio (B) and time to the solvents ratio (C) on the total phenolic content in the extract in superheated solvent extraction method
*Temp= temperature; W/E= water:ethanol ratio.

Application of instrumentation extraction techniques, such as superheated solvent, can reduce the extraction time and increase the final yield (Patel *et al*., 2021). Longer extraction combined with higher temperatures can increase the possibility of undesirable reactions (hydrolysis, enzymatic oxidation of the phenolic compounds, etc.) and consequently affect the level of extracted polyphenols (Oubannin *et al*., 2024; Biesaga & Pyrzynska, 2013). The high temperature and pressure used in the superheated solvent method lead to a change in the polarity of the solvent, which makes it possible to extract both polar and non-polar bioactive compounds from the plant tissue (Cavalcanti *et al*., 2021; Shang, Kim, & Um, 2014). In addition, in such conditions, the solvent permeability into the plant cells increases during the extraction and the highest extraction output is achieved over a shorter period of time (Khan, Aslam, & Makroo, 2019).

The Optimal Parameters Calculated after Implementation of the Design

Evaluating the design information provides an efficient way to assess and optimize the process parameters in a minimum number of experimental runs (Nde & Foncha, 2020). Following the implementation of the experimental design, optimization studies were conducted to determine the main process parameters for both conventional and superheated solvent extraction techniques. The independent variables, specifically the extraction temperature, time, and water: ethanol ratio, were optimized to maximize the extraction yield and total phenolic content.

The optimized parameters, presented in Table 5, were derived from a comprehensive evaluation of the design information, enabling efficient process optimization with the minimal numbers of experimental runs. Considering the design points of each model, the outcome indicated the efficiency of the superheated method in *Salvia leriifolia* leaves extraction.

Table 5- Optimal predicted conditions of *Salvia leriifolia* leaves extraction using conventional and superheated solvent method

The type of extraction	Temperature (˚C)	Time (min)	Water: Eethanol ratio	Yield	Total phenolic content	Desirability
Conventional method	82.57	103.31	50:50	30.96	693.23	0.949
Superheated solvent method	160.00	28.97	74.83:25.17	53.29	737.21	0.960

The optimal conditions for obtaining the highest phenolics and process yield were determined to be the water: ethanol ratio of 50:50 and 74.83:25.17, temperature of 82.57 and 160 °C, and time of 103.31 and 28.97 min for the conventional and superheated solvent extraction methods, respectively. In order to validate the optimal conditions represents by design-expert software, the extraction yield and the phenolic compounds content were measured on experimentally. Based on the optimal conditions of the conventional extraction method, the yield was 29.51% and the total phenols was 569.74 mg GAE/g E; While the yield and phenolic compounds based on the optimal conditions of the extraction using the superheated solvent method were 52.38% and 730.65 mg GAE/g E, respectively. After doing the t-test, there was no significant difference between the data obtained from the software and experimental tests.

Based on our findings, increasing the extracted polyphenols content and the process yield can be achieved using superheated solvent extraction, which has the advantage of time/resources saving compared to the conventional method. This result showed a similarity with the investigations of Eikani, Golmohammad, & Homami (2012), Luque-

Rodriguez, Perez-Juan, & Luque De Castro (2006), Mijangos-Ricardez & Lopez-Luna (2013), and Rahnemoon *et al*. (2018), who found the superheated solvent extraction as a superior method with a high polyphenol extraction amount. Mijangos–Ricardez & López–Luna (2021) applied superheated liquid extraction to isolate phenolic compounds, specifically flavonoids and anthocyanins, from vinification lees. They optimized the extraction parameters (temperature, time, ethanol percent in the extractant and the extractant flow rate), and their findings indicated that superheated liquid extraction reduced the extraction time for flavonoids and anthocyanins compared to the conventional maceration method. Uzel (2018) used a mixture of water and alcohol in the extraction of olive leaves (at 180 ˚C) and showed that the superheated method has the highest recovery of bioactive organic compounds (phenol oleuropein). Rosales-Castro, Honorato-Salazar, Reyes-Navarrete, & Gonzalez-Laredo, (2015) studied *A. fraxinifolius* bark tree extracts (the ethanolic and hot water extraction) and the yields and total phenolic content were measured. Based on the results, there was a significant direct correlation between the yield and total phenolic concentration, where it was higher in young tree barks compared to the extract from mature tree barks.

Analysis of Phenolic Compounds

As mentioned at section 2.5, rosmarinic acid, salvianolic acid and caffeic acid are the three main phenolic compounds in *Salvia leriifolia* plant (Hosseinpoor Mohsen Abadi, Mahdavi, & Rezaei-Seresht, 2016; Modarres *et al*., 2018), therefore, the respective reference compounds were used in this research. The evaluation of phenols in the optimized samples was performed by comparing the HPLC analysis and the retention time with those obtained from standard solutions and the data reported in the relevant literature. HPLC chromatograms of the extracts displayed two major peaks with retention times of approximately 4.28 and 8.74 min, which corresponded to caffeic acid and rosmarinic acid, respectively (Table 6). No salvianolic acid was detected in any of the extract samples.

Table 6- HPLC analysis data for standard phenolic compounds detected in *Salvia leriifolia* leaves extract (conventional extraction and superheated solvent extraction method)

Extraction method	Salvianolic acid	Caffeic acid			Rosmarinic acid		
		Retention time(min)	Peak area (%)	Quantification (g/100 g dried extract)	Retention time(min)	Peak area (%)	Quantification (g/100 g dried extract)
Conventional extraction	Not detected	4.30	6.09	0.03	8.78	93.91	1.18
Superheated solvent extraction	Not detected	4.28	2.35	0.05	8.74	97.65	6.04

Based on our results, the content of caffeic acid was determined as 0.03 and 0.05 g/100 g dried extract using conventional and superheated solvent extraction techniques, respectively. Modarres *et al*. (2014) reported 0.15, 0.20, and 0.07 mg/g dry extract of caffeic acid in root, leaf, and callus extracts of *Salvia leriifolia*, respectively, using 60% aqueous ethanol as solvent. According to the literature, there is only a limited number of studies on the presence of salvianolic acids in *Salvia* species, most of which report trace or very low levels (Hao *et al*., 2012; Wang *et al*., 2014; Wu, Zhu, Zhang, Yang, & Zhou, 2012). Furthermore, the plant age was shown to significantly affect phenolic content (Shahi *et al*., 2025). In the present study, the highest rosmarinic acid level was observed in leaf extracts, with a value of

1.18 g/100 g dried extract using the conventional method and 6.04 g/100 g dried extract using the superheated solvent method. Modarres *et al*. (2014) identified rosmarinic acid as the primary phenolic constituent, with a content of 0.33, 4.65 and 6.39 mg/g dried extract in root, leaf, and callus of *Salvia leriifolia*, respectively. Shahi *et al*. (2025) and Vishwakarma *et al*. (2013) similarly concluded that rosmarinic acid constitutes a major portion of polyphenolic compounds in *Salvia* species and exhibits strong antioxidant properties.

Conclusion

In this research, RSM was employed to optimize the extraction of phenolic compounds from *Salvia leriifolia* leaves using both conventional and superheated solvent methods. Based on the analysis of variance (ANOVA) results and high correlations coefficients, the developed regression models proved highly effective in predicting key process variables (extraction time, temperature, solvent ratio) and maximizing total polyphenol yield and content. The superheated solvent technique demonstrated superior efficiency compared to the traditional approach. To achieve the highest extraction yield and total phenolic content, the recommended condition for *Salvia leriifolia* leaves was superheated solvent extraction at 74.83: 25.17 (v/v) water:ethanol mixture and 160 °C for 28.97 minutes. The HPLC analysis of the optimized treatments revealed significantly higher levels of total phenolic content (mainly rosmarinic acid and caffeic acid) in the superheated solvent extracts than in those obtained by the conventional method. In addition to the above results, further studies should focus on exploring the scalability and industrial applicability of the superheated solvent extraction for utilization in food and pharmaceutical sectors.

Author Contributions

Mahboobe Sarabi-Jamab: Methodology, Investigation, Formal analysis, Project administration, Editing. **Elaheh Mansouri:** Conceptualization, Investigation, Writing. **Aram Bostan:** Methodology, Editing.

Founding Source

This work is based upon research funded by Dr. M. Modarres and also Research Institute of Food Science and Technology (RIFST) under project No. 24095003.

References

1. Adamez, J.D., Samino, E.G., Sanchez, E.V., & Gonzalez-Gomez, D. (2012). In vitro estimation of the antibacterial activity and antioxidant capacity of aqueous extracts from grape-seeds (*Vitis vinifera* L.). *Food Control, 24*(1-2), 136-141. https://doi.org/10.1016/j.foodcont.2011.09.016
2. Al-Farsi, M.A., & Lee, C.Y. (2008). Optimization of phenolics and dietary fibre extraction from date seeds. *Food Chemistry, 108*(3), 977-985. https://doi.org/10.1016/j.foodchem.2007.12.009
3. Alara, O.R., Abdurahman, N.H., & Ukaegbu, C.I. (2021). Extraction of phenolic compounds: A review. *Current Research in Food Science, 4*, 200-214. https://doi.org/10.1016/j.crfs.2021.03.011
4. Aliakbarian, B., Fathi, A., Perego, P., & Dehghani, F. (2012). Extraction of antioxidants from winery wastes using subcritical water. *The Journal of Supercritical Fluids, 65*, 18-24. https://doi.org/10.1016/j.supflu.2012.02.022
5. Alupului, A., Calinescu, I., & Lavric, V. (2012). Microwave extraction of active principles from medicinal plants. *UPB Science Bulletin, Series B, 74*(2), 129-142. available at: http://www.scientificbulletin.upb.ro/rev_docs_arh/2012-2-full/13_Alupului_129_142.pdf
6. Azmir, J., Zaidul, I.S.M., Rahman, M.M., Sharif, K.M., Mohamed, A., Sahena, F., Jahurul, M.H. A., Ghafoor, K., Norulaini, N.A.N., & Omar, A.K.M. (2013). Techniques for extraction

of bioactive compounds from plant materials: A review. *Journal of Food Engineering, 117*(4), 426-436. https://doi.org/10.1016/j.jfoodeng.2013.01.014
7. Biesaga, M., & Pyrzynska, K. (2013). Stability of bioactive polyphenols from honey during different extraction methods. *Food Chemistry, 136*(1), 46-54. https://doi.org/10.1016/j.foodchem.2012.07.095
8. Butsat, S., & Siriamornpun, S. (2016). Effect of solvent types and extraction times on phenolic and flavonoid contents and antioxidant activity in leaf extracts of *Amomum chinense* C. *International Food Research Journal, 23*(1). available at: http://www.ifrj.upm.edu.my/contents.php?volume=23&issue=1)
9. Cavalcanti, V.P., Aazza, S., Bertolucci, S.K.V., Rocha, J.P.M., Coelho, A.D., Oliveira, A.J.M., Mendes, L.C., Pereira, M.M.A., Morais, L.C., Forim, M.R., Pasqual, M., & Dória, J. (2021). Solvent mixture optimization in the extraction of bioactive compounds and antioxidant activities from garlic (*Allium sativum* L.). *Molecules, 26*(19), 6026. https://doi.org/10.3390/molecules26196026
10. Cea Pavez, I., Lozano-Sánchez, J., Borrás-Linares, I., Nuñez, H., Robert, P., & Segura-Carretero, A. (2019). Obtaining an extract rich in phenolic compounds from olive pomace by pressurized liquid extraction. *Molecules, 24*(17), 3108. https://doi.org/10.3390/molecules24173108
11. Chew, K., Ng, S., Thoo, Y., & Khoo, M. (2011). Effect of ethanol concentration. Extraction time and extraction temperature on the recovery of phenolic compounds andantioxidant capacity of *Centella asiatica* extracts. *International Food Research Journal, 18*, 566-573. http://www.ifrj.upm.edu.my/contents.php?volume=18&issue=2)
12. Da Porto, C., Porretto, E., & Decorti, D. (2013). Comparison of ultrasound-assisted extraction with conventional extraction methods of oil and polyphenols from grape (*Vitis vinifera* L.) seeds. *Ultrasonics Sonochemistry, 20*(4), 1076-1080. https://doi.org/10.1016/j.ultsonch.2012.12.002
13. Eikani, M.H., Golmohammad, F., & Homami, S.S. (2012). Extraction of pomegranate (*Punica granatum* L.) seed oil using superheated hexane. *Food and Bioproducts Processing, 90*(1), 32-36. https://doi.org/10.1016/j.fbp.2011.01.002
14. Farhoush, R., Rahimzadeh, M., Pourazarang, H., & Seyedi, S. (2004). Extraction and separation of antioxidative compounds from *Salvia leriifolia* leaves. *Journal of Agricultural Science and Technology (JAST), 6*, 57-69. available at: http://jast.modares.ac.ir/article-23-9057-en.html)
15. Garcia-Marino, M., Rivas-Gonzalo, J.C., Ibanez, E., & Garcia-Moreno, C. (2006). Recovery of catechins and proanthocyanidins from winery by-products using subcritical water extraction. *Analytica Chimica Acta, 563*(1-2), 44-50. https://doi.org/10.1016/j.aca.2005.10.054
16. Hamad, A., & Hartanti, D. (2023). Effects of extraction time on total phenolic and flavonoid contents and antioxidant activities of a polyherbal drink. IOP Conference Series: Earth and Environmental Science, 1200, 012047. https://doi.org/10.1088/1755-1315/1200/1/012047
17. Hao, G., Ji, H., Li, Y., Shi, R., Wang, J., Feng, L., & Huang, L. (2012). Exogenous ABA and polyamines enhanced salvianolic acids contents in hairy root cultures of *Salvia miltiorrhiza* Bge. f. alba. *Plant Omics, 5*(5), 446-452. available at: http://www.pubmedcentral.nih.gov/articlerender.fcgi?tool=pmcentrez&artid=PMC3356712)
18. Hayrapetyan, H., Hazeleger, W.C., & Beumer, R.R. (2012). Inhibition of *Listeria monocytogenes* by pomegranate (*Punica granatum*) peel extract in meat paté at different temperatures. *Food Control, 23*(1), 66-72. https://doi.org/10.1016/j.foodcont.2011.06.012

19. Hosseinpoor Mohsen Abadi, Z., Mahdavi, B., & Rezaei-Seresht, E. (2016). Contents of aerial parts of *Salvia leriifolia* Benth. *Journal of Chemical Health Risks*, *6*(3). available at: https://jchr.org/index.php/JCHR/article/view/323)
20. Hosseinzadeh, H., Sadeghnia, H.R., Imenshahidi, M., & Fazly Bazzaz, B.S. (2009). Review of the pharmacological and toxicological effects of *Salvia leriifolia*. *Iranian Journal of Basic Medical Sciences, 12*(1), 1-8. https://doi.org/10.22038/ijbms.2009.5125
21. Japon-Lujan, R., & de Castro, M.L. (2006). Superheated liquid extraction of oleuropein and related biophenols from olive leaves. *Journal of Chromatography A, 1136*(2), 185-191. https://doi.org/10.1016/j.chroma.2006.09.081
22. Jia, Q., Zhu, R., Tian, Y., Chen, B., Li, R., Li, L., Wang, L., Che, Y., Zhao, D., & Mo, F. (2019). *Salvia miltiorrhiza* in diabetes: A review of its pharmacology, phytochemistry, and safety. *Phytomedicine, 58*, 152871. https://doi.org/10.1016/j.phymed.2019.152871
23. Khan, S.A., Aslam, R., & Makroo, H.A. (2019). High pressure extraction and its application in the extraction of bio-active compounds: A review. *Journal of Food Process Engineering, 42*(1), e12896. https://doi.org/10.1111/jfpe.12896
24. Ledesma-Escobar, C.A., Priego-Capote, F., & de Castro, M.D.L. (2015). Comparative study of the effect of auxiliary energies on the extraction of Citrus fruit components. *Talanta, 144*, 522-528. https://doi.org/10.1016/j.talanta.2015.07.011
25. Li, H.-B., Wong, C.-C., Cheng, K.-W., & Chen, F. (2008). Antioxidant properties in vitro and total phenolic contents in methanol extracts from medicinal plants. *LWT-Food Science and Technology, 41*(3), 385-390. https://doi.org/10.1016/j.lwt.2007.03.011
26. Loizzo, M.R., Tundis, R., Conforti, F., Menichini, F., Bonesi, M., Nadjafi, F., Statti, G.A., Tzakou, O., & Menichini, F. (2010). *Salvia leriifolia* Benth (Lamiaceae) extract demonstrates in vitro antioxidant properties and cholinesterase inhibitory activity. *Nutrition Research, 30*(12), 823-830. https://doi.org/10.1016/j.nutres.2010.09.016
27. Lopez-Salas, L., Exposito-Almellon, X., Borras-Linares, I., Lozano-Sanchez, J., & Segura-Carretero, A. (2024). Design of experiments for green and GRAS solvent extraction of phenolic compounds from food industry by-products-A systematic review. *TrAC Trends in Analytical Chemistry*, *171*, 117536. https://doi.org/10.1016/j.trac.2024.117536
28. Luque-Rodríguez, J., de Castro, M.L., & Pérez-Juan, P. (2007). Dynamic superheated liquid extraction of anthocyanins and other phenolics from red grape skins of winemaking residues. *Bioresource Technology, 98*(14), 2705-2713. https://doi.org/10.1016/j.biortech.2006.09.019
29. Luque-Rodriguez, J.M., Perez-Juan, P., & Luque De Castro, M.D. (2006). Extraction of polyphenols from vine shoots of *Vitis vinifera* by superheated ethanol− water mixtures. *Journal of Agricultural and Food Chemistry*, *54*(23), 8775-8781. https://doi.org/10.1021/jf061855j
30. Malenica, D., Kass, M., & Bhat, R. (2025). Optimization of antioxidant extraction from agro-industrial wastes using ultrasound & response surface methodology. *Food Chemistry Advances, 7*, 100966. https://doi.org/10.1016/j.focha.2025.100966
31. Mijangos-Ricardez, O.F., & Lopez-Luna, J. (2013). Superheated liquid extraction of the phenolic fraction from alperujo, a semisolid residue. available at: https://www.researchgate.net/publication/272998865)
32. Mijangos–Ricardez, O.F., & López–Luna, J. (2021). Optimization of superheated liquid extraction of the phenolic fraction from vinification lees. *Journal of Chemical, Biological and Physical Sciences, 11(3),* 351-361. https://doi.org/10.24214/jcbps.A.11.3.35161
33. Modarres, Asili, J., Lahouti, M., Gangali, A., Iranshahy, M., & Sahebkar, A. (2014). Simultaneous determination of Rosmarinc acid, Salvianolic acid B and Caffeic acid in *Salvia lerifolia* benth root, leaf and callus extracts using a high performance liquid chromatography

with diode-array detection technique. *Journal of Liquid Chromatography and Related Technologies, 37*, 1721-1730. https://doi.org/10.1080/10826076.2013.807466

34. Modarres, M., Esmaeilzadeh Bahabadi, S., & Taghavizadeh Yazdi, M.E. (2018). Enhanced production of phenolic acids in cell suspension culture of *Salvia leriifolia* Benth. using growth regulators and sucrose. *Cytotechnology, 70*(2), 741-750. https://doi.org/10.1007/s10616-017-0178-0
35. Modarres, M., & Yazdi, M.E.T. (2021). Elicitation improves phenolic acid content and antioxidant enzymes activity in *Salvia leriifolia* cell cultures. *Iranian Journal of Science and Technology, Transactions A: Science*, 1-7. https://doi.org/10.1007/s40995-021-01070-y
36. Morales-Munoz, S., Luque-Garcıa, J., & de Castro, M.L. (2003). Acidified pressurized hot water for the continuous extraction of cadmium and lead from plant materials prior to ETAAS. *Spectrochimica Acta Part B: Atomic Spectroscopy, 58*(1), 159-165. https://doi.org/10.1016/s0584-8547(02)00216-1
37. Nde, D.B., & Foncha, A.C. (2020). Optimization methods for the extraction of vegetable oils: a review. *Processes, 8*(2), 209. https://doi.org/10.3390/pr8020209
38. Osorio-Tobon, J.F. (2020). Recent advances and comparisons of conventional and alternative extraction techniques of phenolic compounds. *Journal of Food Science and Technology, 57*(12), 4299-4315. https://doi.org/10.1007/s13197-020-04433-2
39. Oubannin, S., Bijla, L., Ahmed, M.N., Ibourki, M., El Kharrassi, Y., Devkota, K., Bouyahya, A., Maggi, F., Caprioli, G., & Sakar, E.H. (2024). Recent advances in the extraction of bioactive compounds from plant matrices and their use as potential antioxidants for vegetable oils enrichment. *Journal of Food Composition and Analysis, 128*, 105995. https://doi.org/10.1016/j.jfca.2024.105995
40. Patel, M., Dave, K., & Patel, P. (2021). A review on different extraction method of plants: Innovation from ancient to modern technology. *International Journal Biology Pharmacology Allied Science, 10*(12), 511-527. https://doi.org/10.31032/IJBPAS/2021/10.12.1044
41. Rahnemoon, P., Sarabi Jamab, M., Javanmard Dakheli, M., Bostan, A., & Safari, O. (2018). Comparison of two methods of solvent extraction of phenolic compounds from pomegranate (*Punica granatum* L.) peels. *Journal of Agricultural Science and Technology, 20*(5), 939-952. https://doi.org/10.1016/j.fbio.2021.101331
42. Rosales-Castro, M., Honorato-Salazar, J.A., Reyes-Navarrete, M.G., & Gonzalez-Laredo, R.F. (2015). Antioxidant phenolic compounds of ethanolic and aqueous extracts from pink cedar (*Acrocarpus fraxinifolius* Whight & Arn.) bark at two tree ages. *Journal of Wood Chemistry and Technology, 35*(4), 270-279. https://doi.org/10.1080/02773813.2014.946619
43. Sagdic, O., Ozturk, I., & Kisi, O. (2012). Modeling antimicrobial effect of different grape pomace and extracts on *S. aureus* and *E. coli* in vegetable soup using artificial neural network and fuzzy logic system. *Expert Systems with Applications, 39*(8), 6792-6798. https://doi.org/10.1016/j.eswa.2011.12.047
44. Shahi, N.N., Abrishamchi, P., Radjabian, T., & Salami, S.A. (2025). Impact of plant age on phenolic acids production in *Salvia leriifolia* Benth. as medicinal plant: Insights into the contributions of enzymes and biosynthetic pathways. *South African Journal of Botany, 184*, 794-805. https://doi.org/10.1016/j.sajb.2025.05.021
45. Shang, Y.F., Kim, S.M., & Um, B.-H. (2014). Optimisation of pressurised liquid extraction of antioxidants from black bamboo leaves. *Food Chemistry, 154*, 164-170. https://doi.org/10.1016/j.foodchem.2013.12.050
46. Singleton, J., & Stikeleather, L. (1999). A solvent extractor system for the rapid extraction of lipids and trace bioactive micronutrients in oilseeds. *Journal of the American Oil Chemists' Society, 76*(12), 1461-1466. https://doi.org/10.1007/s11746-999-0185-1

47. Tan, M.C., Tan, C.P., & Ho, C.W. (2013). Effects of extraction solvent system, time and temperature on total phenolic content of henna (*Lawsonia inermis*) stems. *International Food Research Journal*, *20*(6), 3117. available at: https://www.researchgate.net/publication/266081397_Effects_of_extraction_solvent_system_time_and_temperature_on_total_phenolic_content_of_henna_Lawsonia_inermis_stems
48. Tepe, B., Donmez, E., Unlu, M., Candan, F., Daferera, D., Vardar-Unlu, G., . . . Sokmen, A. (2004). Antimicrobial and antioxidative activities of the essential oils and methanol extracts of *Salvia cryptantha* (Montbret et Aucher ex Benth.) and *Salvia multicaulis* (Vahl). *Food Chemistry, 84*(4), 519-525. https://doi.org/10.1016/S0308-8146(03)00267-X
49. Tomasi, I.T., Santos, S.C., Boaventura, R.A., & Botelho, C.M. (2023). Optimization of microwave-assisted extraction of phenolic compounds from chestnut processing waste using response surface methodology. *Journal of Cleaner Production, 395*, 136452. https://doi.org/10.1016/j.jclepro.2023.136452
50. Tomšik, A., Pavlić, B., Vladić, J., Cindrić, M., Jovanov, P., Sakač, M., Mandić, A., & Vidović, S. (2017). Subcritical water extraction of wild garlic (*Allium ursinum* L.) and process optimization by response surface methodology. *The Journal of Supercritical Fluids*, *128*, 79-88. https://doi.org/10.1016/j.supflu.2017.05.012
51. Uzel, R.A. (2018). Effect of extraction method and extraction solvent on recovery of phenolic compounds from olive leaves in Kemalpaşa-İzmir (Turkey): Oleuropein recovery as a case example. *Separation Science and Technology, 53(10),* 1531-1539. https://doi.org/10.1080/01496395.2018.1442861
52. Vishwakarma, S., Singh, P., Shukla, M., Singh, U., & Singh, R. (2013). Antioxidant activities of some tuberous plant leaves. *International Journal of Pharmaceutical Sciences Review and Research, 20*(1), 28. available at: http://www.ijpsr.com/bft-article/antioxidant-activities-of-some-tuberous-plant-leaves/)
53. Wang, T., Zhang, H., Wang, L., Jiang, Y., Zhang, L., Zhou, Y., Yang, R., Ding, C., & Wang, X. (2014). A simple and reliable method for distinguishing danshen in salvia: simultaneous quantification of six active compositions by HPLC. *Journal of Chromatographic Science*, *52*(9), 992-998. https://doi.org/10.1093/chromsci/bmt140
54. Wang, Z., Pan, Z., Ma, H., & Atungulu, G.G. (2011). Extract of phenolics from pomegranate peels. *The Open Food Science Journal*, *5*(1). https://doi.org/10.2174/1874256401105010017
55. Wenzel, J., Samaniego, C.S., Wang, L., Nelson, L.S., Ketchum, K., Ammerman, M., & Zand, A. (2015). Superheated liquid and supercritical denatured ethanol extraction of antioxidants from Crimson red grape stems. *Food Science & Nutrition, 3*(6), 569-576. https://doi.org/10.1002/fsn3.246
56. Wijngaard, H.H., Ballay, M., & Brunton, N. (2012). The optimisation of extraction of antioxidants from potato peel by pressurised liquids. *Food Chemistry*, *133*(4), 1123-1130. https://doi.org/10.1016/j.foodchem.2011.01.136
57. Wong, J.C.J., Khoiroh, I., Gan, S., & Croft, A.K. (2025). Deep eutectic solvents for protein extraction: mechanisms, performance, and green metrics. *Journal of Molecular Liquids*, 128636. https://doi.org/10.1016/j.molliq.2025.128636
58. Wu, W., Zhu, Y., Zhang, L., Yang, R., & Zhou, Y. (2012). Extraction, preliminary structural characterization, and antioxidant activities of polysaccharides from *Salvia miltiorrhiza* Bunge. *Carbohydrate Polymers, 87*(2), 1348-1353. https://doi.org/10.1016/j.carbpol.2011.09.024

نشریه پژوهشهای علوم و صنایع غذایی ایران
https://ifstrj.um.ac.ir

مقاله پژوهشی

جلد ۲۲، شماره ۳، مرداد- شهریور، ص. ۳۰۲-۲۸۵

بهینه‌سازی روش‌های استخراج متداول با حلال و فوق داغ جهت استخراج ترکیبات پلی‌فنلی از برگ گیاه نوروزک

محبوبه سرابی جماب[1*]- الهه منصوری[1]- آرام بستان[2]

تاریخ دریافت: ۱۴۰۴/۱۰/۰۵

تاریخ پذیرش: ۱۴۰۵/۰۱/۲۳

چکیده

کارایی روش استخراج در بازیابی ترکیبات فنلی زیست‌فعال به شدت به مکانیسم و شرایط عملیاتی آن وابسته است. پلی‌فنول‌ها از برگ‌های گیاه نوروزک با استفاده از روش‌های متداول استخراج با حلال و فوق داغ استخراج شدند. طرح آزمایشی مرکب مرکزی از روش آماری سطح پاسخ برای ارزیابی اثرات نسبت حلال، دما و زمان بر بازده فرآیند و محتوای فنلی کل به کار گرفته شد. بهینه‌سازی نشان داد که اصلاح در فرآیند استخراج تا حد زیادی بر راندمان روش استخراج تأثیر می‌گذارد. طبق نتایج، روش استخراج با حلال فوق داغ در مقایسه با روش استخراج متداول با حلال به‌طور قابل توجهی کارآمدتر بود و بالاترین بازده ۵۳/۲۹ درصد و محتوای فنلی کل ۷۳۷/۲۱ میلی‌گرم معادل اسید گالیک به گرم عصاره استخراج شده تحت شرایط بهینه (۲۵/۱۷ درصد حلال اتانولی در دمای استخراج ۱۶۰ درجه سانتی‌گراد به‌مدت ۲۸/۹۷ دقیقه) به‌دست آمد. در مقابل، بهینه‌سازی روش استخراج متداول با حلال، حداکثر بازده استخراج و فنول کل را به‌ترتیب به ۳۰/۹۶ درصد و ۶۹۳/۲۳ میلی‌گرم معادل اسید گالیک به گرم عصاره استخراج شده (با استفاده از ۵۰ درصد حلال اتانولی در دمای استخراج ۸۲/۵۷ درجه سانتی‌گراد به‌مدت ۱۰۳/۳۱ دقیقه) رساند. این اولین گزارش در مورد بهینه‌سازی استخراج ترکیبات فنولی با حلال فوق داغ از برگ گیاه نوروزک است.

واژه‌های کلیدی: استخراج با حلال فوق داغ، استخراج متداول، پلی‌فنول‌ها، روش سطح پاسخ، نوروزک

۱- گروه پژوهشی زیست‌فناوری مواد غذایی، مؤسسه پژوهشی علوم و صنایع غذایی، مشهد، ایران
(*- نویسنده مسئول: Email: m.sarabi@rifst.ac.ir)
۲- گروه پژوهشی نانوفناوری مواد غذایی، مؤسسه پژوهشی علوم و صنایع غذایی، مشهد، ایران

https://doi.org/10.22067/ifstrj.2026.97188.1537

Iranian Food Science and Technology Research Journal
Homepage: https://ifstrj.um.ac.ir

Research Article
Vol. 22, No. 3, July- August. 2026, p. 303-317

Effect of Ultrasonication on Texture Profile Analysis, Microbiome Phylogeny, and Prediction of Fatty Acid Metabolic Pathways in Siahmazgi Cheese

S.A. Mehrzad[1], F. Shahidi[1*], N. Davati[2*], M. Karami[2]

1- Department of Food Science and Technology, Faculty of Agriculture, Ferdowsi University of Mashhad, Mashhad, Iran
2- Department of Food Science and Technology, Faculty of Food Industry, Bu-Ali Sina University, Hamedan, Iran
(*- Corresponding Authors Email: fshahidi@um.ac.ir, n.davati@basu.ac.ir)

Received: 27.12.2025
Revised: 10.04.2026
Accepted: 21.04.2026
Available Online: 19.05.2026

How to cite this article:
Mehrzad, S.A., Shahidi, F., Davati, N., & Karami, M. (2026). Effect of ultrasonication on texture profile analysis, microbiome phylogeny, and prediction of fatty acid metabolic pathways in Siahmazgi cheese. *Iranian Food Science and Technology Research Journal*, *22*(3), 303-317.
https://doi.org/10.22067/ifstrj.2026.97209.1539

Abstract

Siahmazgi cheese ripens through the metabolic activities of the indigenous microbiota present in unpasteurized milk. To ensure its safety, non-thermal processing methods such as ultrasound are required. This study aimed to determine the textural changes and the phylogeny relationships of the microbiome in Siahmazgi cheese affected by ultrasonication, followed by a metabolomics analysis of fatty acids (FAs). Microscopic changes in cheese texture affected by ultrasonication (0, 5, 10 min) were examined through processing of SEM images by ImageJ. Texture profile analysis was also performed using a texture analyzer. Phylogenetic and metabolomics analyses of the microbiome were carried out using Geneious Prime. Correlations between microbes, metabolites, and metabolic pathways using Cytoscape. Phylogenetic analysis showed that the microbiome of cheeses treated with the same sonication exhibited similar genetic heatmaps until the third month, while the non-sonicated sample at the sixth month of ripening displayed the highest biodiversity. *Staphylococcus equorum*, *Acinetobacter johnsonii*, *Lactobacillus zeae*, *Macrococcus caseolyticus*, *Leuconostoc mesenteroides*, and *Lactiplantibacillus plantarum* were identified as key contributors to FAs metabolism. Hexadecanoic acid, octadecanoic acid, (9Z,12Z,15Z)-octadecatrienoic acid, and (9Z)-hexadecenoic acid were identified as the main FAs from lipid metabolism, and the biosynthesis of unsaturated FAs. Texture of samples prepared from 5 min-sonication showed the highest pore number (2345) and porosity (0.046352). Hardness, adhesiveness, cohesiveness, gumminess, and chewiness were the lowest in 5-min sonicated samples and the highest in 10-min sonicated samples during ripening. If a porous soft texture in the Siahmazgi cheese is desired, sonication for 5 min is recommended. Additionally, the results of this study provide a comprehensive understanding of the effect of sonication on texture, microbiome, and the prediction of metabolic pathways of FAs in Siahmazgi cheese, which supportthe development of non-thermal technologies for traditional cheeses.

Keywords: Metabolomics, Siahmazgi cheese, Texture profile analyzer, Ultrasonication

https://doi.org/10.22067/ifstrj.2026.97209.1539

Introduction

Siahmazgi cheese, a traditional dairy product from northern Iran, is distinguished by its rich microbial biodiversity, unique texture, characteristic flavor, and high nutritional value. Its natural fermentation, driven by milk indigenous microorganisms, leads in production specific biochemical compounds that set it apart from industrially manufactured cheeses (Fox, Guinee, Cogan, & McSweeney, 2017; Montel *et al*., 2014). Siyahmazgi cheese is a semi-hard, high-fat cheese traditionally prepared in the village of Siyahmazgi in Gilan province. It was originally made from sheep's and goat's milk, but cow's milk is now also used. This cheese undergoes prolong maturation period for six months in a sheepskin, which gives it unique physicochemical and textural properties. However, as Siahmazgi cheese is traditionally made from raw milk without pasteurization, it is susceptible to contamination by pathogenic and spore-forming bacteria, including Clostridium species, which are commonly found in artisanal cheeses (Brändle, Domig, & Kneifel, 2016; Lopez- Brea, Gómez- Torres, & Arribas, 2017). Thermal treatments, while remain the most effective means of reducing microbial risk, can adversely affect the native microbiota responsible for fermentation, potentially altering the cheese's texture, flavor, and aroma (Beresford & Williams, 2004; Settanni & Moschetti, 2010). Non-thermal technologies, particularly ultrasonication, have emerged as promising approaches to enhance the safety and quality of dairy products without compromising their sensory or functional properties. Ultrasonication, through acoustic cavitation, can modify protein networks, enzyme activity, microbial composition, and metabolic pathways in cheese production (Feng, Barbosa-Cánovas, & Weiss, 2011). Changes in microbial composition can affect fatty acid (FA) metabolism, including synthesis and degradation, which in turn influence sensory and functional characteristics. Integrating phylogenetic analysis with metabolomics enables detailed assessment of microbial relationships, identification of FA-producing bacteria, and prediction of associated metabolic pathways.

Previous studies have investigated the effects of ultrasound at frequencies of 20, 40 and 60 kHz for 20 minutes on ultrafiltered and pasteurized Iranian white cheese (Jalilzadeh, Hesari, Peighambardoust, & Javidipour, 2018). In addition, the effect of using *Streptococcus thermophilus*, whose cell walls were lysed by ultrasonication, in the production of Cremoso cheese was also investigated (Peralta, Bergamini, & Hynes, 2019). Another example involves conducting ultrasound pretreatment of milk containing probiotic *Lactobacillus plantarum*. Results of this study indicated that, ultrasound treatment improved the growth and metabolic activity of the probiotic bacteria, leading to enhanced antioxidant activity in the final product. The ultrasound treatment increased cell membrane permeability and significantly improved the fermentation process, resulting in higher quality fermented milk (Gholamhosseinpour & Hashemi, 2019). High-intensity ultrasound leads to enhance texture and stability of products like yogurt and cheese (Guimarães *et al.*, 2018). The ultrasonication times of 5 and 10 minutes were selected based on preliminary trials and previous reports indicating that short‑ to moderate‑duration ultrasound is sufficient to induce structural modifications in dairy matrices without causing excessive protein denaturation or fat coalescence (Carrillo-Lopez *et al.*, 2020). Very short treatments (<3 minutes) do not typically generate measurable microstructural changes, while prolonged exposure (>12–15 minutes) may lead to overheating, loss of moisture, or undesirable textural defects (Jalilzadeh *et al*., 2018). Therefore, 5 and 10 minutes were chosen as representative moderate intensities capable of altering the cheese microstructure while maintaining product integrity and technological feasibility.

This study builds on prior research by evaluating the effects of ultrasonication on the texture,

microbiome phylogeny, and FA metabolism of Siahmazgi cheese. The findings provide insights into non-thermal processing for improving product quality, supporting standardization, and guiding industrial-scale production while preserving the traditional characteristics of this unique cheese.

Materials and Methods

Cheese Preparation

Siahmazgi cheese was produced using the traditional method commonly practiced in Siahmazgi village, Gilan Province. Sheep's milk collected by local nomads in Asadabad (Hamadan, Iran) was filtered and, for treated samples, sonicated (VCX 750, 22.5 kHz, 750 W, titanium probe) for 10 min before enzyme addition. The milk was heated to 35 °C, rennet (0.004%) was added, and then it was heated to 55–60 °C for about 15 min until curd formation. The curd was kneaded to remove whey, drained at room temperature for 24 h, then placed in container and covered with pasteurized whey containing 10% salt. The cheese was finally ripened at 10 °C and 40% humidity for 6 months (Jalilzadeh *et al*., 2018). The different cheese treatments, affected by ultrasonication and ripening time, included: A (0 min ultrasound, 0 months ripening), AB (5 min, 0 months), B (10 min, 0 months), C (0 min, 90 days), CD (5 min, 90 days), D (10 min, 90 days), E (0 min, 180 days), EF (5 min, 180 days), and F (10 min, 180 days) were prepared. The microbiome analysis was performed on the samples treated for 0, and 10 minutes of ultrasonication, while the other analyses were carried out on the samples treated for 0, 5 and 10 minutes of ultrasonication.

Phylogeny Analysis of Microbiomes and Metabolomics Analysis of FAs

16S rRNA metagenomic analysis was performed by extracting total DNA from cheese samples, followed by amplification of the V3–V5 region. To examine the effect of ultrasonication treatment on microbiome-mediated FA metabolism, general associations between dominant bacterial taxa and FAs were first determined. Metabolomic enrichment analyses were subsequently performed to evaluate how bacterial communities at different ripening stages and ultrasonic treatment influenced lipid-related metabolic pathways. Microbial functional prediction was conducted using PICRUSt via the Microbiome Analyst platform (Chong, Liu, Zhou, & Xia, 2020; Dhariwal *et al*., 2017; Lu *et al*., 2023). Microbiome data were filtered based on variance and prevalence, normalized using total sum scaling (TSS), and left unrarefied. Metabolomics data were processed without filtering or normalization due to a limited number of features, and auto-scaling was applied before integration. Integrated analyses included correlation heatmaps, Procrustes analysis, and metabolic network construction. Associations between microbial features and experimental metadata were assessed using general linear models, with MaAsLin2 applied to microbiome data and Limma for metabolomics data (Chong *et al*., 2020; Lu *et al*., 2023). Microbiome and metabolomics datasets were mapped onto the KEGG metabolic network to identify enriched lipid-related pathways. Microbe–metabolite correlations were visualized using interactive correlation heatmaps based on distance correlation, with defined thresholds for correlation strength and significance (Prediction potential score = 0.05; differential significance = 0.05; AGORA database). Fatty acid–microbe–pathway networks were constructed and visualized using Cytoscape v3.9.1 to identify highly connected taxa and metabolic pathways. Procrustes analysis was conducted by ordinating microbiome and metabolomics datasets into a shared multivariate space and optimally rotating and scaling configurations to assess structural alignment between microbial community composition and FA metabolic profiles. Fat was extracted from cheese samples using a 2-propanol-based method and separated by rotary evaporation. The extracted fat was transesterified with hexane and methanolic potassium to produce fatty acid methyl esters

(FAMEs). FAMEs were analyzed by gas chromatography (GC-FID), identified using retention times of standards, and reported as percentages of total fatty acids (Gholamhosseinpour & Hashemi, 2019).

Microscopic Changes in Cheese Texture

The microstructure of cheese samples at the end of the ripening period was examined using a scanning electron microscope (SEM) (FEI Quanta 450 FEG, FEI Company, Hillsboro, OR, USA). Cheese cubes were taken from the central part of the blocks, fixed and dehydrated according to standard protocols, and then mounted and gold-coated prior to imaging. The SEM images were analyzed using ImageJ software 1.40g (Java 1.6.0-05).

Texture Profile Analysis (TPA)

TPA was performed using an STM-series texture analyzer (Santam Engineering Design Co. Ltd., Tehran, Iran). Cheese samples were cut into rectangular segments (approximately 2 × 2 × 2 cm) and equilibrated to room temperature (25 ± 2 °C) before testing. A cylindrical probe (50 mm diameter) was used in step test mode. Test conditions included sample type (rectangular prism), sample thickness (2 cm), sample weight (approximately 6 g), initial distance (150 mm), test speed (60 mm/min), number of steps (4), and activation of the "Link steps" option. Compression steps were set to 6 mm, 0 mm, 6 mm, and 0 mm, respectively.

Statistical Analysis

All TPA data and porosity (image-derived parameters) were performed in triplicate for each treatment and ripening time. Data are expressed as mean ± standard deviation (n = 3). All TPA and porosity data were analyzed using two-way analysis of variance (ANOVA), considering ultrasonic treatment time and ripening time as fixed factors, followed by Tukey's post hoc test to compare means. Statistical analyses were carried out using SPSS software (IBM SPSS Statistics, version 22, IBM Corp., Armonk, NY, USA). Differences were considered statistically significant at $p < 0.05$.

Results and Discussion

Phylogenetic Analysis of Microbiomes in Siahmazgi Cheese

The genetic heat maps in Fig. 1 (a1, b1, c1, d1, e1, f1) display the alignment of 16S rRNA gene sequences among the OTUs identified in the microbiomes of various Siahmazgi cheese samples. Structural similarity within the microbiome refers to the presence of identical or closely related species, as well as similar microbial diversity in terms of the type and number of microorganisms. During the first three months of ripening, the observed microbiome similarity among samples made from non-sonicated raw milk (a1 and c1), as well as those from sonicated milk (b1 and d1), is expected. This is because the samples underwent identical treatments, and only the progression of fermentation during the first three months of ripening produced minor differences in their microbiomes. The most distinct microbiome was found in sample e1, which exhibited the highest species diversity compared to the other samples. The high microbial diversity of e1 might due to the absence of ultrasonic treatment of the raw milk at the start of cheese production, which allowed the intrinsic microbiota of milk to remain intact. Consequently, with a broader range of microorganisms present and sufficient time for growth during six months of fermentation and ripening, a large microbial community developed in this sample. Other comparative patterns, similarity and dissimilarity matrix, follow trends similar to those observed in the genetic heat maps. The presence of certain species from the Enterobacteriaceae family in the samples may result from sheep grazing on fields contaminated with wastewater and animal manure, leading to their transfer into the milk (Hrenovic & Ivankovic, 2009). The microbial load introduced during cheese production, originating from added salt, utensils, and the hands of individuals involved in cheese

handling, also contributes to the microbial diversity of the final product. Thus, in addition to lactic acid bacteria (LAB), the presence of *Acinetobacter* and *Staphylococcus* was confirmed. The occurrence of various members of the Acinetobacteraceae family (Hrenovic & Ivankovic, 2009) and *Staphylococcus* in saline environments such as cheese, has previously been reported (Jørgensen, Mørk, & Rørvik, 2005).

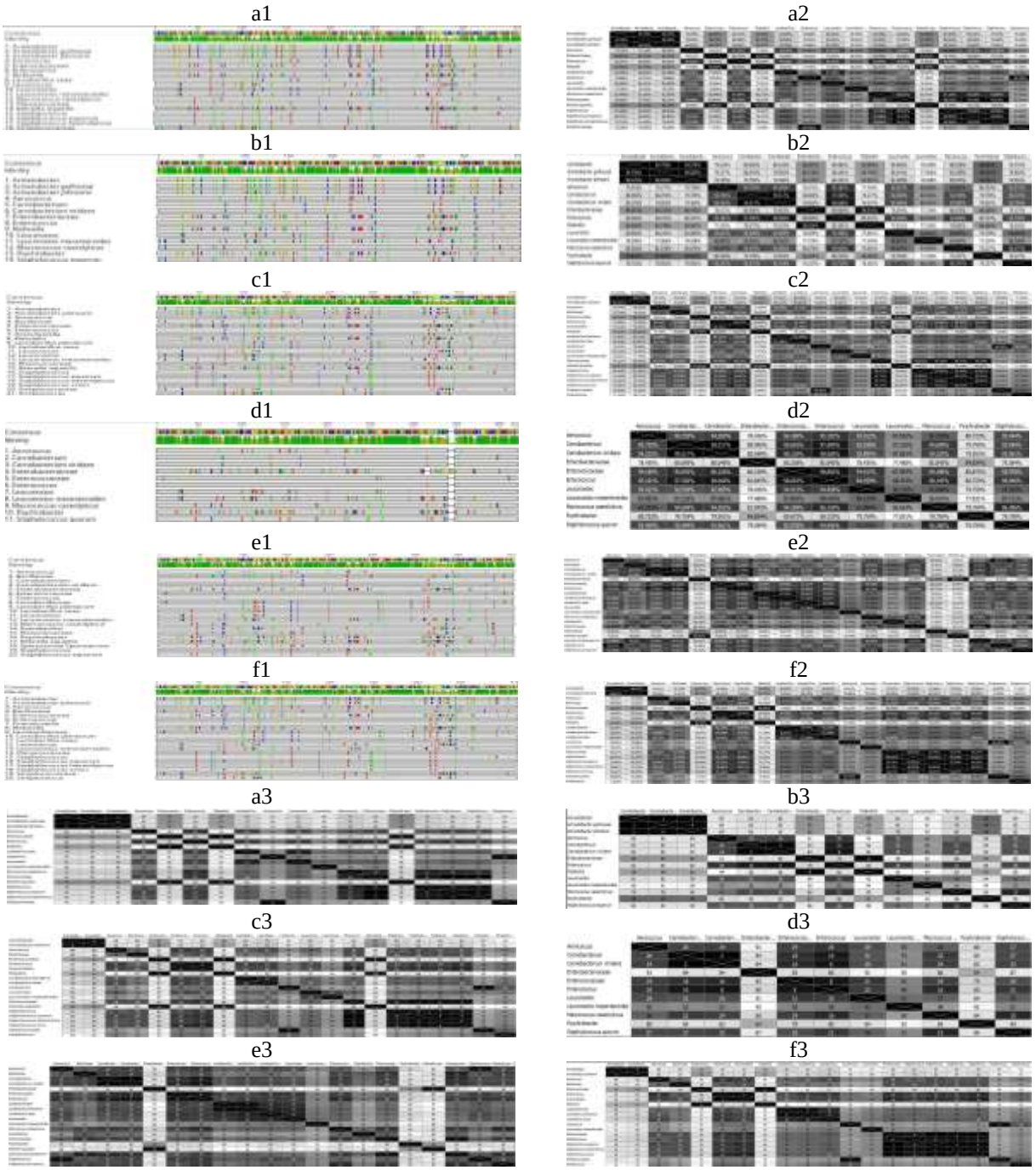

Fig. 1. Genetic heatmap (a1-f1), %identity (a2-f2) and differences matrix (a3-f3) of nucleotide sequence for cheese samples (a-f)

White, lowest %identity; black, highest %identity. The differences showed with the color intensity rate of each cell. Black, lowest difference; white, highest difference.

Pathways Enrichment of FAs

As shown in Fig. 2 (a), the network provides insight into the lipolysis process during siahmazgi cheese ripening and microbe-driven FA transformation. In addition, correlations between dominant species, genera and families, and FAs in cheese samples are shown in Fig. 2 (b1-b3). Based on Fig. 2 (a, b1–b3), all or some of the species and genera associated with these FAs are present in all samples of Siahmazgi cheese and may subsequently be involved in all metabolic pathways associated with the lipids presented in the network, thereby influencing the subsequent development of flavor of Siahmazgi cheese. Metabolomics enrichment (Fig. 2a) of the FA profile produced in Siahmazgi cheese samples indicated that FAs produced by the microbiome through different lipid metabolic pathways are involved. Based on this network, *S. equorum*, *A. johnsonii*, *L. zeae*, *M. caseolyticus*, *L. mesenteroides*, and *L. plantarum* were identified as key players, while hexadecanoic acid, octadecanoic acid, (9Z,12Z,15Z)-octadecatrienoic acid, and (9Z)-hexadecenoic acid were identified as the main FAs in lipid metabolism pathways. *Lactobacillus* spp., *Leuconostoc* spp., and *Staphylococcus* spp. were identified as releasing (lipases) or transforming (isomerases, hydratases, β-oxidation enzymes) FAs during ripening (Collins, McSweeney, & Wilkinson, 2003). The release of free FFAs (palmitic, stearic, oleic, and linoleic acids as flavour precursors) occurs due to lipolysis attributed by endogenous milk lipase, microbial lipases or esterases (Collins *et al.*, 2003). Conjugated linoleic acid (CLA) is a bioactive fatty acid with recognized health-promoting properties, and its production during dairy fermentation has been widely attributed to lactic acid bacteria (LAB) (Sosa-Castañeda *et al.*, 2015). Several LAB species, particularly *Lactobacillus plantarum*, are capable of converting linoleic acid into CLA or related derivatives through isomerization, hydration, dehydration, or isomerase-mediated reactions (Liu *et al.*, 2011). In addition to LAB, cheese surface microbiota such as *Macrococcus* and *Staphylococcus* play an important role in lipid metabolism, as they possess lipases and other enzymes that generate volatile and non-volatile fatty acid (FA) derivatives, including short-chain free fatty acids, methyl ketones, and esters that contribute to flavor development in hard cheese (Mazhar, Kilcawley, Hill, & McAuliffe, 2020). Environmental Gram-negative bacteria, such as *Acinetobacter*, may also be involved in long-chain FA catabolism through β-oxidation and related degradation pathways, consistent with their association with FA elongation and degradation processes (Ren & Palmer, 2023). Ultrasonic treatment of milk prior to cheese manufacture can influence lipid metabolism by modifying the indigenous microbiota through selective cell damage or inactivation, releasing intracellular enzymes such as lipases, and altering milk fat globule structure, which increases triglyceride exposure to enzymatic hydrolysis. These changes can affect both the quantity of free fatty acids produced and the microbial taxa responsible for FA metabolism (Hickey, Kilcawley, Beresford, & Wilkinson, 2007). Accordingly, the present study examined the effects of ultrasonic treatment (0, and 10 minute) on FA metabolic patterns and the microbial species associated with these processes. In control samples, dominant taxa such as *Leuconostoc mesenteroides* and *Staphylococcus equorum* were correlated with key long-chain fatty acids, including linoleic, α-linolenic, hexadecanoic, and octadecanoic acids, which are central metabolites in unsaturated FA biosynthesis, FA elongation, and degradation pathways. Across all samples, some genera such as *Lactobacillus*, *Leuconostoc*, *Macrococcus*, *Staphylococcus*, and *Acinetobacter* were associated with linoleic acid metabolism and potential CLA formation. Similar distribution patterns between microbiome-based functional predictions and measured FA profiles, together

with Procrustes analysis, demonstrated a moderate but significant concordance between microbial community structure and FA metabolism during ripening, supporting a functional link between cheese microbiota and lipid transformation processes.

Microscopic Changes in Texture of **Siahmazgi** Cheese Samples

According to Table 1 and Fig. 3, the effects of ultrasonication for 0, 5, and 10 minutes on the microscopic structure of cheese showed substantial changes in both porosity and pore number.

Table 1- Porosity analysis of Siahmazgi cheese samples in the 6 months of ripening by Image J

Sample	Porosity (0-10)	Pores detected	Magnification
Control (E)	0.008560 ± 0.0007^{c}	278± 10^{d}	1000x
	0.008243 ± 0.0009^{d}	676± 12^{c}	5000x
Ultrasound 5 min (EF)	0.046352 ± 0.0034^{a}	2244 ± 37^{b}	1000x
	0.028852 ± 0.0021^{b}	2345 ± 24^{a}	5000x
Ultrasound 10 min (F)	0.003073± 0.0013^{f}	115± 5^{e}	1000x
	0.005694 ± 0.0009^{e}	294± 8^{d}	5000x

Different letters in each column indicate significant differences among the samples ($p < 0.05$).

Based on SEM image analysis, the control sample showed very low porosity values (0.0085–0.0082%) and a limited number of pores (278–676). However, 5 minutes of ultrasonication resulted in a remarkable 5- to 6-fold increase in both pore number (2244–2345) and porosity (0.04635–0.046352) compared with the control.

Ultrasonication affects cheese microstructure and fermentation primarily through cavitation, which disrupts protein interactions, opens the casein network, and creates microvoids that alter matrix porosity. Cavitation and sonoporation transiently increase cell membrane permeability, enhancing nutrient and metabolite transfer, stimulating microbial activity, and accelerating biochemical reactions. Short-term or low-intensity ultrasound generally promotes microbial growth and metabolic performance, whereas prolonged treatment can damage membranes, cause intracellular leakage, and inactivate cells, with species-specific sensitivity (*E. aerogenes* and *B. subtilis* being more susceptible than *Staphylococcus* spp. (Carrillo-Lopez *et al.*, 2021). Low-frequency ultrasound (20–30 kHz) has been shown to enhance β-galactosidase release, lactose hydrolysis, organic acid production, proteolysis, lipolysis, and bioactive compounds formation. Short-term ultrasonication increases porosity in cheese and protein gels by partially disaggregating protein networks and creating microcavities, due to physical (microstreaming, shear stress, membrane disruption) and chemical effects (free radical formation, lipid peroxidation, protein unfolding). In contrast, 10-minute treatment reduces porosity and pore number via protein reaggregation and matrix compaction (Chandrapala, Zisu, Palmer, Kentish, & Ashokkumar, 2011), whereas 5-minute ultrasonication enhances porosity through fat globule disruption and improved fat–protein distribution (Chen *et al.*, 2025). During ripening, microbial fermentation, gas production, enzyme activity, and moisture changes further modify pore structure (Yavuz, Kasavi, & Öner, 2021). Overall, short-term ultrasound produces porous cheese, while longer treatments yield denser, more uniform textures.

The structural differences observed among the nine treatments align closely with recent findings regarding the influence of ultrasound on dairy protein networks. High‑intensity ultrasound is known to induce localized cavitation, shear forces, and microstreaming, which collectively disrupt the protein matrix and promote the formation of more open and porous structure. In the present study, cheeses treated for 5 and 10 min displayed greater porosity and a less compact microstructure compared with the control, consistent with

previously reported ultrasound‐mediated loosening of protein gel networks (Teng *et al*., 2020).

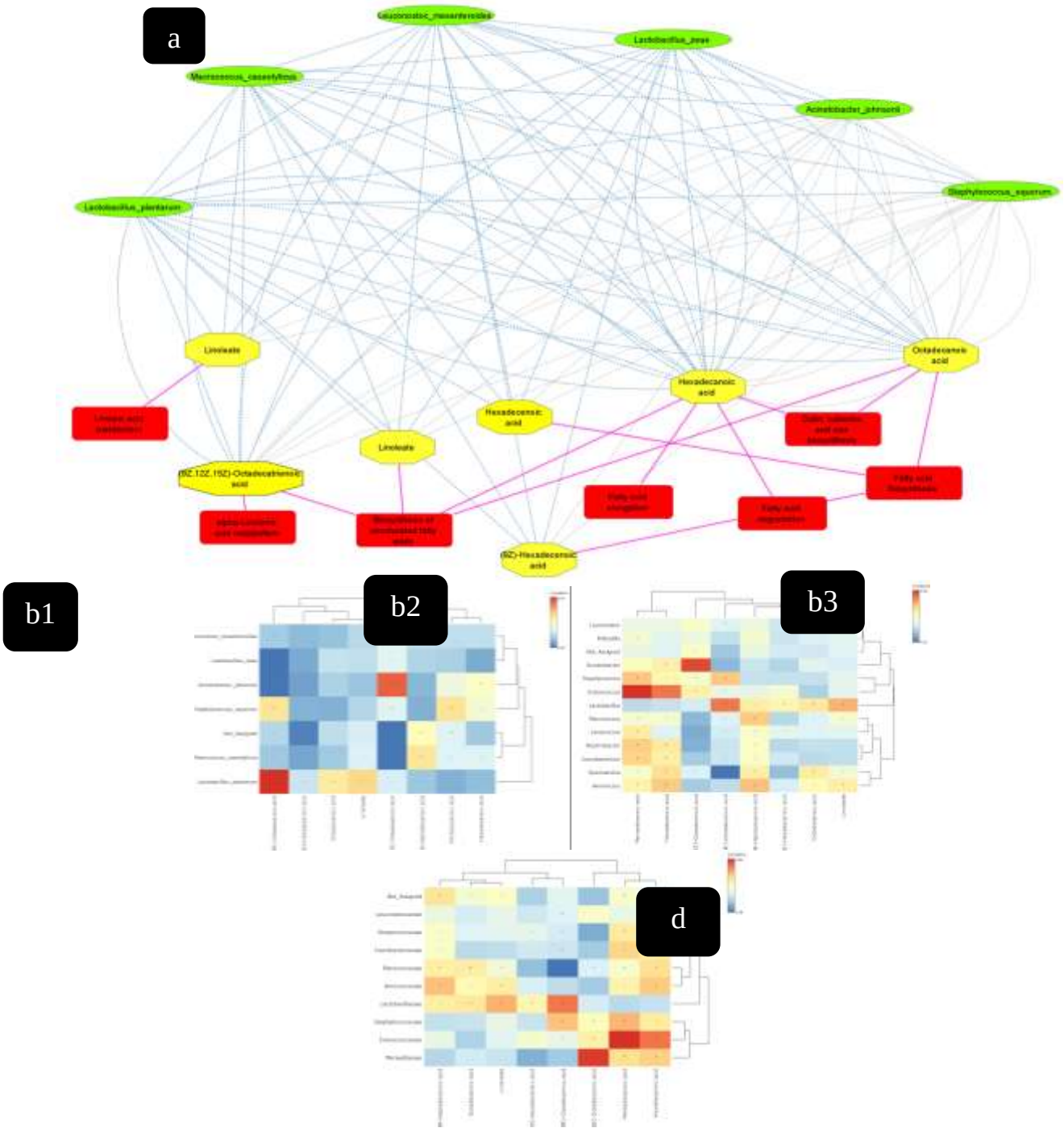

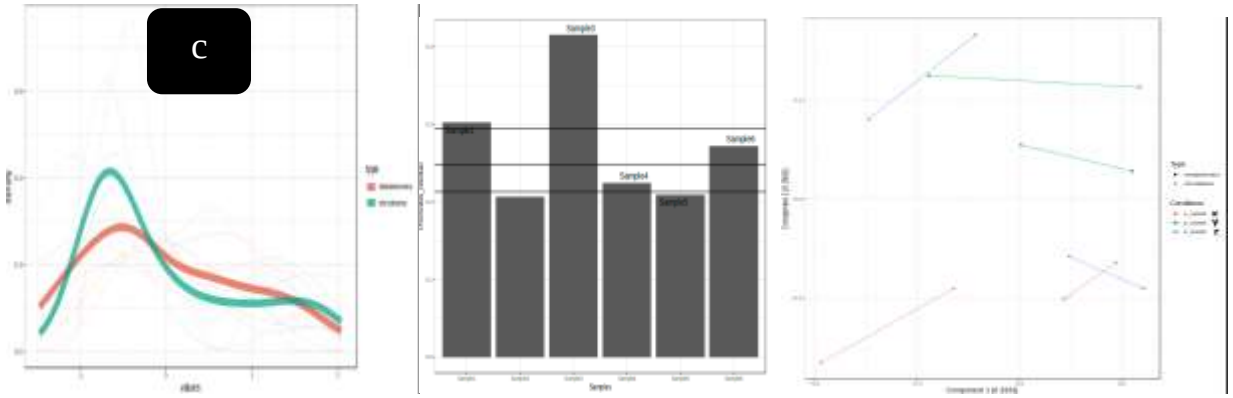

Fig. 2. The network among microbiome, FAs and lipid metabolic pathways in Siahmazgi cheese samples by Cytoscape. Rectangle: Metabolic pathway, Pentagon: FA; Elliptical: Bacteria spp., (a). The heatmap visualization of FAs produced by the dominant bacteria species (b1), genus (b2), family (b3). Density Plot **against log2 of read counts (c). Procrustes analysis, Residuals and ordination plot (d)**

The enhanced pore formation observed in the 10‑min treatment corresponds with evidence showing that prolonged exposure increases cavitational activity and modifies casein micelle aggregation. Similar microstructural patterns—characterized by expanded cavities and weakened protein junctions—have been reported in fresh cheeses exposed to high‑power ultrasound during storage (Chen *et al*., 2025). Furthermore, the quantitative porosity analysis in our study agrees with multi‑scale evaluations demonstrating that ultrasound can significantly alter cheese matrix architecture, leading to increased pore density and heterogeneity. Overall, these comparisons confirm that the structural modifications observed in Siahmazgi cheese are consistent with the broader literature describing ultrasound‑induced alterations in cheese microstructure.

Texture Profile Analysis

The results obtained from the TPA of Siahmazgi cheese samples are presented in Table 2. Hardness values showed notable changes due to both ultrasound treatment and ripening time. At 0 months, hardness increased from 8.52 ± 1.45 N in the control to 10.01 ± 0.45 N with 5-minute ultrasound and 17.79 ± 1.20 N with 10-minute treatment, reflecting immediate protein matrix compaction. By 3 months, hardness decreased in all samples, 1.36 ± 0.15 N (control), 2.13 ± 0.15 N (5 min), and 4.29 ± 0.32 N (10 min). At 6 months, hardness values were 2.11 ± 0.22 N for the control, 1.71 ± 0.22 N for 5 minutes, and 11.35 ± 0.85 N for 10 minutes.

These results indicate that the 10-minute ultrasound treatment consistently produced higher hardness, consistent with SEM observations of reduced porosity and increased structural cohesion. Adhesiveness remained negative in all treatments. At 0 months, values were −0.30 ± 0.05 N for the control, −0.28 ± 0.05 N for the 5-minute treatment, and −0.80 ± 0.10 N for the 10-minute ultrasound treatment, indicating a strong increase in surface stickiness with prolonged sonication. By 3 months, adhesiveness decreased to −0.05 ± 0.02 N (control), −0.03 ± 0.02 N (5 min), and −0.15 ± 0.03 N (10 min). At 6 months, adhesiveness increased again, with the 10-minute treatment remaining the highest at −0.50 ± 0.07 N, while the 5-minute sample showed the lowest value (−0.05 ± 0.02 N). At 0 months, cohesiveness increased slightly with ultrasound, from 0.93 ± 0.03 in the control to 0.94 ± 0.03 (5 min) and 0.96 ± 0.01 (10 min). By 3 months, cohesiveness dropped sharply in the control (0.37 ± 0.02), while the 5-minute (0.74 ± 0.05) and 10-minute (0.85 ± 0.04) treatments retained much higher structural integrity. At 6 months, cohesiveness declined in the 5-minute sample (0.57 ± 0.05), whereas the 10-minute treatment maintained a high value of 0.93 ± 0.02. Overall, ultrasound,

especially the 10-minute duration, significantly enhances and preserves casein network integrity during ripening. Springiness remained consistently high in all treatments. At 0 months, values were 0.95 ± 0.02 (control), 0.93 ± 0.01 (5 min), and 0.96 ± 0.01 (10 min), with only minor differences. After 3 months, springiness increased in the 5-minute sample (0.99 ± 0.03), exceeding the control (0.92 ± 0.01) and approaching the 10-minute treatment (0.94 ± 0.02). By 6 months, the 5-minute treatment again showed the highest springiness (0.99 ± 0.02), followed by the 10-minute (0.97 ± 0.01) and the control (0.90 ± 0.01).

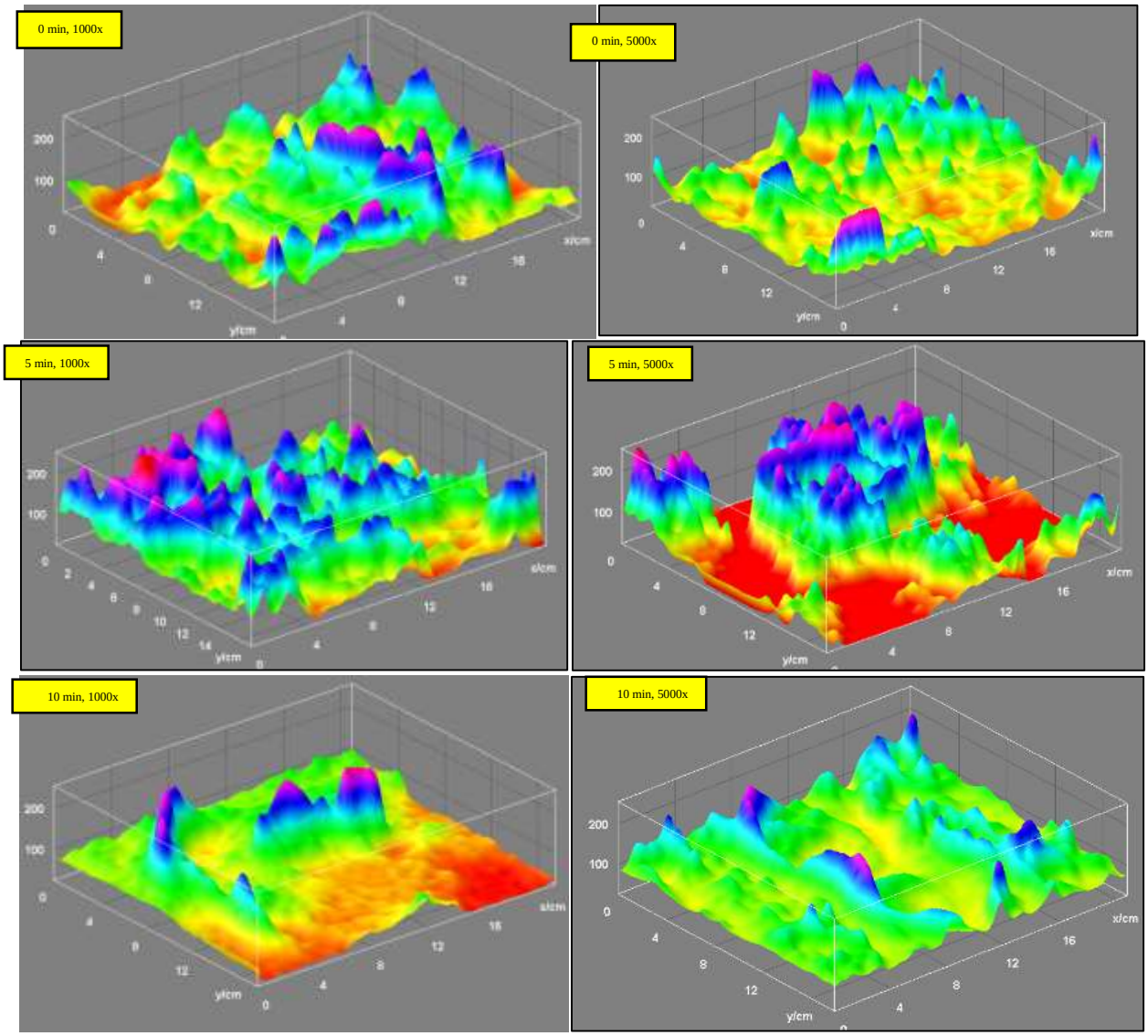

Fig. 3. The SEM of Siahmazgi cheese in the 6 months of ripening affected by 0, 5, and 10 min ultrasound

These results indicate that even short sonication enhances and maintains elasticity during ripening. At 0 months, gumminess values were 7.92 ± 0.55 N for the control, 9.23 ± 0.55 N for the 5-minute treatment, and 17.07 ± 1.15 N for the 10-minute treatment. At 3 months, gumminess was 1.57 ± 0.08 N for the 5-minute treatment, higher than the control (0.51 ± 0.08 N) but lower than the 10-minute treatment (3.65 ± 0.28 N). At 6 months, gumminess in the 5-minute sample decreased to 0.97 ± 0.18 N, below the control (1.69 ± 0.18 N). In contrast, the 10-minute treatment resulted in very high gumminess (10.50 ± 0.78

N) and a firmer, more resistant texture, indicating persistent structural integrity. At 0 months, chewiness increased from 7.52 ± 0.48 N in the control to 8.61 ± 0.48 N with 5-minute ultrasound, while the 10-minute treatment produced a much stronger effect (16.39 ± 1.08 N). By 3 months, chewiness values decreased but remained higher in sonicated samples—0.47 ± 0.07 N (control), 1.55 ± 0.07 N (5 min), and 3.43 ± 0.25 N (10 min). At 6 months, chewiness in the 5-minute sample declined to 0.96 ± 0.16 N, below the control (1.50 ± 0.16 N), whereas the 10-minute treatment maintained a very high value (10.18 ± 0.72 N). This study demonstrates that both ultrasound duration and ripening time significantly influence the texture and chewiness of Siahmazgi cheese. The effects of ultrasound followed a nonlinear pattern depending on exposure duration. At 0 months, both 5- and 10-minute ultrasound treatments increased hardness, cohesiveness, gumminess, and chewiness compared to the control, with the 10-minute treatment, the denser, most cohesive structure were achieved. Prolonged sonication enhanced protein–fat interactions, promoted reorganization of the casein network into a compact matrix, and reduced porosity, consistent with mechanisms of acoustic cavitation (Chandrapala *et al.*, 2011). This dense network remained stable during six months of ripening, resulting in a texture comparable to semi-hard cheeses, whereas the 5-minute treatment provided moderate reinforcement, suitable for soft to semi-soft textures. During the first three months, softening of all cheeses happened due to proteolysis, but ultrasound appeared to moderate the softening trend by synergistically interacting with microbial and enzymatic activity. Enhanced proteolysis in sonicated samples likely reflects increased enzyme accessibility and stimulation of lactic acid bacteria (LAB), supporting controlled softening without excessive structural degradation. By six months, moisture loss and reduced proteolytic activity contributed to matrix firming and further structural stability (Lucey, Johnson, & Horne, 2003). The control exhibited extensive softening and low cohesiveness due to uncontrolled proteolysis, while ultrasound treatments enhanced matrix uniformity, fat globule disruption, and protein–fat bonding, consistent with previous reports in Siahmazgi and other cheeses like Cheddar and Gouda (Bermúdez- Aguirre, Mawson, & Barbosa- Cánovas, 2008; Jalilzadeh, Hesari, Peighambardoust, & Javidipour, 2018). Differences in response among cheeses are attributed to inherent variations in casein matrix density, fat distribution, and microbial activity. Overall, ultrasound effectively modulated Siahmazgi cheese texture, with 10-minute treatment producing a firm, cohesive, and resilient matrix suitable for semi-hard cheese varieties, while 5-minute sonication provided moderate softening, demonstrating the method's potential for tailoring cheese textural properties during ripening.

Table 2- Effect of ultrasound treatment and ripening periods on the TPA of the cheese samples

Formulation	Hardness (N)	Adhesiveness (N)	Cohesiveness	%Springiness	Gumminess (N)	Chewiness (N)
A	8.52 ± 1.45^{c}	-0.3 ± 0.05^{d}	0.93 ± 0.03^{a}	0.95 ± 0.02^{a}	7.92 ± 0.55^{c}	7.52 ± 0.48^{c}
AB	10.01 ± 0.45^{c}	-0.28 ± 0.05^{a}	0.94 ± 0.03^{d}	0.93 ± 0.01^{a}	9.23 ± 0.55^{c}	8.61 ± 0.48^{c}
B	17.79 ± 1.20^{a}	-0.80 ± 0.1^{e}	0.96 ± 0.01^{a}	0.96 ± 0.01^{a}	17.07 ± 1.15^{a}	16.39 ± 1.08^{a}
C	1.36 ± 0.15^{f}	-0.05 ± 0.02^{a}	0.37 ± 0.02^{e}	0.92 ± 0.01^{b}	0.51 ± 0.08^{f}	0.47 ± 0.07^{g}
CD	2.13 ± 0.15^{e}	-0.03 ± 0.02^{a}	0.74 ± 0.05^{c}	0.99 ± 0.03^{a}	1.57 ± 0.08^{f}	1.55 ± 0.07^{e}
D	4.29 ± 0.32^{d}	-0.15 ± 0.03^{b}	0.85 ± 0.04^{b}	0.94 ± 0.02^{a}	3.65 ± 0.28^{d}	3.43 ± 0.25^{d}
E	2.11 ± 0.22^{e}	-0.08 ± 0.02^{a}	$0.80 \pm 0.05b^{c}$	0.90 ± 0.01^{b}	1.69 ± 0.18^{e}	1.50 ± 0.16^{e}
EF	1.71 ± 0.22^{e}	-0.05 ± 0.02^{a}	0.57 ± 0.05^{d}	0.99 ± 0.20^{a}	0.97 ± 0.18^{e}	0.96 ± 0.16^{f}
F	11.35 ± 0.85^{b}	-0.50 ± 0.07^{c}	0.93 ± 0.02^{a}	0.97 ± 0.01^{a}	10.50 ± 0.78^{b}	10.18 ± 0.72^{b}

Different letters in each column indicate significant differences among the samples ($p < 0.05$).

Conclusion

The results of this study demonstrated that ultrasound treatment significantly influenced the physicochemical, microbiological, and structural characteristics of Siahmazgi cheese during ripening. Compared with the control samples, ultrasonic treatment cheeses (5 and 10 min) showed notable modifications in microstructure, including increased porosity and pore number as revealed by SEM image analysis. These structural changes were accompanied by measurable variations in texture profile parameters throughout the ripening period. In addition, ultrasound treatment contributed to a reduction in pathogenic microorganisms compared with the untreated control samples, indicating its potential as a supportive non‑thermal processing technique to improve microbial safety in traditional cheeses. Overall, moderate ultrasound treatment, particularly at 5 min, produced favorable structural and quality changes while maintaining desirable textural characteristics of the cheese. Therefore, ultrasound processing can be considered a promising technology for improving the quality and safety of traditional Siahmazgi cheese. However, this study had some limitations. The investigation was conducted at a laboratory scale with limited ultrasound treatment conditions and a relatively small number of samples. In addition, sensory evaluation and detailed biochemical analyses of flavor compounds were not included. Further studies are recommended to evaluate a wider range of ultrasound intensities and treatment durations, investigate the long‑term effects on flavor development and consumer acceptance, and assess the scalability of this technology for industrial cheese production.

Author Contributions

Somayehalsadat Mehrzad: conducted the experiments, collected and processed the data, and prepared a draft of the manuscript. **Fakhri Shahidi and Nafiseh Davati**: supervised and designed the experiments, interpreted the data, contributed to the writing of the original draft, and revised the manuscript. **Mostafa Karami**: co-supervisor on this project; provided general guidance throughout the development of the work.

Acknowledgments

We gratefully appreciate the cooperation of all the current study participants from Ferdowsi University and Bu-Ali Sina University.

Funding Source

This study was financially supported by Ferdowsi University of Mashhad, Mashhad, Iran [grant No.3/55720].

References

1. Beresford, T., & Williams, A. (2004). The microbiology of cheese ripening. In *Cheese: Chemistry, Physics and Microbiology, 1*, 287-317. Elsevier. https://doi.org/10.1016/S1874-558X(04)80071-X
2. Bermúdez Aguirre, D., Mawson, R., & Barbosa Cánovas, G. (2008). Microstructure of fat globules in whole milk after thermosonication treatment. *Journal of Food Science, 73*(7), E325-E332. https://doi.org/10.111/j.1750-3841.2008.00875.X
3. Brändle, J., Domig, K., & Kneifel, W. (2016). Relevance and analysis of butyric acid producing clostridia in milk and cheese. *Food Control, 67*, 96-113. https://doi.org/10.1016/j.foodcont.2016.02.038
4. Carrillo-Lopez, L.M., Garcia-Galicia, I.A., Tirado-Gallegos, J.M., Sanchez-Vega, R., Huerta-Jimenez, M., Ashokkumar, M., & Alarcon-Rojo, A.D. (2021). Recent advances in the application of ultrasound in dairy products: Effect on functional, physical, chemical,

microbiological and sensory properties. *Ultrasonics Sonochemistry, 73*, 105467. https://doi.org/10.1016/j.ultsonch.2021.105467

5. Chandrapala, J., Zisu, B., Palmer, M., Kentish, S., & Ashokkumar, M. (2011). Effects of ultrasound on the thermal and structural characteristics of proteins in reconstituted whey protein concentrate. *Ultrasonics Sonochemistry, 18*(5), 951-957. https://doi.org/10.1016/j.ultsonch.2010.12.016
6. Chen, X., Wei, L., Mao, Y., Zhao, A., Pu, M., Liu, Y., & Wang, B. (2025). A comparative study of ultrasound and thermal processing: Effects on goat milk stability and protein structure. *Journal of Dairy Science*, *108*(4), 3273-3286. https://doi.org/10.3168/jds.2024-25918
7. Chong, J., Liu, P., Zhou, G., & Xia, J. (2020). Using MicrobiomeAnalyst for comprehensive statistical, functional, and meta-analysis of microbiome data. *Nature Protocols*, *15*(3), 799-821. https://doi.org/10.1038/s41596-019-0264-1
8. Collins, Y.F., McSweeney, P.L., & Wilkinson, M.G. (2003). Lipolysis and free fatty acid catabolism in cheese: a review of current knowledge. *International Dairy Journal*, *13*(11), 841-866. https://doi.org/10.1016/S0958-6946(03)00109-2
9. Dhariwal, A., Chong, J., Habib, S., King, I.L., Agellon, L.B., & Xia, J. (2017). MicrobiomeAnalyst: a web-based tool for comprehensive statistical, visual and meta-analysis of microbiome data. *Nucleic Acids Research, 45*(W1), W180-W188. https://doi.org/10.1093/nar/gkx295
10. Feng, H., Barbosa-Cánovas, G.V., & Weiss, J. (2011). *Ultrasound technologies for food and bioprocessing* (Vol. 1): Springer. https://doi.org/10.1007/978-1-4419-7472-3
11. Fox, P.F., Guinee, T.P., Cogan, T.M., & McSweeney, P.L. (2017). *Fundamentals of cheese science* (Vol. 1): Springer. https://doi.org/10.1007/978-1-4899-7681-9_1
12. Gholamhosseinpour, A., & Hashemi, S.M.B. (2019). Ultrasound pretreatment of fermented milk containing probiotic *Lactobacillus plantarum* AF1: Carbohydrate metabolism and antioxidant activity. *Journal of Food Process Engineering, 42(1),* e12930. https://doi.org/10.1111/jfpe.12930
13. Guimarães, J.T., Silva, E.K., Alvarenga, V.O., Costa, A.L.R., Cunha, R.L., Sant'Ana, A.S., . . . Cruz, A.G. (2018). Physicochemical changes and microbial inactivation after high-intensity ultrasound processing of prebiotic whey beverage applying different ultrasonic power levels. *Ultrasonics Sonochemistry*, *44*, 251-260. https://doi.org/10.1016/j.ultsonch.2018.02.012
14. Hickey, D., Kilcawley, K., Beresford, T., & Wilkinson, M. (2007). Lipolysis in cheddar cheese made from raw, thermized, and pasteurized milks. *Journal of Dairy Science*, *90*(1), 47-56. https://doi.org/10.3168/jds.S0022-0302(07)72607-3
15. Hrenovic, J., & Ivankovic, T. (2009). Survival of *Escherichia coli* and *Acinetobacter junii* at various concentrations of sodium chloride. *EurAsian Journal of Biosciences, 3* . https://doi.org/10.5053/ejobios.2009.3.0.18
16. Jalilzadeh, A., Hesari, J., Peighambardoust, S., & Javidipour, I. (2018). The effect of ultrasound treatment on microbial and physicochemical properties of Iranian ultrafiltered feta-type cheese. *Journal of Dairy Science*, *101*(7), 5809-5820. https://doi.org/10.3168/jds.2017-14352
17. Jørgensen, H., Mørk, T., & Rørvik, L. (2005). The occurrence of *Staphylococcus aureus* on a farm with small-scale production of raw milk cheese. *Journal of Dairy Science*, *88*(11), 3810-3817. https://doi.org/10.3168/jds.S0022-0302(05)73066-6
18. Liu, P., Shen, S.-r., Ruan, H., Zhou, Q., Ma, L.-l., & He, G.-q. (2011). Production of conjugated linoleic acids by *Lactobacillus plantarum* strains isolated from naturally fermented Chinese pickles. *Journal of Zhejiang University Science B, 12*(11), 923-930. https://doi.org/10.1631/jzus.B1100072

19. Lopez Brea, S. G., Gómez Torres, N., & Arribas, M.Á. (2017). Spore forming bacteria in dairy products. *Microbiology in Dairy Processing: Challenges and Opportunities*, 11-36. https://doi.org/10.1002/9781119115007.ch2
20. Lu, Y., Zhou, G., Ewald, J., Pang, Z., Shiri, T., & Xia, J. (2023). MicrobiomeAnalyst 2.0: comprehensive statistical, functional and integrative analysis of microbiome data. *Nucleic Acids Research, 51*(W1), W310-W318. https://doi.org/10.1093/nar/gkad407
21. Lucey, J., Johnson, M., & Horne, D. (2003). Invited review: Perspectives on the basis of the rheology and texture properties of cheese. *Journal of Dairy Science, 86*(9), 2725-2743. https://doi.org/10.3168/jds.S0022-0302(03)73869-7
22. Mazhar, S., Kilcawley, K.N., Hill, C., & McAuliffe, O. (2020). A systems-wide analysis of proteolytic and lipolytic pathways uncovers the flavor-forming potential of the gram-positive bacterium *Macrococcus caseolyticus* subsp. *caseolyticus*. *Frontiers in Microbiology, 11*, 1533. https://doi.org/10.3389/fmicb.2020.01533
23. Montel, M.-C., Buchin, S., Mallet, A., Delbes-Paus, C., Vuitton, D.A., Desmasures, N., & Berthier, F. (2014). Traditional cheeses: Rich and diverse microbiota with associated benefits. *International Journal of Food Microbiology, 177*, 136-154. https://doi.org/10.1016/j.ijfoodmicro.2014.02.019
24. Peralta, G.H., Bergamini, C.V., & Hynes, E.R. (2019). Disruption treatments on two strains of *Streptococcus thermophilus*: levels of lysis/permeabilisation of the cultures, and influence of treated cultures on the ripening profiles of Cremoso cheese. *International Dairy Journal, 92*, 11-20. https://doi.org/10.1016/j.idairyj.2019.01.002
25. Ren, X., & Palmer, L.D. (2023). Acinetobacter metabolism in infection and antimicrobial resistance. *Infection and Immunity, 91*(6), e00433-00422. https://doi.org/10.1128/iai.00433-22
26. Settanni, L., & Moschetti, G. (2010). Non-starter lactic acid bacteria used to improve cheese quality and provide health benefits. *Food Microbiology, 27*(6), 691-697. https://doi.org/10.1016/j.fm.2010.05.023
27. Sosa-Castañeda, J., Hernández-Mendoza, A., Astiazarán-García, H., Garcia, H., Estrada-Montoya, M., González-Córdova, A., & Vallejo-Cordoba, B. (2015). Screening of *Lactobacillus* strains for their ability to produce conjugated linoleic acid in milk and to adhere to the intestinal tract. *Journal of Dairy Science, 98*(10), 6651-6659. https://doi.org/10.3168/jds.2014-8515
28. Teng, F., He, M., Xu, J., Chen, F., Wu, C., Wang, Z., & Li, Y. (2020). Effect of ultrasonication on the stability and storage of a soy protein isolate-phosphatidylcholine nanoemulsions. *Scientific Reports, 10*(1), 14010. https://doi.org/10.1038/s41598-020-70462-8
29. Yavuz, M., Kasavi, C., & Öner, E.T. (2021). Developments in effective use of volatile organic compound analysis to assess flavour formation during cheese ripening. *Journal of Dairy Research, 88*(4), 461-467. https://doi.org/10.1017/S0022029921000790

نشریه پژوهشهای علوم و صنایع غذایی ایران
https://ifstrj.um.ac.ir

مقاله پژوهشی
جلد ۲۲، شماره ۳، مرداد- شهریور ۱۴۰۵، ص. ۳۱۷-۳۰۳

تأثیر فراصوت بر تحلیل مشخصات بافت، فیلوژنی میکروبیوم و پیش‌بینی مسیرهای متابولیکی اسیدهای چرب در پنیر سیاه‌مزگی

سمیه السادات مهرزاد[۱]- فخری شهیدی[۱*]- نفیسه دعوتی[۲*]- مصطفی کرمی[۲]

تاریخ دریافت: ۱۴۰۴/۱۰/۰۶
تاریخ پذیرش: ۱۴۰۵/۰۲/۰۱

چکیده

پنیر سیاه‌مزگی از طریق فعالیت‌های متابولیکی میکروبیوتای بومی موجود در شیر پاستوریزه‌نشده دچار رسیدگی می‌شود. برای تضمین ایمنی این محصول، به‌کارگیری روش‌های فرآوری غیرحرارتی مانند فراصوت ضروری است. هدف این مطالعه بررسی تغییرات بافتی و روابط فیلوژنتیکی میکروبیوم پنیر سیاه‌مزگی تحت تأثیر تیمار فراصوت و به‌دنبال آن انجام تحلیل متابولومیک اسیدهای چرب بود. تغییرات میکروسکوپی بافت پنیر تحت تیمارهای فراصوت (۰، ۵ و ۱۰ دقیقه) از طریق پردازش تصاویر SEM با استفاده از نرم‌افزار ImageJ ارزیابی شد. همچنین تحلیل پروفیل بافت با دستگاه سنجش بافت انجام گرفت. تحلیل‌های فیلوژنتیکی و متابولومیکی میکروبیوم با استفاده از نرم‌افزار Geneious Prime و بررسی ارتباطات بین میکروب‌ها، متابولیت‌ها و مسیرهای متابولیکی با استفاده از Cytoscape انجام شد. نتایج تحلیل فیلوژنتیکی نشان داد میکروبیوم پنیرهای تیمارشده با فراصوت مشابه (از نظر مدت زمان) تا ماه سوم رسیدگی، الگوهای حرارتی ژنتیکی مشابهی داشتند، در حالی‌که نمونه بدون تیمار در ماه ششم رسیدگی بیشترین تنوع زیستی را نشان داد. گونه‌های *Staphylococcus equorum*، *Acinetobacter johnsonii*، *Lactobacillus zeae*، *Macrococcus caseolyticus*، *Leuconostoc mesenteroides* و *Lactiplantibacillus plantarum* به‌عنوان عوامل کلیدی دخیل در متابولیسم اسیدهای چرب شناسایی شدند. هگزادکانوئیک اسید، اکتادکانوئیک اسید، (9Z,12Z,15Z)-اُکتادکاترینوئیک اسید و (9Z)-هگزادسنوئیک اسید نیز به‌عنوان اسیدهای چرب اصلی حاصل از متابولیسم لیپیدها و زیست‌سنتز اسیدهای چرب غیراشباع شناسایی شدند. نمونه‌های تیمارشده با ۵ دقیقه فراصوت بیشترین تعداد حفره (۲۳۴۵ عدد) و تخلخل (۰/۰۴۶۳۵۲) را داشتند. در طول دوره رسیدگی، سختی، چسبندگی، انسجام، صمغی‌بودن و قابلیت جویدن در نمونه‌های تیمار ۵ دقیقه‌ای کمترین و در نمونه‌های تیمار ۱۰ دقیقه‌ای بیشترین مقدار را نشان دادند. بنابراین، در صورتی‌که هدف دستیابی به بافتی نرم و متخلخل در پنیر سیاه‌مزگی باشد، تیمار فراصوت به‌مدت ۵ دقیقه توصیه می‌شود. افزون بر این، نتایج این پژوهش درک جامعی از تأثیر فراصوت بر ویژگی‌های بافتی، ساختار میکروبی و پیش‌بینی مسیرهای متابولیکی اسیدهای چرب در پنیر سیاه‌مزگی ارائه می‌کند که می‌تواند در توسعه فناوری‌های غیرحرارتی برای پنیرهای سنتی مؤثر باشد.

واژه‌های کلیدی: پنیر سیاه‌مزگی، تحلیل پروفیل بافت، فراصوت، متابولومیکس

۱- گروه علوم و صنایع غذایی، دانشکده کشاورزی، دانشگاه فردوسی مشهد، مشهد، ایران
۲- گروه علوم و صنایع غذایی، دانشکده صنایع غذایی، دانشگاه بوعلی‌سینا، همدان، ایران
(*- نویسندگان مسئول: Email: fshahidi@um.ac.ir, Email: n.davati@basu.ac.ir)

https://doi.org/10.22067/ifstrj.2026.97209.1539

Iranian Food Science and Technology Research Journal
Homepage: https://ifstrj.um.ac.ir

Short Research Article
Vol. 22, No. 3, July- August. 2026, p. 319-330

Rapid Authentication of Bandeng (Chanos chanos) Oil Nanoemulsion Using Fourier Transform Infrared (FTIR) Spectroscopy Combined with Chemometrics

M. Masrukan[1*], F. Tunnisa[2], A.N. Ikhsan[3]

1- Department of Food Technology, Faculty of Science and Technology, Universitas Widya Mataram, Yogyakarta, Indonesia
(*- Corresponding Author Email: mrukan@widyamataram.ac.id)
2- Department of Biotechnology, The Graduate School of Universitas Gadjah Mada, Yogyakarta, Indonesia
3- Department of Pharmaceutics, Faculty of Pharmacy, Universitas Gadjah Mada, Yogyakarta, Indonesia

Received: 17.11.2025	**How to cite this article:**
Revised: 13.04.2026	Masrukan, M., Tunnisa, F., & Ikhsan, A.N. (2026). Rapid authentication of Bandeng (Chanos chanos) oil nanoemulsion using fourier transform infrared (FTIR) spectroscopy combined with chemometrics. *Iranian Food Science and Technology Research Journal, 22*(3), 319-330. https://doi.org/10.22067/ifstrj.2026.96524.1514
Accepted: 13.04.2026	
Available Online: 24.05.2026	

Abstract

A high level of polyunsaturated fatty acid (PUFA) in bandeng oil nanoemulsion (BON) makes it risky to be adulterated using low-quality oils such as palm oil (PO). Authentication of BON is essential to guarantee product quality and safety. Adulterated nanoemulsion is particularly challenging to identify because the surfactant matrix and aqueous phase mask the characteristic odor, color, and specific chemical markers detectable in bulk oils. This research aims to perform the authentication of BON using FTIR spectroscopy combined with chemometrics. Adulteration models were built using palm oil as an adulterant, bandeng oil as a pure component, and nanoemulsion matrix. All samples were analyzed using ATR-FTIR spectroscopy at 4000–650 cm^{-1} wavenumbers. Chemometrics technique, such as principal component analysis (PCA), partial least squares regression (PLSR), and principal component regression (PCR), was performed to separate and quantify BON from adulterant. PCA successfully separated BON from palm oil (PO) as an adulterant. Therefore, PLSR using normal spectra at wavenumbers 1500- 650 cm^{-1} had the best value based on highest R^2_{cal} value 0.9503; R^2_{pred} value 0.8761; lowest RMSEC 0.145; RMSEP 0.245. It can be concluded that FTIR spectroscopy combined with chemometrics was claimed as rapid, accurate, and suitable for authenticating BON from PO as an adulterant in nanoemulsion form.

Keywords: Fish oil nanoemulsion, Fingerprint, Partial least squares regression, Principal component analysis, Principal component regression

https://doi.org/10.22067/ifstrj.2026.96524.1514

Introduction

Fish oils are known as sources of polyunsaturated fatty acids (PUFA) and essential omega-3 unsaturated fatty acids such as eicosapentaenoic acid (EPA) and docosahexaenoic acid (DHA). Fish oils come mainly from oily fishes, such as cod, salmon, sardine, anchovy, and mackerel (Nieva-Echevarría, Goicoechea, & Guill'en, 2017; Chandrasekar, Belur, & Regupathi, 2018). Omega-3 fatty acid consumption has several beneficial effects on human health, such as antioxidant activity (Ikhsan, Syifa, Mustafidah, & Rohman, 2021) being recognized as effective against cardiovascular and inflammatory diseases, among others (Nichols, McManus, Krail, Sinclair, & Miller, 2014).

Recently, bandeng oil has been the focus of growing interest due to its nutritional advantages. Bandeng had a good quantity of protein, amino acids, vitamins, and polyunsaturated fatty acids. It contains rich levels of unsaturated fatty acids (50.74%), with monounsaturated fatty acids (MUFA) and polyunsaturated fatty acids (PUFA) constituting 34.47 and 16.27%, respectively (Murthy *et al*., 2016). Therefore, oil extracted from bandeng has the potential to be developed as a source of fish oil.

Bandeng oil has large-scale market potential. First, it can be the source of vitamin A and D and the long-chain n-3 fatty acids. Fish-oil products based on natural fish oil or their derivatives are frequently introduced to the market as a functional food (emulsion) or medicines, because consumption of seafood directly may be attributed to taste, price, contamination concerns such as heavy metals, and availability (Kennedy, Luo, & Ausman, 2012). Nanoemulsion-based delivery systems offer many potential benefits for incorporating omega-3 oils into foods and beverages. Fish oil nanoemulsion has been introduced to enrich foodstuffs, including meat, bakery, and dairy products such as yogurt (Zhong, Yang, Cao, Liu, & Qin, 2018; Jamshidi, Cao, Xiao, Simal-Gandara, 2020). The nanoemulsion method can effectively improve the oxidative stability of fish oil and mask unpleasant fishy flavour in fortified products.

Authentication of bandeng oil nanoemulsion (BON) is essential to prevent adulteration, ensure quality, nutritional value, and product safety for consumers. Driven by economic, unethical fats and oils, producers may intentionally or unintentionally mislabel and adulterate high-quality fish oils (Rohman, Putri, Irnawati Windarsih, Nisa, & Lestari, 2021). Adulteration involves the addition of cheaper oils. The potential adulterants of fish oil nanoemulsion are plant oils or vegetable oils. Fish oil is mainly adulterated using palm oil (PO) because of its physicochemical property similarities and lower prices (Putri, Rohman, & Riyanto, 2019).

Due to the increasing demand for fish oil nanoemulsions, it is essential to have a fast and accurate method to verify identification and detection of potential adulterants. Analytical methods that can be employed for authentication are gas chromatography-mass spectrometry (GC-MS) (Gul, Nasrullah, Nissar, Saifi, & Abdin, 2018), nuclear magnetic resonance (NMR) (Amargianitaki & Spyros, 2017), ultraperformance liquid chromatography (UPLC) (Setyaningsih, Saputro, Carrera, Palma, & García-Barroso, 2019), and Fourier transform infrared (FTIR) spectroscopy (Putri *et al*., 2019; Ikhsan *et al*., 2021b). While GC-MS, NMR, and UPLC offer high specificity, they are often associated with higher costs, longer analysis times, and more complex sample preparation, making them less suitable for rapid, high-throughput screening. FTIR spectroscopy, in contrast, provides a fast, solvent-free, and cost-effective alternative suitable for routine authentication.

FTIR spectroscopy is the most commonly used technique to determine authentication analysis, especially in fats and oils. It is also considered green analytical chemistry because it requires less solvent (Choiri, Sulaiman, & Rohman, 2020; Ikhsan *et al*., 2021b). FTIR spectroscopy combined with multivariate analysis has been applied for authentication of

virgin olive oil (Tay, Singh, Krishnan, & Gore, 2002), virgin coconut oil (Manaf, Che Man, Hamid, Ismail, & Abidin, 2007), and snakehead fish oil (Syifa, Irnawati, Riyanta, & Rohman, 2020). However, a literature search suggests that there is no information available related to the use of FTIR spectroscopy in BON, especially related to authentication.

The objective of this study is to authenticate BON that has been adulterated with palm oil using FTIR spectroscopy combined with chemometrics. Further analysis was conducted to distinguish BON as a pure product, and palm oil nanoemulsion (PON) as well as mixture oil nanoemulsion (MON) as fake products based on their FTIR spectra using the principal component analysis (PCA) method. However, partial least squares regression (PLSR) and principal component regression (PCR) calibration were intended for quantitative analysis adulteration models.

Materials and Methods

Bandeng was obtained from a local fish breeder in Pati, Central Java, Indonesia. Fish oil extraction was conducted in Sekolah Pasca Sarjana, Universitas Gadjah Mada, Yogyakarta, Indonesia. Meanwhile, the palm oil and other nanoemulsion components were purchased from Brataco (Yogyakarta, Indonesia).

Preparation of Adulteration Model's

Fish oil adulteration models were prepared by mixture bandeng oil and palm oil at varying concentrations ranging from 0% to 100% (v/v), as randomly generated using Excel software (Microsoft Inc, USA) (Mustafidah, Irnawati, Lukitaningsih, & Rohman, 2021). A total of 25 mixture samples (MON) were prepared with different bandeng-to-palm oil ratios, along with three replicates each of pure bandeng oil nanoemulsion (BON) and pure palm oil nanoemulsion (PON), resulting in 31 samples in total (Table 1).

Nanoemulsions were formulated according to a low-energy emulsification method (Chong *et al*., 2018). Each oil mixture was combined with 1500 µL Tween 80, 500 µL Span 80, and 16,000 µL distilled water, then premixed using a magnetic stirrer hotplate (IKA C MAG HS 7) at 800 rpm and 60 °C for 10 min. Subsequent homogenization was performed at 15,000 rpm for 5 min with a high-speed disperser (Ultra-Turrax T25, IKA). The resulting nanoemulsions were stored at 4 °C until further analysis. All samples were prepared in three independent batches over two separate days to account for preparation variability.

FTIR Spectroscopy Analysis

An FTIR spectrophotometer (Thermo Scientific Nicolet iS10, Madison, WI) was used to analyze all nanoemulsion samples based on Putri *et al*. (2019) research. Various wavenumber between 4000 – 650 cm^{-1} was used for measurement using 16 cm^{-1} resolution and each spectrum was the average of 32 scans to ensure a high signal-to-noise ratio (Rohman *et al*., 2020). Horizontal Attenuated Total Reflectance (HATR) composed ZnSe crystal was used for sampling accessory. Before analyzing each sample, a correction was performed by scanning a background spectrum of room air in the same condition. The sampling accessory was cleaned using n-hexane and acetone after FTIR spectrophotometer analysis was conducted.

Data Matrix Construction and Spectral Processing

The spectral data were organized into a matrix of dimensions 31 × 1680, where rows represented individual samples (25 MON, 3 PON, 3 BON) and columns corresponded to the 1680 absorbance values acquired across the wavenumber range of 4000–650 cm^{-1}. Prior to chemometric analysis, the raw spectra were preprocessed using baseline correction (linear baseline fit between 1800 cm^{-1} and 800 cm^{-1}) followed by vector normalization (standard normal variate, SNV) to minimize scattering effects and enhance spectral comparability. For derivative spectra, Savitzky-Golay filtering with a 9-point window and second-order polynomial was

used to compute first and second derivatives. Wavenumber selection was performed by evaluating several spectral sub-regions based on their chemical relevance and signal-to-noise ratio. The range 1500–650 cm^{-1} was identified as optimal for modeling, as it contains characteristic bands of lipid functional groups (e.g., C=O stretching, C–H bending) and showed the highest discriminative power in preliminary PCA (Crouse, Rousseau, & Grover, 2024).

Table 1- Composition of nanoemulsion samples used in adulteration models: milkfish oil and palm oil mixtures

Sample Codes	Milkfish oil (µL)	Palm oil (µL)	Tween80 (µL)	Span80 (µL)	Distilled water (µL)
MON1	590	1410	1500	500	16000
MON2	280	1720	1500	500	16000
MON3	960	1040	1500	500	16000
MON4	140	1860	1500	500	16000
MON5	290	1710	1500	500	16000
MON6	850	1150	1500	500	16000
MON7	660	1340	1500	500	16000
MON8	1590	410	1500	500	16000
MON9	1470	530	1500	500	16000
MON10	380	1620	1500	500	16000
MON11	640	1360	1500	500	16000
MON12	480	1520	1500	500	16000
MON13	630	1370	1500	500	16000
MON14	1310	690	1500	500	16000
MON15	560	1440	1500	500	16000
MON16	840	1160	1500	500	16000
MON17	920	1080	1500	500	16000
MON18	860	1140	1500	500	16000
MON19	430	1570	1500	500	16000
MON20	1260	740	1500	500	16000
MON21	1700	300	1500	500	16000
MON22	530	1470	1500	500	16000
MON23	1020	980	1500	500	16000
MON24	270	1730	1500	500	16000
MON25	280	1720	1500	500	16000
PON1	0	2000	1500	500	16000
PON2	0	2000	1500	500	16000
PON3	0	2000	1500	500	16000
BON1	2000	0	1500	500	16000
BON2	2000	0	1500	500	16000
BON3	2000	0	1500	500	16000

MON: Mixture oil nanoemulsion, PON: Palm oil nanoemulsion, BON: Bandeng oil nanoemulsion

Preparation of Calibration and Validation Samples

The samples for validation were prepared using the same spanned samples concentration as in samples for calibration. The validation was performed using the leave one out technique. The performance of the calibration models was evaluated using the following statistical parameters: The optimal number of PLSR and PCR was selected based on the minimum RMSECV (*Root mean square error of cross-validation*). The model with the highest Coefficient of determination for calibration (R^2cal) and prediction (R^2pred), together with the lowest RMSEC (*Root mean square error of calibration*) and RMSEP (*Root mean square error of prediction*) was chosen for the authentication of bandeng oil nanoemulsion.

Chemometrics analysis

Principal component analysis (PCA) was performed using Minitab 19 (Minitab Inc.,

USA). Quantification partial least squares regression (PLSR) and principal component regression (PCR) was used for quantitative analysis using TQ Analyst™ (Thermo Fisher Scientific Inc., USA) (Miller & Miller, 2018). For PLSR and PCR, the number of latent variables (LVs) was selected based on the minimum RMSEC.

Results and Discussion

Generally, animal fats and oils can be differed based on the composition of fatty acids each fat and oils. The carbon chain length and unsaturation degree of different fatty acids can be detected using various analysis instruments such as high-performance liquid chromatography (HPLC), gas chromatography (GC), and Fourier transforms infrared (FTIR) spectroscopy (Fahy *et al*., 2005). Therefore, using FTIR spectroscopy, adulteration practice can be detected using fingerprint FTIR spectra of each oil. FTIR spectroscopy was claimed rapid and effective in authenticating fish oil adulteration from adulterants or different fish oils. However, in nanoemulsion form, various matrices from nanoemulsion surfactants and other components may affect the authentication method (Hertiani *et al*., 2019; Kresnawati, Shantiningsih, & Martien, 2020).

The initial FTIR scanning was performed across the broad spectral range of 4000–650 cm^{-1} to capture the complete fingerprint region. However, to optimize the model for discrimination and quantification, a systematic wavenumber selection was conducted by comparing several spectral sub-regions: (1) the full range (4000–650 cm^{-1}), (2) the high-frequency region (3100–2800 cm^{-1}) associated with C–H stretching vibrations reflecting fatty acid chain length and unsaturation, (3) the fingerprint region (1800–650 cm^{-1}), and (4) a narrower fingerprint sub-region (1500–650 cm^{-1}). For each region, a PLSR model was built using normal spectra and evaluated by leave-one-out cross-validation (LOOCV) and independent external validation. The statistical results are summarized in Table 2.

Table 2- Performance of PLSR models built on different spectral regions (normal spectra).

Spectral region (cm^{-1})	LV	R^2cal	RMSEC	R^2pred	RMSEP
4000–650	7	0.892	0.210	0.801	0.312
3100–2800	4	0.745	0.335	0.689	0.421
1800–650	6	0.935	0.158	0.865	0.268
1500–650	5	0.9503	0.145	0.8761	0.245

LV: number of latent variables selected based on minimum RMSEC

The region 1500–650 cm^{-1} yielded the highest R^2cal (0.9503) and R^2pred (0.8761), along with the lowest RMSEC (0.145) and RMSEP (0.245). Although the region 2800–3100 cm^{-1} contains information about fatty acid chain length and unsaturation, it showed substantial spectral overlap between bandeng oil and palm oil in the nanoemulsion matrix. Moreover, a broad band around 3000–3500 cm^{-1}, due to O–H stretching from water present in the nanoemulsion, introduced baseline variability that reduced discriminatory power. In contrast, the 1500–650 cm^{-1} region contains key functional group vibrations such as C=O stretching (~1745 cm^{-1}), C–H bending (~1465 cm^{-1}), and C–O stretching (~1160 cm^{-1}), which are more sensitive to differences in triglyceride composition.

Subsequently, within the selected region (1500–650 cm^{-1}), different spectral

preprocessing techniques were compared: normal spectra, first derivative, and second derivative. The results for both PLSR and PCR are presented in Table 3.

Table 3- The optimization of multivariate calibration (PLSR and PCR) at 1500-650 cm^{-1} wavenumber regions

	Wavelength (cm^{-1})	Spectra	RMSEC	R^2_{cal}	RMSEP	R^2_{pred}
		Normal	***0.145***	***0.9503***	***0.245***	***0.8761***
PLSR	1500-650	1st derivative	0.256	0.8354	0.339	0.7120
		2nd derivative	0.368	0.6144	0.400	0.5987
		Normal	0.276	0.8068	0.300	0.8109
PCR	1500-650	1st derivative	0.335	0.6966	0.353	0.6747
		2nd derivative	0.330	0.7061	0.370	0.6417

*The selection condition was marked with italicized bold

For the optimal PLSR model (1500–650 cm^{-1}, normal spectra), the calibration slope was 0.948 and the intercept was 0.025. The response variable (adulteration level) was expressed as the mass fraction of palm oil in the total oil phase, ranging from 0 to 1 (0–100%). Therefore, the RMSEC of 0.145 and RMSEP of 0.245 correspond to mean prediction errors of approximately 14.5% and 24.5% of the full adulteration range, respectively.

The lowest adulteration level tested was 10% palm oil (MON samples with 90% bandeng oil). The PLSR model showed acceptable prediction accuracy at this level (prediction error ~12%). The limit of detection (LOD) and limit of quantification (LOQ) were estimated as 3.3 × RMSEC / slope and 10 × RMSEC / slope, yielding approximate values of 5% and 15% palm oil, respectively. This sensitivity is adequate for detecting economically motivated adulteration, which typically occurs at higher levels.

Partial least squares regression (PLSR) and principal component regression (PCR) can be observed in Table 3. In PLSR and PCR, linearity and error occurred was used to analyze the relationship between absorbance and concentration of each component. Statistical parameters, namely coefficient of determination for calibration (R^2_{cal}), coefficient of determination for prediction (R^2_{pred}), root mean square error of calibration (RMSEC), as well as root mean square error of prediction (RMSEP) in normal spectra, 1st derivative spectra, and 2nd derivative spectra, were evaluated. RMSEC and R^2_{cal} were used to evaluate calibration models; however, RMSEP and R^2_{pred} were used to evaluate real cases and compared to the reference value obtained. For both PLSR and PCR, normal spectra provided the best performance. Therefore, the normal spectra in the 1500–650 cm^{-1} region were used for the final quantitative adulteration models.

The method of choice for the authentication models was based on the highest values of coefficient of determination for calibration (R^2_{cal}) and coefficient of determination for prediction (R^2_{pred}), followed by the lowest values of root mean square error of calibration (RMSEC) and root mean square error of prediction (RMSEP). The normal spectra of FTIR spectra at wavenumbers of 1500 - 650 cm^{-1} were the highest R^2_{cal} values (0.9503); R^2_{pred} (0.8761); followed by the lowest RMSEC (0.145), and the lowest RMSEP (0.245) using PLSR. Moreover, using PCR as the selection method resulted R^2_{cal}; R^2_{pred}; RMSEC; and RMSEP value was 0.8068; 0,8109; 0.276; and 0.300 respectively

The authentication method was performed using 4000 - 650 cm^{-1} because fingerprint spectra can be observed in this area (Rohman *et al*., 2020). The FTIR spectra of bandeng oil nanoemulsion (BON), palm oil nanoemulsion

(PON), and mixture oil nanoemulsion (MON) can be observed in Fig. 1. Moreover, in Fig. 1, the various peaks corresponding to specific functional groups can be observed.

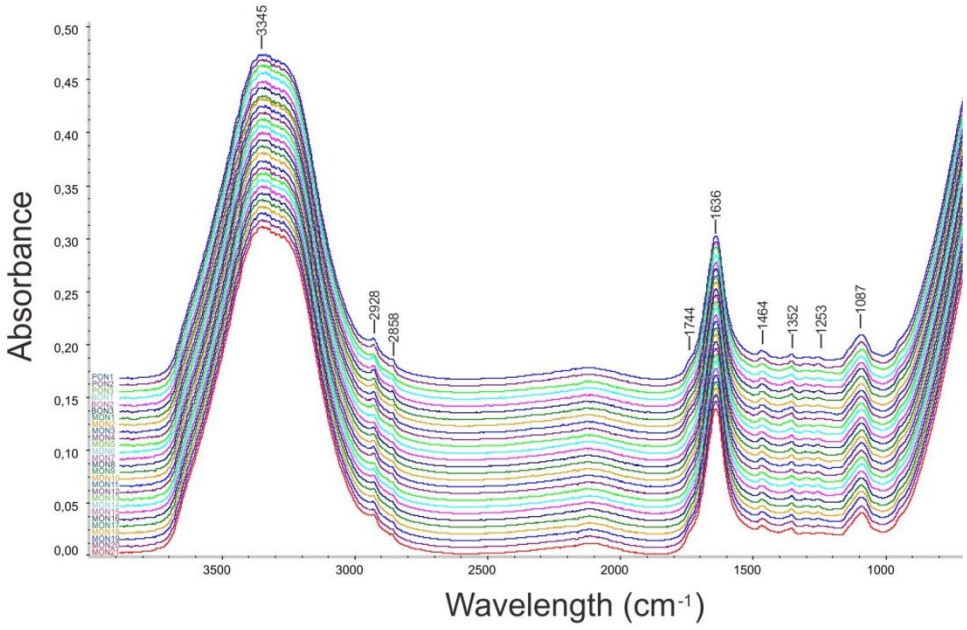

Fig. 1. The FTIR spectra of BON, PON, and MON at 4000 – 650 cm^{-1} wavenumber regions

Each peak and its functional group were compiled and observed in Table 4. A wide peak in every sample at 3000– 3500 cm^{-1} corresponds to water presence in nanoemulsion form. After wavenumber optimization, the highest R^2_{cal} – R^2_{pred} value and lowest RMSEP– RMSEC was obtained at 1500-650 cm^{-1} compared other wavenumber regions. Hence, this area can be used for quantitative analysis from adulteration models.

Table 4- Functional groups responsible in FTIR spectra between BON, PON, and MON at 4000 – 650 cm^{-1} wavenumber regions

Wavenumber (cm^{-1})	Functional Group
3345	-OH Stretch
2928	-CH_2 stretch (asymmetric)
2858	-CH_2 stretch (symmetric)
1744	-C=O ester stretch
1636	=C-H stretch (cis)
1464	-CH_2 bending
1352	-CH_3 bending
1253	-C-O ester stretch
1087	=C-H stretch (cis)

Principal component analysis (PCA) was used to discriminate each component from adulteration models at 4000– 650 cm^{-1} wavenumbers. PCA is an unsupervised pattern recognition that builds a discrimination model based on the similarity of the new variables (principal component) derived from wavenumber intensity as old variables (Miller & Miller, 2018). Discrimination of the authentication model can be observed in Fig. 2. The bandeng oil nanoemulsion (BON), which was labelled as a pure product, was grouped in specific regions. However, palm fish oil nanoemulsion (PON), labeled as adulterated nanoemulsion, was grouped in other specific regions and located distant from

the BON group. It is caused by the difference of FTIR spectra between these two oils, in which BON comes from animals and PON from plants.

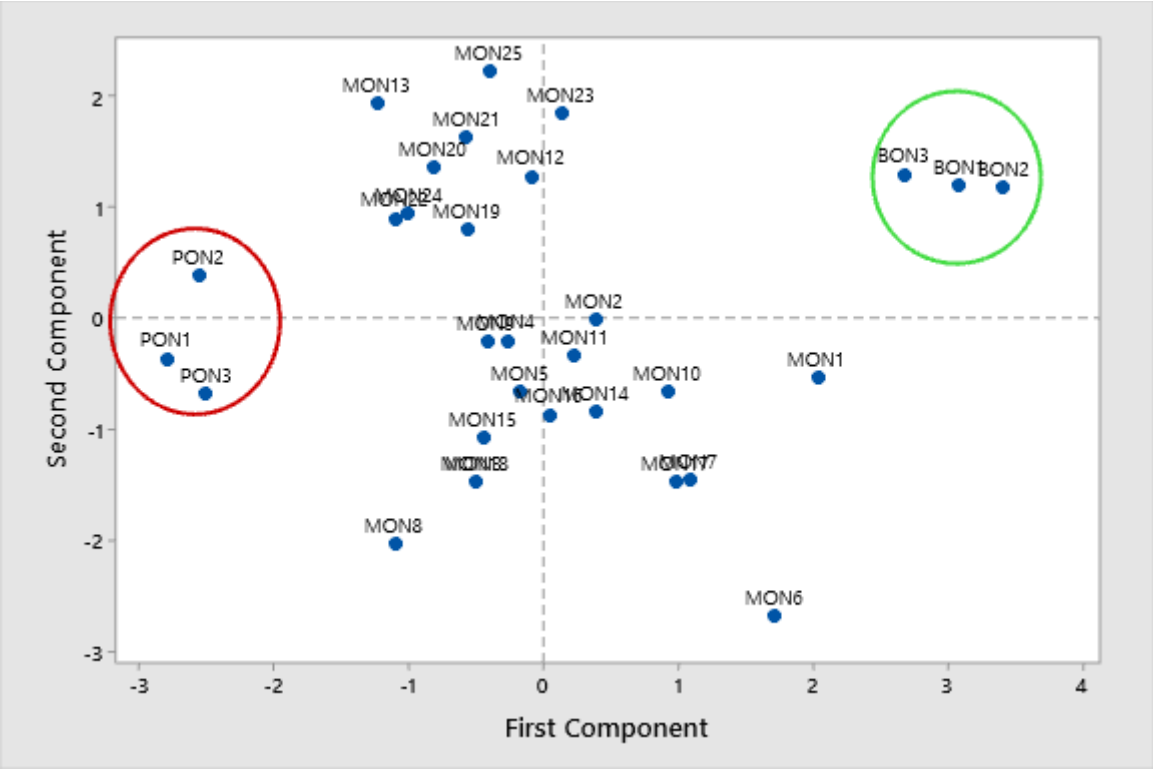

Fig. 2. The score plot between BON (green circle), PON (red circle), and MON

Based on the results, PCA has successfully discriminated BON from adulterant in the distant area between adulterants. The quantitative analysis using PLSR also yielded good analysis results, providing high accuracy and low errors method for the authentication of BON from PON as an adulterant in nanoemulsion form.

Conclusion

A combination of Fourier transform infrared (FTIR) spectroscopy with principal component analysis (PCA) and partial least squares regression (PLSR) was used for rapid authentication of BON. PCA discriminated and grouped BON from palm oil as an adulterant. The simultaneous analysis method was based on variable absorbances values of the normal spectra at 1500– 650 cm^{-1} based on the highest accuracy and lowest errors. This method was claimed rapid and effective to authenticate BON from PON as an adulterant.

Conflict of Interest

The authors declare no conflict of interest.

Acknowledgments

The authors send their gratitude to the Department of Food Technology, Faculty of Science and Technology, Universitas Widya Mataram, Yogyakarta, Indonesia, and Department of Pharmaceutics, Faculty of Pharmacy, Universitas Gadjah Mada, Yogyakarta, Indonesia.

Funding Source

The authors gratefully acknowledge the financial support from the Directorate General of Research and Development of the Ministry of Higher Education, Science, and Technology of the Republic of Indonesia for publication assistance in a reputable journal in 2025.

Author Contributions

Masrukan: Conceptualization, Funding acquisition, Data curation, Formal analysis, Investigation, Methodology, Project administration, Resources, Supervision, Writing– original draft, Writing– review and editing. **Fitra Tunnisa**: Conceptualization, Data curation, Formal analysis, Investigation, Software, Validation, Writing– original draft, Writing– review and editing. **Arif Nur Ikhsan**: Conceptualization, Investigation, Software, Validation, Visualization, Writing– original draft, Writing– review and editing.

References

1. Amargianitaki, M., & Spyros, A. (2017). NMR-based metabolomics in wine quality control and authentication. *Chemical and Biological Technologies in Agriculture*, *4*(9), 1–12. https://doi.org/10.1186/s40538-017-0092-x
2. Chandrasekar, V., Belur, P.D., & Regupathi, I. (2016). Effect of hydroxybenzoic acids antioxidants on the oxidative stability of sardine oil. *Resource-Efficient Technologies*, *2*(1), 114–118. https://doi.org/10.18799/24056529/2016/5/88
3. Choiri, S., Sulaiman, T.N.S., & Rohman, A. (2020). Development and application of atr-ftir spectroscopy for mixture homogeneity in pharmaceutical application. *International Journal of Pharmaceutical Research, 12*(4), 7-16. https://doi.org/10.31838/ijpr/2020.12.04.003
4. Chong, W.T., Tan, C.P., Cheah, Y.K., Lajis, A.F.B., Dian, N.L.H.M., Kanagaratnam, S., & Lai, O.I. (2018). Optimization of process parameters in preparation of tocotrienol-rich red palm oil-based nanoemulsion stabilized by Tween80-Span 80 using response surface methodology. *PLoS ONE, 13*(8), 272-278. https://doi.org/10.1371/journal.pone.0202771
5. Crouse, S.H., Rousseau, R.W., & Grover, M.A. (2024). A feature selection method for overlapping peaks in vibrational spectroscopy using nonnegatively constrained classical least squares. *Computers & Chemical Engineering, 189*, 108785. https://doi.org/10.1016/j.compchemeng.2024.108785
6. Fahy, E., Subramaniam, S., Brown, H.A., Glass, C.K., Merrill, A.H.J., Murphy, R.C., Raetz, C.R., Russell, D.W., Seyama, Y., Shaw, W., Shimizu, T., Spener, F., van-Meer, G., VanNieuwenhze, M.S., White, S.H., Witztum, J.L., & Dennis, E.A. (2005). A comprehensive classification system for lipids. *Journal of Lipid Research, 46*(5), 839-861. https://doi.org/10.1194/jlr.E400004-JLR200
7. Gul, I., Nasrullah, N., Nissar, U., Saifi, M., & Abdin, M.Z. (2018). Development of DNA and GC-MS fingerprints for authentication and quality control of *Piper nigrum* L. and its adulterant *Carica papaya* L. *Food Analytical Methods, 11*(4), 1209–1222. https://doi.org/10.1007/s12161-017-1088-7
8. Hertiani, T., Tunjung-Pratiwi, S.U., Haryadi, E.C., Triatmoko, B., Yuswanto, A., & Martien, R. (2019). Evaluation of the efficacy and toxicity of massoia oil nanoemulsion. *Pakistan Journal of Pharmaceutical Sciences, 32*(4), 1519-1528. https://doi.org/10.36721/pjps/32/4/01.07.2019/5332/1519-1528
9. Ikhsan, A.N., Syifa, F., Mustafidah, M., & Rohman, A. (2021a). Implementation of chemometrics as a solution to detecting and preventing falsification of herbal medicines in Southeast Asia: A review. *Journal of Applied Pharmaceutical Science, 11*(9), 139–148. https://doi.org/10.7324/JAPS.2021.110917
10. Ikhsan, A.N., Rohman, A., Putri, A., Syifa, F., Mustafidah, M., & Martien, R. (2021b). Application of FTIR spectroscopy and chemometrics for the prediction of radical scavenging activities of fish oils. *Indonesian Journal of Pharmacy, 32*(2), 166-174. https://doi.org/10.22146/ijp.1004

11. Jamshidi, A., Cao, H., Xiao, J., & Simal-Gandara, J. (2020). Advantages of techniques to fortify food products with the benefits of fish oil. *Food Research International, 137*, 109353. https://doi.org/10.1016/j.foodres.2020.109353
12. Kennedy, E.T., Luo, H., & Ausman, L.M. (2012). Cost implications of alternative sources of (n-3) fatty acid consumption in the United States. *The Journal of Nutrition, 142*(3), 605S–609S. https://doi.org/10.3945/jn.111.152736
13. Kresnawati, Y., Shantiningsih, R.R., & Martien, R. (2020). Optimization of soybean oil, tween 80, peg 400 in formulation of beta carotene nanoemulsion. *Research Journal of Pharmacy and Technology, 13*(12), 5692-5698. https://doi.org/10.5958/0974-360X.2020.00991.9
14. Manaf, M.A., Che Man, Y.B., Hamid, N.S.A., Ismail, A., & Abidin, S.Z. (2007). Analysis of adulteration of virgin coconut oil by palm kernel olein using fourier transform infrared spectroscopy. *Journal of Food Lipids, 14*(2), 111–121. https://doi.org/10.1111/j.1745-4522.2007.00066.x
15. Miller, J.N., & Miller, J.C. (2018). *Statistics and Chemometrics for Analytical Chemistry*. 7th ed. Philadelphia: Coronet Books Inc.
16. Murthy, L.N., Padiyar, P., Rao, M., Asha, K., Jesmi, D., Girija, P., Prasad, M., & Ravishankar, C. (2016). Nutritional profile and heavy metal content of cultured milkfish (Chanos chanos). *Fishery Technology, 53*, 245–249.
17. Mustafidah, M., Irnawati, I., Lukitaningsih, E., & Rohman, A. (2021). Authentication analysis of milkfish fish oil using the combination of FTIR spectroscopy and chemometrics. *Food Research, 5*(2), 272-278. https://doi.org/10.26656/fr.2017.5(2).607
18. Nichols, P.D., McManus, A., Krail, K., Sinclair, A.J., & Miller, M. (2014). Recent advances in omega-3: health benefits, Sources, Products and bioavailability. *Nutrients, 6*(9), 3727–3733. https://doi.org/10.3390/nu6093727
19. Nieva-Echevarría, B., Goicoechea, E., & Guill'en, M.D. (2017). Polyunsaturated lipids and vitamin A oxidation during cod liver oil in vitro gastrointestinal digestion- Antioxidant effect of added BHT. *Food Chemistry, 232*, 733–743. https://doi.org/10.1016/j.foodchem.2017.04.057
20. Putri, A.R., Rohman, A., & Riyanto, S. (2019). Authentication of Patin (*Pangasius micronemus*) fish oil adulterated with palm oil using FTIR spectroscopy combined with chemometrics. *International Journal of Applied Pharmaceutics, 11*(3), 195–199. https://doi.org/10.22159/ijap.2019v11i3.30947
21. Rohman, A., Ghazali, M.A.B., Windarsih, A., Irnawati, Riyanto, S., Yusof, F.M., & Mustafa, S. (2020). Comprehensive review on application of FTIR spectroscopy coupled with chemometrics for authentication analysis of fats and oils in the food products. *Molecules, 25*(22), 5485. https://doi.org/10.3390/molecules25225485
22. Rohman, A., Putri, A.R., Irnawati, Windarsih, A., Nisa, K., & Lestari, L.A. (2021). The employment of analytical techniques and chemometrics for authentication of fish oils: A review. *Food Control, 124*, 107864. https://doi.org/10.1016/j.foodcont.2021.107864
23. Setyaningsih, W., Saputro I.E., Carrera, C.A., Palma, M., & García-Barroso, C. (2019). Fast determination of phenolic compounds in rice grains by ultraperformance liquid chromatography coupled to photodiode array detection: Method development and validation. *Journal Agriculture Food Chemistry, 67*(10), 3018-3027. https://doi.org/10.1021/acs.jafc.8b05430
24. Syifa, F., Irnawati, Riyanta, S., & Rohman, A. (2020). Authentication analysis of snakehead fish oil using combination of ftir spectra and chemometrics. *International Journal of Pharmaceutical Research, 13*(1), 160-167. https://doi.org/10.31838/ijpr/2021.13.01.025

25. Tay, A., Singh, R.K., Krishnan, S.S., & Gore, J.P. (2002). Authentication of olive oil adulterated with vegetable oils using Fourier transform infrared spectroscopy. *LWT- Food Science Technology*, *35*(1), 99–103. https://doi.org/10.1006/fstl.2001.0864
26. Zhong, J., Yang, R., Cao, X., Liu, X., & Qin, X. (2018). Improved physicochemical properties of yogurt fortified with fish oil/γ-Oryzanol by nanoemulsion technology. *Molecules*, *23*(1), 56. https://doi.org/10.3390/molecules23010056

نشریه پژوهشهای علوم و صنایع غذایی ایران
https://ifstrj.um.ac.ir

مقاله کوتاه پژوهشی

جلد ۲۲، شماره ۳، مرداد- شهریور ۱٤۰۵، ص. ۳۳۰-۳۱۹

احراز هویت سریع نانوامولسیون روغن باندنگ (Chanos chanos) با استفاده از طیف‌سنجی مادون قرمز تبدیل فوریه (FTIR) همراه با شیمی‌سنجی

ماس روکان[۱*]- فیترا تونیسا[۲]- عارف نور ایخسان[۳]

تاریخ دریافت: ۱۴۰۴/۰۸/۲۶
تاریخ پذیرش: ۱۴۰۵/۰۱/۲۴

چکیده

سطح بالای اسید چرب چند غیراشباع (PUFA) در نانوامولسیون روغن باندنگ (BON)، تقلب در آن را با استفاده از روغن‌های بی‌کیفیت مانند روغن پالم (PO) خطرناک می‌کند. احراز هویت BON برای تضمین کیفیت و ایمنی محصول ضروری است. شناسایی نانوامولسیون تقلبی به‌ویژه چالش برانگیز است زیرا ماتریس سورفکتانت و فاز آبی، بو، رنگ و نشانگرهای شیمیایی خاص قابل تشخیص در روغن‌های فله را می‌پوشانند. هدف از این تحقیق، احراز هویت BON با استفاده از طیف‌سنجی FTIR همراه با شیمی‌سنجی است. مدل‌های تقلب با استفاده از روغن پالم به‌عنوان یک ماده تقلبی، روغن باندنگ به‌عنوان یک جزء خالص و ماتریس نانوامولسیون ساخته شدند. همه نمونه‌ها با استفاده از طیف‌سنجی ATR-FTIR در طول موج‌های ۴۰۰۰ تا ۶۵۰ (cm^{-1}) تجزیه و تحلیل شدند. تکنیک‌های شیمی‌سنجی، مانند تجزیه و تحلیل مؤلفه‌های اصلی (PCA)، رگرسیون حداقل مربعات جزئی (PLSR) و رگرسیون مؤلفه‌های اصلی (PCR)، برای جداسازی و تعیین کمیت BON از ماده تقلبی انجام شد. PCA با موفقیت BON را از روغن پالم (PO) به‌عنوان یک ماده تقلبی جدا کرد. بنابراین، PLSR با استفاده از طیف‌های نرمال در طول موج‌های ۱۵۰۰ تا ۶۵۰ (cm^{-1})، بهترین مقدار را بر اساس بالاترین مقدار R_2cal برابر با ۰/۹۵۰۳؛ مقدار R_2pred برابر با ۰/۸۷۶۱؛ کمترین RMSEC برابر با ۰/۱۴۵؛ و RMSEP برابر با ۰/۲۴۵ داشت. می‌توان نتیجه گرفت که طیف‌سنجی FTIR همراه با روش‌های شیمی‌سنجی، روشی سریع، دقیق و مناسب برای تشخیص BON از PO به‌عنوان یک ماده‌ی تقلبی در شکل نانوامولسیون است.

واژه‌های کلیدی: اثر انگشت، تحلیل مؤلفه‌های اصلی، رگرسیون حداقل مربعات جزئی، رگرسیون مؤلفه‌های اصلی، نانوامولسیون روغن ماهی

۱- گروه صنایع غذایی، دانشکده علوم و فناوری، دانشگاه ویدیا ماتارام، یوگیاکارتا، اندونزی
(*- نویسنده مسئول: Email: mrukan@widyamataram.ac.id)
۲- گروه بیوتکنولوژی، دانشکده تحصیلات تکمیلی دانشگاه گادجاه ماداه، یوگیاکارتا، اندونزی
۳- گروه داروسازی، دانشکده داروسازی، دانشگاه گادجاه ماداه، یوگیاکارتا، اندونزی

https://doi.org/10.22067/ifstrj.2026.96524.1514

بسم الله الرحمن الرحیم

مندرجات

نشریه پژوهشهای علوم و صنایع غذایی ایران

با شماره پروانه ۱۲۴/۸۴۷ و درجه علمی–پژوهشی شماره ۳/۱۱/۸۱۰ از وزارت علوم، تحقیقات و فناوری ۸۸/۵/۱۰

"براساس مصوبه وزارت عتف از سال ۱۳۹۸، کلیه نشریات دارای درجه "علمی–پژوهشی" به نشریه "علمی" تغییر نام یافتند. "

جلد ۲۲ **شماره ۳** **مرداد- شهریور ۱۴۰۵**

ناشر: دانشگاه فردوسی مشهد

این نشریه درپایگاه‌های زیر نمایه شده است:

AGRIS، Scopus، CABI، DOAJ، EBSCO، Google scholar، Internet Archive، پایگاه استنادی جهان اسلام (ISC)، سامانه نشریات علمی ایران، پایگاه اطلاعات علمی جهاد دانشگاهی (SID)، بانک اطلاعات نشریات کشور (MAGIRAN)، مرجع دانش CIVILICA

پست الکترونیکی: ifstrj@um.ac.ir

مقالات این شماره در سایت https://ifstrj.um.ac.ir به‌صورت مقاله کامل نمایه شده است.

این نشریه به تعداد ۶ شماره در سال و به‌صورت آنلاین منتشر می‌شود.

نشریه علمی
پژوهشهای علوم و صنایع غذایی ایران

جلد ۲۲ شماره ۳
سال ۱۴۰۵
شماره پیاپی ۹۹
شاپا: ۴۱۶۱-۱۷۳۵

عنوان مقالات

مقالات پژوهشی

مقاله کوتاه